Theoretical Studies of Positronium Formation in Positron Collisions with Lithium and Hydrogen Atoms

Martin Stephen Thomas Watts

ProQuest Number: 10045757
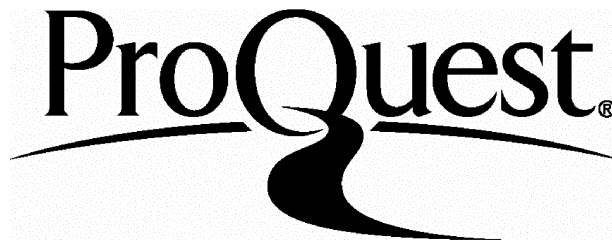
ProQuest 10045757

Abstract

The Kohn variational method has been used to study elastic scattering and positronium (Ps) formation in positron collisions with atomic hydrogen and lithium, in the energy region where only these two channels are open.

In common with other alkali metals, lithium is interesting in that its valence electron is sufficiently weakly bound that positronium formation is exothermic, and hence an open channel for incident positrons of zero energy. For such a process, Wigner's threshold theory predicts an s-wave cross section which has an inverse dependence on the wavenumber, k, of the projectile as $k \rightarrow 0$.

Using a model potential and very elaborate trial functions, a detailed investigation of s- and p-wave positron-lithium scattering has been made in the energy range 0–1.84eV, and preliminary results have also been obtained for d-wave scattering. The s-wave Ps formation cross section, as calculated variationally, appears to be in accordance with the Wigner theory, although this partial wave contributes negligibly to the Ps channel across most of the energy range considered. The p and d partial waves make a much more substantial contribution to the rearrangement process.

New cross sections for positron-hydrogen scattering have been calculated for the energy region close to the positronium formation threshold, and results have been compared with the predictions of R-matrix threshold theory.

Acknowledgements

Contents

Chapter 1

Introduction

1.1 The Positron

1.1.1 Prediction and Observation

It was as a consequence of the publication of Dirac's highly successful paper on the relativistic theory of the electron (1928) that the existence of the positron was first theoretically postulated. The relativistic wave equation contained in this publication explained several hitherto inexplicable quantum mechanical phenomena, including fine-structure effects in atomic hydrogen and electron spin, but had the apparent drawback of predicting states corresponding to negative solutions of the energy equation

$$E = \sqrt{p^2c^2 + m_e^2c^4} \tag{1.1}$$

for which no physical explanation could initially be found. It was not understood why, when there existed an infinite number of these states into which an electron could fall, no such transitions from positive states had actually been observed to occur.

In an effort to account for the lack of any experimental evidence for the negative energy states, Dirac proposed his 'sea of electrons' theory, where it was supposed that free space was, in fact, composed of an infinite density of electrons occupying all the states of negative energy. Transitions from positive to negative states would thus be forbidden by the Pauli exclusion principle, although there still remained the possibility

of the reverse process, which would leave the 'sea' with a hole in it. It was quickly realised that such a hole would have the characteristics of a particle with a charge equal to that of the electron, but with opposite sign, although the firm prediction of a new type of elementary particle did not immediately follow—at a time when the proton and electron were the only known sub-atomic particles, and inextricably connected with the concepts of positive and negative charge, there was considerable opposition to the idea of the existence of a positive electron, and much effort was devoted to demonstrating that the holes would actually behave like protons. It was Weyl (1931) who conclusively refuted this latter interpretation, leading Dirac (1931) to identify the negative energy solutions with an 'anti-electron', or positron, remarking incidentally that there ought also to exist anti-protons, possessing a negative charge, corresponding to holes in a similar negative energy sea of protons.

The first experimental observation of the positron was made, completely independently of Dirac, by Anderson (1932), who photographed an anomalous ionisation track in a cloud chamber whilst investigating cosmic radiation. The range of the ionisation was that of an electron, but the curvature of the track, brought about by a magnetic field applied across the chamber, was in the opposite sense, leading Anderson to conclude that what had been witnessed was genuinely a positive electron. Not being conversant with Dirac's theory of the positron, however, Anderson was unable immediately to make the connection between prediction and observation, and it remained for Blackett and Occhialini (1933), who recorded many more occurrences of positrons in a cloud chamber using more sophisticated techniques, to link the two. This confirmation, rejecting as it did the idea that protons and electrons were the sole constituents of matter, marked the beginning of modern elementary particle physics.

The positron and the electron possess equal charges of opposite sign, and consequently opposite magnetic dipole moments, but in all other respects they resemble each

other. This fundamental difference between them, however, gives rise to some interesting differences in their behaviour in the presence of matter. The distinguishability of the electron and positron also means that they are not subject to the Pauli exclusion principle when interacting with one another.

1.1.2 Positron Interactions with Matter

In a vacuum, the positron is a stable particle with an infinite lifetime, but in the presence of atoms and molecules, where there is a high concentration of electrons, it is always prone to annihilate (the electron falling into the 'hole' of Dirac's sea theory), resulting in the emission of electromagnetic radiation. When the positron and electron have parallel spins, triplet annihilation produces three gamma ray quanta with energies totalling 1022keV, the sum of the rest mass energies of the two particles. If the spins are anti-parallel, singlet annihilation may take place via the production of two gamma photons, each with an energy of 511keV. In each case, the number of photons emitted on annihilation is determined by the necessity for conservation of both momentum and angular momentum.

In positron scattering from atoms and molecules the cross section for direct annihilation is extremely small in comparison with that for other collision processes to the extent that it can effectively be disregarded in calculations of cross sections. Where energetically viable, it is much more likely that annihilation will take place via the formation of the bound state of a positron and an electron known as positronium (Ps). This purely leptonic 'atom' has a reduced mass almost exactly one half that of the hydrogen atom, so that, neglecting fine structure effects, its energy eigenvalues are one half those of the corresponding hydrogenic eigenstates. The ground state thus has an energy of −6.8eV, although some fine structure splitting occurs between the singlet and triplet eigenstates, referred to as para- and ortho-positronium respectively. The most significant difference between these two types is in their mean lifetimes. Each decays

according to the exponential form

$$P \sim \exp{-t/\tau,} \qquad (1.2)$$

where for para-Ps, which decays via two gamma photons, $\tau = 1.25 \times 10^{-10}$sec. Ortho-Ps, decaying with the emission of three photons, has a much longer lifetime of $\tau = 1.41 \times 10^{-7}$sec, making experimental observation of its behaviour rather easier.

The characteristic decay rates for the two forms of Ps facilitate the investigation of positron behaviour in gases by means of lifetime studies, one of the earliest experimental techniques in positron physics. The lifetime of a positron is determined by detecting the gamma radiation given off on emission of the positron from a source (typically Na^{22}) immersed in the gas, and also that emitted on annihilation, the two types of radiation being distinguishable by their differing energies. By collecting data for many such events, a lifetime spectrum is built up, from which information can be extracted about the fraction of positrons annihilating freely, or via positronium formation, by a process of fitting and subtracting exponentials corresponding to the various components.

Despite the very small cross section for free annihilation, lifetime spectra usually exhibit a substantial component due to this process because some positrons slow down from the high energies with which they are emitted, by means of elastic and inelastic collisions, to energies where positronium formation is not possible. The Ps formation threshold, E_{thr}, is the difference between the binding energy of the positronium in its ground state, E_{Ps}, and that of the atom or molecule under investigation, E_B, that is

$$E_{thr} = E_{Ps} - E_B. \qquad (1.3)$$

Positrons with energies between zero and E_{thr} cannot form Ps, and must therefore ultimately annihilate freely. Such a region of the energy spectrum exists for many atoms with the notable exception of the alkalis, for which the atomic valence electron is less tightly bound than Ps, giving a negative value for E_{thr}. This is an interesting

10

feature of the present work on e$^+$-Li scattering, since it means that Ps formation is an open channel even for positrons of zero energy. Connected with the weak binding energy of the lithium atom is its very high polarisability, which gives rise to a complex set of correlations and distortions when situated in the field of the positron, and the complicated nature of the positron-atom interaction thus provides a severe challenge for theoretical approximation methods.

For many atoms and molecules, the positronium formation threshold lies below the first excitation threshold, producing a region, known as the Öre gap, where Ps formation is the only possible inelastic process. This part of the energy spectrum is of particular interest for the studies reported here of both e$^+$-H and e$^+$-Li scattering.

Although lifetime experiments were previously an important tool for investigating positron behaviour in gases, the development of moderators capable of producing well collimated beams of positrons has enabled direct measurements of scattering cross sections to be obtained, and most experimental interest now tends to focus on this latter method. Recently, Stein *et al.* (1985, 1988, 1990) have measured total cross sections for positron scattering from alkali metals, and this has, in part, provided the stimulus for the present theoretical investigations of positron-lithium scattering.

Total cross sections for positron scattering from a given atom or molecule at low energies tend to be smaller than for the corresponding case of electron scattering, owing to the cancellation, in the former case, of the static and polarization terms in the interaction potential, which are repulsive and attractive respectively. For electrons, the two components are both attractive, and combine to increase the overall strength of the interaction. The alkalis are again peculiar here, in that positron total cross sections are higher at low energies than in electron scattering and this is almost certainly due to the presence of the open positronium channel at all energies.

Electron and positron total cross sections are compared in figures 1.1 and 1.2, for a
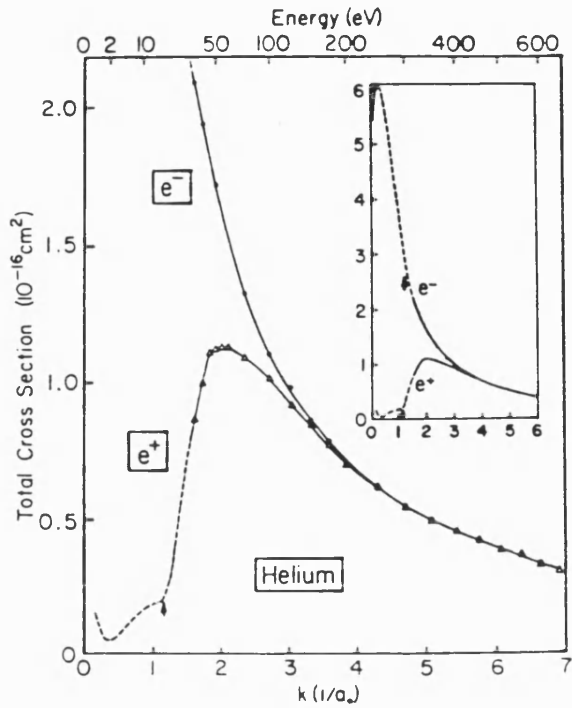
Figure 1.1: Comparison of positron-helium and electron-helium total cross sections, obtained from Kauppila *et al.* (1981).
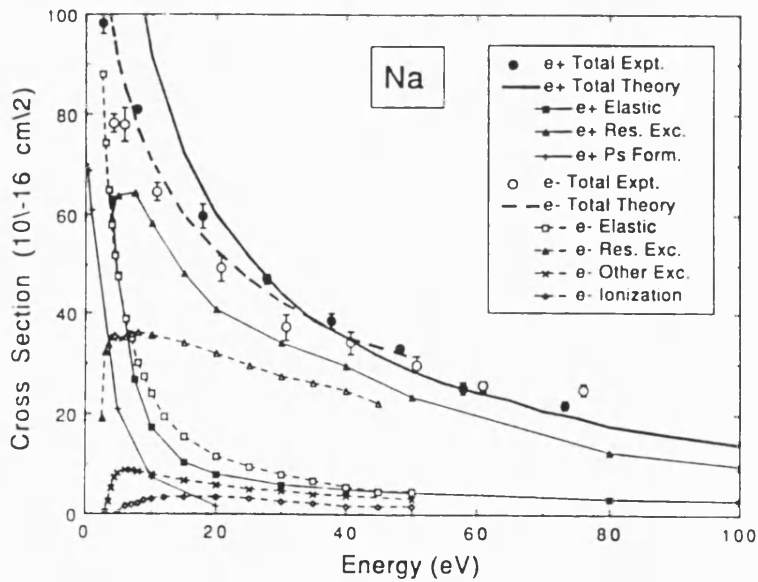
Figure 1.2: Comparison of positron-sodium and electron-sodium total cross sections, taken from Kauppila and Stein (1990).

noble gas atom and for an alkali. Note that the two cross sections converge at higher energies, as the polarization and exchange components in the interaction become less significant.

1.2 Variational Methods

1.2.1 Introduction

The work presented in this thesis has made extensive use of two variational techniques: the Rayleigh-Ritz method, for treating bound state problems, and the Kohn method for the calculation of scattering cross sections. The methods have in common that they each make use of stationary properties arrived at by considering how the functional

$$I = \; < \Psi|H - E|\Psi > \tag{1.4}$$

changes with respect to variations in the trial wavefunction Ψ, when Ψ approaches the correct solution of the Schrödinger equation.

The Rayleigh-Ritz variational principle considers the case where Ψ tends to zero at infinity rapidly enough that it is normalisable, and the stationary property here is associated with the energy eigenvalues, E_n, of the Hamiltonian. The Rayleigh-Ritz method is particularly powerful since, in addition to the stationary feature, it also yields a rigorous upper bound on these eigenvalues.

The Kohn method, on the other hand, considers the case where the trial function is not normalisable, but has a given asymptotic form at long ranges. The stationary quantities here are the tangent of the phase shift, for purely elastic scattering, or the elements of the reactance matrix, K, for the multi-channel case. Except in the special limiting case of collisions at zero energy, the Kohn method gives no rigorous bound in the way that the Rayleigh-Ritz method does, since the stationary feature can, in general, be a maximum, minimum or point of inflection. In practice, though, a well-behaved set of results will often exhibit a local maximum for the tangent of the phase shift,

or the diagonal elements of the K-matrix, under certain recognisable circumstances, producing what might be termed at least an 'empirical' lower bound. For reasons to be discussed, it is usually necessary to treat the results of a Kohn calculation with more caution than those of a Rayleigh-Ritz problem, although the method is capable of yielding cross sections of very high accuracy when used correctly.

1.2.2 The Rayleigh-Ritz Variational Method

Consider a Hamiltonian H with eigenvalues E_n corresponding to the orthonormal set of eigenfunctions ϕ_n, i.e. $H\phi_n = E_n\phi_n$, and let I be the functional

$$I = < \Phi_n^t \mid H - E_n \mid \Phi_n^t >, \tag{1.5}$$

where Φ_n^t is a trial function which differs from an exact eigenfunction ϕ_n by an amount $\delta\phi$ such that

$$\Phi_n^t = \phi_n + \delta\phi. \tag{1.6}$$

The above integral (1.5) can thus be written

$$I = < \phi_n + \delta\phi \mid H - E_n \mid \phi_n + \delta\phi >$$
$$= < \phi_n \mid H - E_n \mid \phi_n > +2 < \delta\phi \mid H - E_n \mid \phi_n > + < \delta\phi \mid H - E_n \mid \delta\phi > \tag{1.7}$$

where we have exploited the Hermiticity of the Hamiltonian operator. The first two terms on the right hand side are both zero, and so equating (1.5) and (1.7) the resulting identity is

$$< \Phi_n^t \mid H - E_n \mid \Phi_n^t > \equiv < \delta\phi \mid H - E_n \mid \delta\phi > \tag{1.8}$$

and hence the exact energy eigenvalue is given by

$$E_n = \frac{< \Phi_n^t \mid H \mid \Phi_n^t > - < \delta\phi \mid H \mid \delta\phi >}{< \Phi_n^t \mid \Phi_n^t > - < \delta\phi \mid \delta\phi >}. \tag{1.9}$$

Dropping the terms $< \delta\phi \mid H \mid \delta\phi >$ and $< \delta\phi \mid \delta\phi >$, which are of second order in $\delta\phi$, gives the well-known Rayleigh-Ritz functional:

$$E_n^v = \frac{< \Phi_n^t \mid H \mid \Phi_n^t >}{< \Phi_n^t \mid \Phi_n^t >}. \qquad (1.10)$$

Hence, we have a variational estimate of the energy of the system, E_n^v, which differs from the exact energy E_n by an amount which has a second order dependence on $\delta\phi$, and thus has the required stationary property. A further useful property of the functional (1.10) is that it provides a rigorous upper bound on the lowest eigenvalue, E_0, of H; that is to say, regardless of Φ_n^t, $E_n^v \geq E_0$. This may be demonstrated by expanding Φ_n^t in terms of the complete set of orthonormal eigenfunctions of H:

$$\Phi_n^t = \sum_j a_j \phi_j. \qquad (1.11)$$

The functional (1.10) therefore has the form

$$\begin{aligned} E_n^v &= \frac{< \sum_i a_i \phi_i \mid H \mid \sum_j a_j \phi_j >}{< \sum_i a_i \phi_i \mid \sum_j a_j \phi_j >} \\ &= \frac{\sum_{i,j} E_j a_j a_i < \phi_i \mid \phi_j >}{\sum_{i,j} a_j a_i < \phi_i \mid \phi_j >}. \end{aligned} \qquad (1.12)$$

But $< \phi_i \mid \phi_j > = \delta_{ij}$, so

$$E_n^v = \frac{\sum_j a_j^2 E_j}{\sum_j a_j^2}. \qquad (1.13)$$

Subtracting E_0 from both sides gives

$$E_n^v - E_0 = \frac{\sum_j a_j^2 (E_j - E_0)}{\sum_j a_j^2}. \qquad (1.14)$$

By definition $E_j \geq E_0$, and the coefficients a_j are real, so it follows that $E_n^v - E_0 \geq 0$.

A Rayleigh-Ritz calculation, then, consists of selecting a form for the trial function and varying its parameters in an attempt to obtain the lowest possible value for the functional (1.10). Increasing the number of parameters on which a given form of

15

function depends allows a closer fit to the exact eigenfunction to be attained, and consequently a more accurate approximation to the exact eigenvalue to be found. A study of the rate of convergence of the eigenvalue estimates with respect to such systematic improvements can then provide information on how accurate the results are.

The form used for the trial function obviously depends to a great extent on the problem being solved, and should ideally contain as much previously known information as possible about the system under study—the better the general form, the fewer the number of variational parameters required to obtain satisfactory convergence. In the case of a Rayleigh-Ritz calculation, however, it is at least possible to say that the required eigenvalue lies below the one computed, no matter how bad the trial function. For the Kohn variational method, on the other hand, no such rigorous bound exists and a sensible choice of trial function is important in order that useful information can be extracted.

1.2.3 The Kohn Variational Method

Rigorous bounded variational methods do exist in scattering theory, but their theoretical complexity makes them less attractive for practical purposes than the Kohn variational method (Kohn, 1948). Although unable to provide a bound on any parameter in the sense in which the Rayleigh-Ritz method does, the Kohn method appears to produce a localised lower bound on the diagonal elements of the K-matrix under certain recognisable circumstances, and has been shown to yield results of high accuracy in a number of cases. In this section the one channel Kohn functional is derived by consideration of the asymptotic form of a wavefunction describing the elastic scattering of a monoenergetic beam of particles by a central potential.

Consider the case of particles, wavenumber k, travelling in the positive z-direction encountering a potential, V, spherically symmetric with respect to the origin of coor-

dinates. The time-independent Schrödinger equation for such a system is

$$(-\nabla^2 + 2V(r))\Psi(\mathbf{r}) = k^2\Psi(\mathbf{r}). \tag{1.15}$$

Exploitation of the axial symmetry of the system allows the total wavefunction to be expanded in terms of the complete orthonormal set of Legendre polynomials, $P_l(\cos\theta)$, so

$$\Psi(\mathbf{r}) = \sum_{l=0}^{\infty} R_l(k,r)P_l(\cos\theta) \tag{1.16}$$

where each term individually is a solution of (1.15). In spherical polar coordinates, the Laplacian operator is given by

$$\nabla^2 = \frac{1}{r^2}\frac{\partial}{\partial r}\left(r^2\frac{\partial}{\partial r}\right) + \frac{1}{r^2\sin\theta}\frac{\partial}{\partial\theta}\left(\sin\theta\frac{\partial}{\partial\theta}\right) + \frac{1}{r^2\sin^2\theta}\frac{\partial^2}{\partial\phi^2}, \tag{1.17}$$

where the second and third terms may conveniently be abbreviated as $-L^2/r^2$, $\mathbf{L}$ being the total angular momentum operator. Since the Legendre polynomials, $P_l(\cos\theta)$, are eigenfunctions of L^2 with eigenvalues $l(l+1)$ the Schrödinger equation is reducible to the radially dependent equation

$$\left(-\frac{1}{r^2}\frac{d}{dr}\left(r^2\frac{d}{dr}\right) + \frac{l(l+1)}{r^2} + 2V(r)\right)R_l(k,r) = k^2R_l(k,r) \tag{1.18}$$

which may be further reduced, via the substitution $u_l(k,r) = rR_l(k,r)$, to

$$\left(-\frac{d^2}{dr^2} + \frac{l(l+1)}{r^2} + 2V(r)\right)u_l(k,r) = k^2u_l(k,r). \tag{1.19}$$

In order that $R_l(k,r)$ be finite everywhere, it is necessary that $u_l(k,r) \to 0$ as $r \to 0$. Provided that $V(r)$ tends towards zero faster than $1/r$ as $r \to \infty$, asymptotic solutions to the above equation are of the form

$$u_l(k,r) = N_l(k)kr\left[j_l(kr) - \tan\eta_l\, n_l(kr)\right] \tag{1.20}$$

where $j_l(kr)$ and $n_l(kr)$ are the spherical Bessel and Neumann functions, and η_l is the phase shift for the lth partial wave. Using the asymptotic forms of $j_l(kr)$ and $n_l(kr)$

the above expression becomes

$$u_l(k,r) \underset{r\to\infty}{\sim} N_l(k) \left[\sin\left(kr - \frac{l\pi}{2} \right) + \tan\eta_l \cos\left(kr - \frac{l\pi}{2} \right) \right]. \qquad (1.21)$$

In order to derive the Kohn functional, we consider a trial function $\Phi_l^t(k,r)$ which is an approximation to $u_l(k,r)$ and necessarily has the same form of asymptotic boundary conditions i.e.

$$\Phi_l^t(k,0) \quad = \quad 0 \qquad (1.22)$$

$$\Phi_l^t(k,r) \underset{r\to\infty}{\sim} N_l(k) \left[\sin\left(kr - \frac{l\pi}{2} \right) + \tan\eta_l^t \cos\left(kr - \frac{l\pi}{2} \right) \right], \qquad (1.23)$$

where η_l^t is the trial phase shift. If the difference, $\delta\phi$, between Φ_l^t and u_l is such that

$$\Phi_l^t \quad = \quad u_l + \delta\phi \qquad (1.24)$$

then the asymptotic conditions require that

$$\delta\phi(k,0) \quad = \quad 0 \qquad (1.25)$$

$$\delta\phi(k,r) \underset{r\to\infty}{\sim} N_l(k) \left(\tan\eta_l^t - \tan\eta_l \right) \cos\left(kr - \frac{l\pi}{2} \right). \qquad (1.26)$$

By analogy with the derivation of the Rayleigh-Ritz functional, consider now the functional

$$I \quad = \quad < \Phi_l^t \mid H - E \mid \Phi_l^t >, \qquad (1.27)$$

where $H = \frac{1}{2}\left[-d^2/dr^2 + l(l+1)/r^2 \right] + V(r)$ and $E = k^2/2$. Using (1.24) this may alternatively be written

$$I \quad = \quad < u_l + \delta\phi \mid H - E \mid u_l + \delta\phi >$$

$$= \quad < u_l \mid H - E \mid \delta\phi > + < \delta\phi \mid H - E \mid \delta\phi > \qquad (1.28)$$

where we have used $(H - E)u_l = 0$. Integrating by parts, twice, we have

$$\int_0^\infty u_l \frac{d^2}{dr^2} \delta\phi\, dr \quad = \quad \left[u_l \frac{d}{dr}\delta\phi \right]_0^\infty - \int_0^\infty \frac{du_l}{dr}\frac{d}{dr}\delta\phi\, dr$$

$$= \quad \left[u_l \frac{d}{dr}\delta\phi - \frac{du_l}{dr}\delta\phi \right]_0^\infty + \int_0^\infty \delta\phi \frac{d^2 u_l}{dr^2} dr, \qquad (1.29)$$

18

which could also be obtained by use of Green's theorem. Thus

$$< u_l \mid H - E \mid \delta\phi > \ = \ < \delta\phi \mid H - E \mid u_l > -\frac{1}{2} \left[u_l \frac{d}{dr}\delta\phi - \frac{du_l}{dr}\delta\phi \right]_0^\infty . \quad (1.30)$$

The first term on the right hand side is zero, and substituting the asymptotic forms of u_l and $\delta\phi$ into the second we obtain

$$
\begin{aligned}
< u_l \mid H - E \mid \delta\phi > \ = \ & \frac{N_l^2}{2} \left[\sin\left(kr - \frac{l\pi}{2}\right) + \tan\eta_l \cos\left(kr - \frac{l\pi}{2}\right) \right] \\
& \times \left(\tan\eta_l^t - \tan\eta_l \right) k \sin\left(kr - \frac{l\pi}{2}\right) \\
& + \frac{N_l^2}{2} k \left[\cos\left(kr - \frac{l\pi}{2}\right) - \tan\eta_l \sin\left(kr - \frac{l\pi}{2}\right) \right] \\
& \times \left(\tan\eta_l^t - \tan\eta_l \right) \cos\left(kr - \frac{l\pi}{2}\right) \\
= \ & \frac{N_l^2}{2} k \left(\tan\eta_l^t - \tan\eta_l \right) \quad (1.31)
\end{aligned}
$$

whereupon

$$I \ = \ \frac{N_l^2}{2} k \left(\tan\eta_l^t - \tan\eta_l \right) + < \delta\phi \mid H - E \mid \delta\phi > . \quad (1.32)$$

Equating (1.32) with (1.27) gives an expression for the exact phase shift:

$$\frac{N_l^2}{2} k \tan\eta_l \ = \ \frac{N_l^2}{2} k \tan\eta_l^t - < \Phi_l^t \mid H - E \mid \Phi_l^t > + < \delta\phi \mid H - E \mid \delta\phi > . (1.33)$$

This result is known as the Kato identity and is analogous to equation (1.9), used in the derivation of the Rayleigh-Ritz functional. Similarly here, we drop the final term, of second order in $\delta\phi$, to obtain our variational estimate, so

$$N_l^2 k \tan\eta_l^v \ = \ N_l^2 k \tan\eta_l^t - 2 < \Phi_l^t \mid H - E \mid \Phi_l^t > . \quad (1.34)$$

This is a general form for the Kohn functional, where the normalisation of the wavefunction may be chosen according to convenience. The more usual form, and the one most appropriate to the later generalisation to a K-matrix formulation, is obtained by selecting $N_l = 1/\sqrt{k}$, thus

$$\tan\eta_l^v \ = \ \tan\eta_l^t - 2 < \Phi_l^t \mid H - E \mid \Phi_l^t > . \quad (1.35)$$

19

As in the bound-state case, the error in the variational estimate has a second order dependence on the error in the trial function, $\delta\phi$, and thus has the required stationary property. Here, however, no further bound property can be found associated with the functional for $k > 0$, although the Kohn functional can be shown (Spruch and Rosenberg, 1960) to give a rigorous upper bound on the scattering length α, which is defined by

$$\alpha = -\lim_{k\to 0}\frac{\tan\eta}{k}.\tag{1.36}$$

By considering exact and trial wavefunctions with the asymptotic forms

$$u_l(k,r) \underset{r\to\infty}{\sim} N_l(k)\left(\cot\eta_l\sin\left(kr - \frac{l\pi}{2}\right) + \cos\left(kr - \frac{l\pi}{2}\right)\right).\tag{1.37}$$

and

$$\Phi_l^t(k,r) \underset{r\to\infty}{\sim} N_l(k)\left(\cot\eta_l^t\sin\left(kr - \frac{l\pi}{2}\right) + \cos\left(kr - \frac{l\pi}{2}\right)\right),\tag{1.38}$$

which differ from (1.21) and (1.23) only by a phase factor, it is possible, by means of a similar derivation, to obtain the Inverse Kohn functional:

$$\cot\eta_l^v = \cot\eta_l^t + 2 < \Phi_l^t \mid H - E \mid \Phi_l^t >\tag{1.39}$$

which has a similar stationary property. Both functional forms have been used in the present work. There in fact exists a limitless number of forms for the Kohn functional, since the way in which the phaseshift is included in the asymptotic forms is arbitrary, provided the multiplying factors for the Neumann and Bessel functions are in the ratio $\tan\eta_l$. This fact proves useful in avoiding some of the problems presented by the irregular behaviour which is an inevitable feature of the Kohn method, described further in section 1.2.4.

As in the case of a Rayleigh-Ritz bound state calculation, the trial function for a variational scattering calculation is chosen carefully according to physical considerations.

Clearly, at points in space far removed from the scattering centre, the wavefunction must be of the form (1.23), to within an overall phase factor, so this determines the long-range structure. At short ranges, however, there are no strict constraints on the form of the wavefunction, and the usual procedure is to expand in terms of some flexible set of basis functions ϕ_i, which become negligible as $r \to \infty$, so that the overall structure of the wavefunction for a particular partial wave would be

$$\Psi^t = \Phi + \sum_{i=1}^{N} c_i \phi_i, \tag{1.40}$$

where, for the s-wave case ($l = 0$), the long-range component is

$$\Phi = \frac{1}{\sqrt{4\pi}} \left[\frac{\sin kr}{kr} + \tan \eta^t \frac{\cos kr}{kr} f(r) \right], \tag{1.41}$$

which can be conveniently abbreviated as

$$\Phi = S + \tan \eta^t C. \tag{1.42}$$

The function $f(r)$ is a shielding factor which is included to prevent the wavefunction becoming singular at $r = 0$.

From (1.35) the variational phase shift is thus given by

$$\tan \eta^v = \tan \eta^t - \sum_{i,j=1}^{N} c_i c_j M_{ij} - 2 \sum_{i=1}^{N} c_i R_i - (S, LS)$$
$$- \tan \eta^t (S, LC) - \tan \eta^t (C, LS) - \tan^2 \eta^t (C, LC), \tag{1.43}$$

where

$$M_{ij} = M_{ji} = (\phi_i, L\phi_j), \tag{1.44}$$

$$R_i = (\phi_i, L\Phi), \tag{1.45}$$

and $L = 2(H - E)$, the brackets in (1.43), (1.44), and (1.45) signifying integrations over all space. The condition that $\tan \eta^v$ is stationary with respect to variations in the

trial phase shift and the linear parameters c_i then yields the set of linear simultaneous equations

$$
\begin{bmatrix}
(C,LC) & \cdots & (C,L\phi_j) & \cdots \\
\vdots & & \vdots & \\
(\phi_i,LC) & \cdots & (\phi_i,L\phi_j) & \\
\vdots & & \vdots &
\end{bmatrix}
\begin{bmatrix}
\tan\eta^t \\
\vdots \\
c_i \\
\vdots
\end{bmatrix}
= -
\begin{bmatrix}
(C,LS) \\
\vdots \\
(\phi_i,LS) \\
\vdots
\end{bmatrix}.
\qquad (1.46)
$$

By expressing this as

$$
AX = -B \qquad (1.47)
$$

it is clear that the variational parameters are given by

$$
X = -A^{-1}B, \qquad (1.48)
$$

and from here it is a straightforward matter to evaluate the variational phase shift by substituting the linear parameters contained in X back into (1.43). In general, the short-range basis functions will also contain non-linear parameters, which require optimisation for well converged results to be obtained. For the variation of these parameters, the whole calculation requires repeating.

1.2.4 Schwartz Singularities

Problems can arise, however, in the variational scattering calculation, owing to the nature of the eigenstates of the operator L. Since the Hamiltonian has a continuous energy spectrum, in which the total energy E is embedded, it is evident that $L = 2(H - E)$ also has a continuous set of eigenvalues which actually pass through zero. Although the matrix A is, in practice, always of finite rank with only $N+1$ eigenvalues, it is possible for it to possess an eigenvalue very close to zero, making its inverse ill-defined. When this occurs, the variational parameters contained in X also become badly behaved, and the tangent of the variational phase shift, instead of being in error by only a small amount, can actually lie anywhere in the region $-\infty$ to $+\infty$.
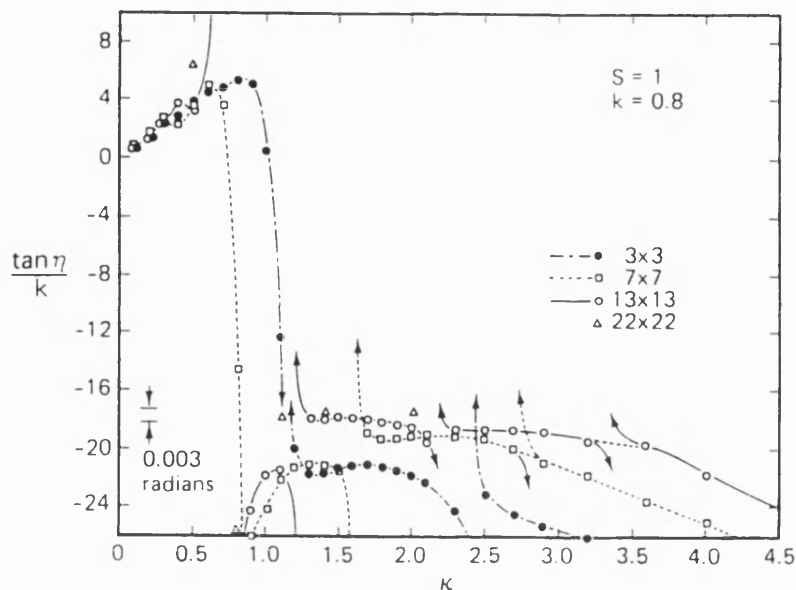
Figure 1.3: Variation of $\tan \eta^v / k$ with respect to κ for s-wave $e^- - H$ elastic scattering, where $k = 0.8$. The different lines correspond to different sizes of basis set. Taken from Schwartz (1961a).

This type of behaviour, which is a very common feature of unbounded Kohn calculations, was first considered by Schwartz (1961a), who observed such irregularities (now referred to as Schwartz singularities) in a variational treatment of electron-hydrogen elastic scattering. In these investigations, he studied the variation of the phase shift with respect to a non-variational scaling parameter, κ, in the wavefunction, in order to map out the occurrences of singularities, and also experimented with varying the total number of linear variational parameters, N. Some of the results of this analysis are shown graphically in figure 1.3.

The important empirical conclusions to be drawn from Schwartz's work are that as N increases, so, in general, do the number of singular points in a given range of the scaling parameter κ, but their region of influence, as a function of κ or as a function of energy, appears to decrease; and also, that as the size of the basis set is increased, the average value of the tangent of the phase shift between singularities tends to flatten

out. This latter observation is very significant, since it means that the singularities become increasingly easier to distinguish as the size of the matrix A grows.

Schwartz singularities are an important feature of this type of variational calculation, and the studies of Schwartz himself generated considerable interest in the subject. Fuller treatments are given by, for example, Nesbet (1968,1969), Brownstein and McKinley (1968), or Harris and Michels (1971). The irregularities are generally avoidable if results are obtained for various different values of some non-variational parameter, and the above considerations born in mind. Armour has successfully used a generalised form of the Kohn functional (see Armour and Humberston, 1991) which introduces a phase parameter τ, such that

$$\tan(\eta^v - \tau) = \tan(\eta^t - \tau) - <\Psi^t|L|\Psi^t> . \tag{1.49}$$

By selecting various different values of τ, and discarding results which lie markedly out of line, the problem of Schwartz singularities is thus reduced considerably. The ordinary forms for the Kohn and Inverse Kohn functionals, (1.35) and (1.39), are reproducible within this formalism by selecting $\tau = 0$ and $\frac{1}{2}\pi$ respectively. For the present studies of positron-hydrogen and positron-lithium scattering, it has been found sufficient to consider only the Kohn and Inverse Kohn methods since, for a large enough basis set, it proves very unlikely that irregular behaviour will be encountered for both methods at the same energy.

1.2.5   The Multi-channel Kohn Method

The single channel formalism discussed above can readily be extended to treat situations where more than one scattering process is possible, by selecting appropriate asymptotic forms for the wavefunction. The stationary property here is associated with the elements of the K-matrix, which is the natural generalisation of the tangent of the phase shift for the multi-channel case.

24

For the purposes of the research presented here, a two channel formulation of the Kohn method is suitable, since at most two scattering processes are considered. The positron-atom collisions which have been investigated result either in elastic scattering, or in positronium (Ps) formation, that is

$$A + e^+ \rightarrow A + e^+ \tag{1.50}$$

$$\rightarrow A^+ + \text{Ps}. \tag{1.51}$$

The total wavefunction for the system, however, is required to represent not only these reactions, but *all* energetically possible scattering processes associated with the system. Thus the additional reactions

$$A^+ + \text{Ps} \rightarrow A^+ + \text{Ps} \tag{1.52}$$

$$\rightarrow A + e^+ \tag{1.53}$$

must also be taken into account.

It is therefore convenient to express the total wavefunction in the two component form

$$\begin{bmatrix} \Psi_1 \\ \Psi_2 \end{bmatrix}$$

where Ψ_1 represents the reactions (1.50) and (1.51), and Ψ_2 describes (1.52) and (1.53). Defining the coordinate ρ to be the separation of the centres of mass of the positive ion, A^+, and the positronium atom, the asymptotic forms of the two components are given by

$$\Psi_1 \underset{r \to \infty}{\sim} Y_{l,0}(\theta, \phi)\sqrt{k}\phi_A \left[j_l(kr) - K_{11}n_l(kr) \right]$$

$$\underset{\rho \to \infty}{\sim} -Y_{l,0}(\theta_\rho, \phi_\rho)\sqrt{2\kappa}\phi_{\text{Ps}}K_{21}n_l(\kappa\rho), \tag{1.54}$$

$$\Psi_2 \underset{\rho \to \infty}{\sim} Y_{l,0}(\theta_\rho, \phi_\rho)\sqrt{2\kappa}\phi_{\text{Ps}} \left[j_l(\kappa\rho) - K_{22}n_l(\kappa\rho) \right]$$

$$\underset{r \to \infty}{\sim} -Y_{l,0}(\theta, \phi)\sqrt{k}\phi_A K_{12}n_l(kr), \tag{1.55}$$

where ϕ_A and ϕ_{Ps} are the wavefunctions for the target and positronium atoms, and κ is the wavenumber of the positronium atom, obtained by a simple consideration of energy conservation: if the binding energies of the target atom and positronium are E_A and E_{Ps} respectively, then we require

$$\frac{k^2}{2} + E_A = \frac{\kappa^2}{4} + E_{\mathrm{Ps}}. \tag{1.56}$$

The K-matrix elements K_{ij} $(i,j = 1,2)$ enable the cross sections for scattering between all combinations of the positron-atom and positronium-ion channels to be calculated. For scattering from channel ν into channel ν', the cross section $\sigma_{\nu\nu'}$ is given by

$$\sigma_{\nu\nu'} = \frac{4(2l+1)}{k_\nu^2} \left| \left(\frac{K}{1 - iK} \right)_{\nu\nu'} \right|^2, \tag{1.57}$$

where, if subscripts 1 and 2 refer to the positron-atom and positronium-ion channels respectively, then $k_1 = k$ and $k_2 = \kappa$. If k and κ are in units of a_0^{-1}, the units of the cross section thus evaluated are πa_0^2.

By taking trial functions with the correct asymptotic forms, but with trial values substituted for the various K-matrix elements, a process of reasoning similar to that used in section 1.2.3 leads to a two channel version of the Kohn functional (Humberston, 1982):

$$\begin{bmatrix} K_{11}^v & K_{12}^v \\ K_{21}^v & K_{22}^v \end{bmatrix} = \begin{bmatrix} K_{11}^t & K_{12}^t \\ K_{21}^t & K_{22}^t \end{bmatrix} - \begin{bmatrix} (\Psi_1^t, L\Psi_1^t) & (\Psi_1^t, L\Psi_2^t) \\ (\Psi_2^t, L\Psi_1^t) & (\Psi_2^t, L\Psi_2^t) \end{bmatrix}. \tag{1.58}$$

All variational K-matrix elements K_{ij} now have the required stationary property with respect to variations in trial functions Ψ_1^t and Ψ_2^t. If the trial functions are again expanded in terms of a flexible set of basis functions, as in the one channel case, the requirement that each of the elements K_{ij}^v is stationary with respect to all linear variational parameters in Ψ_1^t and Ψ_2^t leads to a set of linear simultaneous equations analogous to (1.46). Once these have been solved it is a simple matter to evaluate K^v.

The form of the two channel Kohn functional ensures that the variational K-matrix is symmetric, providing the trial functions possess the correct asymptotic forms, al-

26

though in general the trial K-matrix is not. In solving a two channel Kohn problem using a computer, therefore, any discrepancy between K_{12}^v and K_{21}^v is a consequence of numerical (or programming) errors, which provides a useful check on the accuracy of the calculation. The technicalities of the two channel Kohn method are discussed further in chapter 2, in the context of the positron-hydrogen problem.

Chapter 2

Positron-Hydrogen Scattering

2.1 Introduction

Because the lithium atom in the present work is represented as a hydrogenic model, the positron-lithium problem has been formulated in a very similar way to the previous work on positron-hydrogen scattering, the main differences being the use, in the case of Li, of a more complicated target wavefunction and interaction potential. In view of this similarity, and also of the greater simplicity of the e^+-H system, it seems appropriate first to discuss the Kohn method applied to the positron-hydrogen problem in some detail, making reference to the e^+-Li system where appropriate, before introducing the modifications required for the latter, more complicated, problem in chapter 5.

The Kohn variational method was first applied to the positron-hydrogen problem by Schwartz (1961b), using quite a flexible trial function to calculate s-wave scattering phaseshifts at energies below the Ps formation threshold. With rather more sophisticated computational resources available, Humberston and Wallace (1972) were able to improve on these investigations using more elaborate trial functions. The results of these later studies compared very favourably with those obtained by Bhatia *et al.* (1971), which are believed to be the most accurate available in this energy region, and demonstrated the suitability of the Kohn method for this type of problem.

The theory was successfully modified for the positron-helium problem (Humberston

1973, 1979, Campeanu 1977) and, later, further extended to enable the determination of both elastic scattering and Ps formation cross sections for energies up to the first excitation threshold of the hydrogen atom (Humberston 1982, 1986, Brown and Humberston 1984, 1985). The energy region between the Ps formation and first excitation thresholds, where elastic scattering and Ps formation are the only possible scattering processes, is known as the Öre gap which, for hydrogen, extends from 6.8 to 10.2eV. The present work on positron-lithium scattering has been developed from this later positron-hydrogen theory; the existence of the Ps formation channel at all energies of the incident positron makes its inclusion necessary for any complete theoretical treatment of positron-alkali atom collisions.

The following section describes the two-channel Kohn method as applied to e^+-H scattering, and introduces some typical features of such a calculation. In chapter 3, some results are presented of new investigations of the e^+-H system, undertaken in the light of recent interest in threshold phenomena.

2.2 Positron-Hydrogen s-wave Scattering

2.2.1 Trial Functions

The two-channel Kohn functional, as discussed in chapter 1, takes the form:-

$$\begin{bmatrix} K_{11}^v & K_{12}^v \\ K_{21}^v & K_{22}^v \end{bmatrix} = \begin{bmatrix} K_{11}^t & K_{12}^t \\ K_{21}^t & K_{22}^t \end{bmatrix} - \begin{bmatrix} (\Psi_1, L\Psi_1) & (\Psi_1, L\Psi_2) \\ (\Psi_2, L\Psi_1) & (\Psi_2, L\Psi_2) \end{bmatrix} \qquad (2.1)$$

where the trial functions, Ψ_1 and Ψ_2, between them represent all possible scattering processes associated with the three-body system: Ψ_1 represents positron-hydrogen scattering, resulting either in elastic collisions or in Ps formation; Ψ_2 represents positronium-proton collisions, resulting in elastic scattering or in the formation of atomic hydrogen. The only strict constraints to be imposed on the trial functions are that they possess the correct asymptotic form, and remain finite at the origin of coordinates.
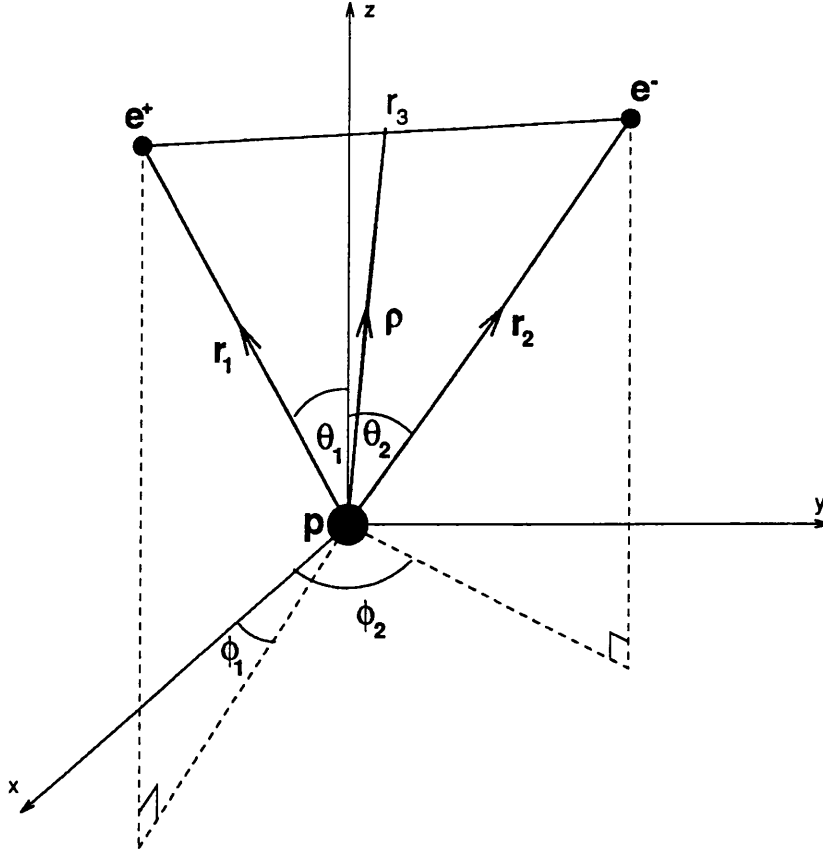
Figure 2.1: The positron-hydrogen system

For s-wave ($l = 0$) positron-hydrogen scattering the trial functions devised were as follows:-

$$\Psi_1 = Y_{00}(\theta_1, \phi_1)\Phi_H(r_2)\sqrt{k}\left\{j_0(kr_1) - K_{11}^t n_0(kr_1)\left[1 - \exp(-\lambda r_1)\right]\right\}$$

$$-Y_{00}(\theta_\rho, \phi_\rho)\Phi_{Ps}(r_3)\sqrt{2\kappa}K_{21}^t\left[n_0(\kappa\rho) + \exp(-\mu\rho)(1 + a\rho + b\rho^2)/\kappa\rho\right]$$

$$+Y_{00}(\theta_1, \phi_1)\Phi_H(r_2)\exp\left(-(\alpha r_1 + \beta r_2 + \gamma r_3)\right)\sum_{i=1}^{N} c_i r_1^{k_i} r_2^{l_i} r_3^{m_i} \tag{2.2}$$

$$\Psi_2 = Y_{00}(\theta_\rho, \phi_\rho)\Phi_{Ps}(r_3)\sqrt{2\kappa}\left\{j_0(\kappa\rho) - K_{22}^t\left[n_0(\kappa\rho) + \exp(-\mu\rho)(1 + a\rho + b\rho^2)/\kappa\rho\right]\right\}$$

$$-Y_{00}(\theta_1, \phi_1)\Phi_H(r_2)\sqrt{k}K_{12}^t n_0(kr_1)\left[1 - \exp(-\lambda r_1)\right]$$

$$+Y_{00}(\theta_1, \phi_1)\Phi_H(r_2)\exp\left(-(\alpha r_1 + \beta r_2 + \gamma r_3)\right)\sum_{j=1}^{N} d_j r_1^{k_j} r_2^{l_j} r_3^{m_j}, \tag{2.3}$$

where k and κ are the positron and positronium wavenumbers respectively. The coordinate nomenclature is illustrated in figure 2.1. The $l = 0$ spherical harmonic is simply

given by

$$Y_{00}(\theta, \phi) = \frac{1}{\sqrt{4\pi}}, \tag{2.4}$$

and the zero order spherical Bessel and Neumann functions have the damped sinusoidal forms

$$j_0(kr) = \frac{\sin kr}{kr} \tag{2.5}$$

$$n_0(kr) = -\frac{\cos kr}{kr}. \tag{2.6}$$

Abbreviating the long-range components as

$$S_1 = Y_{00}(\theta_1, \phi_1)\Phi_{\mathrm{H}}(r_2)\sqrt{k}j_0(kr_1) \tag{2.7}$$

$$C_1 = -Y_{00}(\theta_1, \phi_1)\Phi_{\mathrm{H}}(r_2)\sqrt{k}n_0(kr_1)\left[1 - \exp(-\lambda r_1)\right] \tag{2.8}$$

$$S_2 = Y_{00}(\theta_\rho, \phi_\rho)\Phi_{\mathrm{Ps}}(r_3)\sqrt{2\kappa}j_0(\kappa\rho) \tag{2.9}$$

$$C_2 = -Y_{00}(\theta_\rho, \phi_\rho)\Phi_{\mathrm{Ps}}(r_3)\sqrt{2\kappa}\left[n_0(\kappa\rho) + \exp(-\mu\rho)(1 + a\rho + b\rho^2)/\kappa\rho\right], \tag{2.10}$$

and each short-range correlation term as

$$\phi_i = Y_{00}(\theta_1, \phi_1)\Phi_{\mathrm{H}}(r_2)r_1^{k_i}r_2^{l_i}r_3^{m_i}\exp(-(\alpha r_1 + \beta r_2 + \gamma r_3)), \tag{2.11}$$

leads to a more manageable form of notation for the trial functions:

$$\Psi_1 = S_1 + K_{11}^t C_1 + K_{21}^t C_2 + \sum_{i=1}^{N} c_i\phi_i \tag{2.12}$$

$$\Psi_2 = S_2 + K_{22}^t C_2 + K_{12}^t C_1 + \sum_{j=1}^{N} d_j\phi_j. \tag{2.13}$$

The forms of the S and C terms ensure that the structure of the wavefunction is correct asymptotically, and the exponential factors contained in C_1 and C_2 shield the singularity in the Neumann functions at the origin. The forms for the shielding factors are determined by the requirements that the overall wavefunction behaves like r_1^l as $r_1 \rightarrow 0$, and like ρ^l as $\rho \rightarrow 0$. The differences between the C_1 and C_2 shielding terms

31

are due to that fact that, as $\rho \to 0$ there is no particle at the origin of coordinates, and thus the potential remains finite. This condition means that the second derivative of C_2 must also remain finite as $\rho \to 0$, a constraint which does not exist for C_1 as $r_1 \to 0$ (see Brown, 1986).

The Hylleraas functions ϕ_i constitute the short-range components of the wavefunction, and represent the complicated distortions arising from the various polarization and correlation effects which occur when the three particles are in close proximity. The representation is improved accordingly as the number of such terms in the summation, N, is increased. The exponential factor which multiplies the polynomial expansion causes the short-range functions to vanish in the limit as r_1, r_2 or r_3 tends towards infinity. The non-linear parameters α, β and γ determine how fast these functions are killed off, and are chosen so as to provide the best possible convergence of the scattering calculation.

The linear variational parameters are the trial K-matrix elements and the coefficients $c_i(i = 1, ..., N)$ and $d_j(j = 1, ..., N)$, and the requirement that the elements of the variational K-matrix are each stationary with respect to variations in all these parameters leads to the set of linear simultaneous equations

$$
\begin{bmatrix}
(C_1, LC_1) & (C_1, LC_2) & \cdots & (C_1, L\phi_j) & \cdots \\
(C_2, LC_1) & (C_2, LC_2) & \cdots & (C_2, L\phi_j) & \cdots \\
\vdots & \vdots & & \vdots & \\
(\phi_i, LC_1) & (\phi_i, LC_2) & \cdots & (\phi_i, L\phi_j) & \cdots \\
\vdots & \vdots & & \vdots &
\end{bmatrix}
\begin{bmatrix}
K_{11}^t & K_{12}^t \\
K_{21}^t & K_{22}^t \\
\vdots & \vdots \\
c_i & d_i \\
\vdots & \vdots
\end{bmatrix}
= -
\begin{bmatrix}
(C_1, LS_1) & (C_1, LS_2) \\
(C_2, LS_1) & (C_2, LS_2) \\
\vdots & \vdots \\
(\phi_i, LS_1) & (\phi_i, LS_2) \\
\vdots & \vdots
\end{bmatrix}
\tag{2.14}
$$

Expressing this in the form

$$
AX \; = \; -B, \tag{2.15}
$$

it is thus possible to obtain the variational parameters contained in X by formally inverting the matrix A and performing a matrix multiplication with B. The variationally

determined K-matrix elements are then given (Armour and Humberston, 1991) by

$$K^v = -\begin{bmatrix} I & X^T \end{bmatrix} \begin{bmatrix} (S, LS) & B^T \\ B & A \end{bmatrix} \begin{bmatrix} I \\ X \end{bmatrix}, \tag{2.16}$$

where

$$(S, LS) = \begin{bmatrix} (S_1, LS_1) & (S_1, LS_2) \\ (S_2, LS_1) & (S_2, LS_2) \end{bmatrix}. \tag{2.17}$$

Arguments obtained by using Green's theorem show that the matrices (S, LS) and A are both symmetric (see Appendix B); this substantially reduces the number of matrix elements which require explicit evaluation and, in turn, ensures that the matrix K^v is symmetric, although the trial K-matrix, K^t, in general is not.

2.2.2 Determination of the Matrix Elements

The main computational effort required in calculating the variational K-matrix lies in the determination of the individual elements of the matrices A and B; the actual matrix operations are comparatively trivial. The elements to be computed fall neatly into three categories: long-range–long-range, long-range–short-range, and short-range–short-range. Before they can be integrated, it is first necessary to operate on both the short- and long-range terms with L. The fact that each term is expressed as a product including either the hydrogen or positronium wavefunction simplifies this. Consider, for example, the form of LS_1. We have

$$
\begin{aligned}
LS_1 &= 2(H - E)S_1 \\
&= \left[-\nabla_1^2 - \nabla_2^2 + 2\left(\frac{1}{r_1} - \frac{1}{r_2} - \frac{1}{r_3}\right) - 2E_0 - k^2 \right] Y_{00}\Phi_H(r_2)\sqrt{k}\frac{\sin kr_1}{kr_1}, \tag{2.18}
\end{aligned}
$$

where E_0 is the ground state energy of the hydrogen atom. Since S_1 is separable into functions of r_1 and r_2 only, the relationship

$$\nabla^2(fg) = f\nabla^2 g + 2\nabla f \cdot \nabla g + g\nabla^2 f \tag{2.19}$$

33

enables (2.18) to be reduced to

$$LS_1 = \Phi_H(r_2)\sqrt{k}\left(-\nabla_1^2 + 2\left(\frac{1}{r_1} - \frac{1}{r_3}\right) - k^2\right)Y_{00}\frac{\sin kr_1}{kr_1}$$
$$+ Y_{00}\sqrt{k}\frac{\sin kr_1}{kr_1}\left(-\nabla_2^2 - \frac{2}{r_2} - 2E_0\right)\Phi_H(r_2), \tag{2.20}$$

where the dot product term of (2.19) vanishes for both ∇_1^2 and ∇_2^2. But the last term of (2.20) is evidently zero, since Φ_H is an eigenfunction of $-\frac{1}{2}\nabla_2^2 - r_2^{-1}$ corresponding to the eigenvalue E_0. Thus, the fact that S_1 is expressed in terms of a product involving the hydrogen wavefunction enables us to express LS_1 in a form which ignores the nature of the hydrogenic Hamiltonian and its eigenvalues. Hence, we have

$$LS_1 = \Phi_H\sqrt{k}\left(-\nabla_1^2 + 2\left(\frac{1}{r_1} - \frac{1}{r_3}\right) - k^2\right)Y_{00}\frac{\sin kr_1}{kr_1}. \tag{2.21}$$

Since there is no angular dependence in Y_{00}, the derivatives with respect to the angular variables in ∇_1^2 vanish, and we find that

$$-\nabla_1^2\frac{\sin kr_1}{kr_1} = k^2\frac{\sin kr_1}{kr_1}, \tag{2.22}$$

and thus (2.21) reduces to simply

$$LS_1 = \Phi_H\sqrt{k}\left(\frac{2}{r_1} - \frac{2}{r_3}\right)Y_{00}\frac{\sin kr_1}{kr_1} \tag{2.23}$$

The form for LC_1 can be simplified in a similar way, but here the presence of the shielding factor makes the operation of ∇_1^2 rather more complicated. We find that

$$LC_1 = Y_{00}\Phi_H(r_2)\sqrt{k}\frac{1}{kr_1}\left[e^{-\lambda r_1}\left(2k\lambda\sin kr_1 + \lambda^2\cos kr_1\right)\right.$$
$$\left. + \left(\frac{2}{r_1} - \frac{2}{r_3}\right)\cos kr_1\left(1 - e^{-\lambda r_1}\right)\right]. \tag{2.24}$$

When considering the operation of L on S_2 and C_2, it is convenient to use the alternative form for the Hamiltonian,

$$H = -\nabla_3^2 - \frac{1}{2}\nabla_\rho^2 + \frac{1}{r_1} - \frac{1}{r_2} - \frac{1}{r_3} \tag{2.25}$$

34

and to specify the total energy, E, in terms of the positronium binding energy, E_{Ps}, and wavenumber, κ. Consideration of conservation of energy shows that these are related to E_0 and k by

$$\frac{k^2}{2} + E_0 = \frac{\kappa^2}{4} + E_{Ps}.$$ (2.26)

For example, for LS_2 we have

$$LS_2 = \left[-2\nabla_3^2 - \frac{1}{2}\nabla_\rho^2 + 2\left(\frac{1}{r_1} - \frac{1}{r_2} - \frac{1}{r_3}\right) - 2E_{Ps} - \frac{\kappa^2}{2} \right]$$

$$\times Y_{00}\phi_{Ps}(r_3)\sqrt{2\kappa}\frac{\sin\kappa\rho}{\kappa\rho},$$ (2.27)

which, by a process of vector algebra similar to that used above, leads to

$$LS_2 = \Phi_{Ps}(r_3)\sqrt{2\kappa}\left(-\frac{1}{2}\nabla_\rho^2 + 2\left(\frac{1}{r_1} - \frac{1}{r_2}\right) - \frac{\kappa^2}{2}\right)Y_{00}\frac{\sin\kappa\rho}{\kappa\rho}$$

$$+Y_{00}\frac{\sin\kappa\rho}{\kappa\rho}\sqrt{2\kappa}\left(-2\nabla_3^2 - \frac{2}{r_3} - 2E_{Ps}\right)\Phi_{Ps}(r_3).$$ (2.28)

Since $-\nabla_3^2 - r_3^{-1}$ is just the Hamiltonian operator for the positronium atom, and E_{Ps} is the eigenvalue corresponding to Φ_{Ps}, the last term again vanishes. Also, S_2 is easily shown to be an eigenfunction of $-\nabla_\rho^2$, with eigenvalue κ^2, so we are left with

$$LS_2 = \Phi_{Ps}(r_2)\sqrt{2\kappa}\left(\frac{2}{r_1} - \frac{2}{r_2}\right)Y_{00}\frac{\sin\kappa\rho}{\kappa\rho}.$$ (2.29)

The form for LC_2 is again complicated by the presence of the shielding factor, but derivable by means of a similar procedure to give

$$LC_2 = Y_{00}\phi_{Ps}(r_3)\sqrt{2\kappa}\frac{1}{\kappa\rho}\left\{ \frac{e^{-\lambda\rho}}{2}\left[\rho(\lambda^2 a - 4\lambda b + a\kappa^2) + \rho^2(\lambda^2 b + \kappa^2 b)\right] \right.$$ (2.30)

$$\left. +2\left(\frac{1}{r_1} - \frac{1}{r_2}\right)\left[\cos\kappa\rho - e^{-\lambda\rho}(1 + a\rho + b\rho^2)\right]\right\}.$$ (2.31)

Making use of the symmetry properties of the integrals discussed in Appendix B, we now have all the information required to form the integrands for the long-range–long-range and short-range–long-range matrix elements. In order to compute the short-range–short-range elements, we consider the action of L on ϕ_i. Writing

$$\phi_i = \phi_H(r_2)\chi_i(r_1, r_2, r_3, \theta_1, \phi_1),$$ (2.32)

where

$$\chi_i(r_1, r_2, r_3, \theta_1, \phi_1) = Y_{00}(\theta_1, \phi_1) r_1^{k_i} r_2^{l_i} r_3^{m_i} \exp\left[-(\alpha r_1 + \beta r_2 + \gamma r_3)\right], \quad (2.33)$$

we have

$$L\phi_i = \left[-\nabla_1^2 - \nabla_2^2 + 2\left(\frac{1}{r_1} - \frac{1}{r_2} - \frac{1}{r_3}\right) - k^2 - 2E_0\right]\phi_H \chi_i. \quad (2.34)$$

Then, using (2.19), we get

$$\begin{aligned}
L\phi_i &= -\phi_H \nabla_1^2 \chi_i - \phi_H \nabla_2^2 \chi_i - \chi_i \nabla_2^2 \phi_H - 2(\nabla_2 \phi_H \cdot \nabla_2 \chi_i) \\
&\quad + \left(\frac{2}{r_1} - \frac{2}{r_2} - \frac{2}{r_3} - k^2 - 2E_0\right)\phi_H \chi_i \\
&= -\phi_H(r_2)(\nabla_1^2 + \nabla_2^2)\chi_i - 2\nabla_2 \phi_H \cdot \nabla_2 \chi_i + \left(\frac{2}{r_1} - \frac{2}{r_2} - k^2\right)\phi_H \chi_i, \quad (2.35)
\end{aligned}$$

having again used the fact that $(-\nabla_2^2 - r_2^{-1} - 2E_0)\phi_H(r_2) = 0$. The form for a short-range–short-range integral is thus

$$\begin{aligned}
(\phi_i, L\phi_j) &= \int \chi_i \phi_H \left\{\left[-(\nabla_1^2 + \nabla_2^2)\chi_i\right]\phi_H - 2\nabla_2 \phi_H \cdot \nabla_2 \chi_i \right. \quad (2.36) \\
&\quad \left. + \left(\frac{2}{r_1} - \frac{2}{r_2} - k^2\right)\chi_i \phi_H\right\} d\tau.
\end{aligned}$$

In order to obtain a more convenient expression, we consider alone the term involving in the Laplacian operators ∇_1^2 and ∇_2^2, and integrate by parts, thus

$$\begin{aligned}
\int \chi_i \phi_H \left[-(\nabla_1^2 + \nabla_2^2)\chi_j\right]\phi_H d\tau &= \int \left[\nabla_1(\chi_i \phi_H^2) \cdot \nabla_1 \chi_j + \nabla_2(\chi_i \phi_H^2) \cdot \nabla_2 \chi_j\right] d\tau \\
&= \int \left[\phi_H^2(\nabla_1 \chi_i \cdot \nabla_1 \chi_j + \nabla_2 \chi_i \cdot \nabla_2 \chi_j) \right. \quad (2.37) \\
&\quad \left. + 2\phi_H \chi_i(\nabla_1 \phi_H \cdot \nabla_1 \chi_j + \nabla_2 \phi_H \cdot \nabla_2 \chi_j)\right] d\tau
\end{aligned}$$

Substituting this form back into (2.36), and using the fact that $\nabla_1 \phi_H = 0$, we find that

$$(\phi_i, L\phi_j) = \int \phi_H^2 \left[(\nabla_1 \chi_i \cdot \nabla_1 \chi_j + \nabla_2 \chi_i \cdot \nabla_2 \chi_j) + \left(\frac{2}{r_1} - \frac{2}{r_2} - k^2\right)\chi_i \chi_j\right] d\tau. (2.38)$$

In this form, it is immediately obvious that interchanging i and j has no effect on the value of the integral, and thus the short-range–short-range matrix elements are evidently symmetric in these two variables.

36
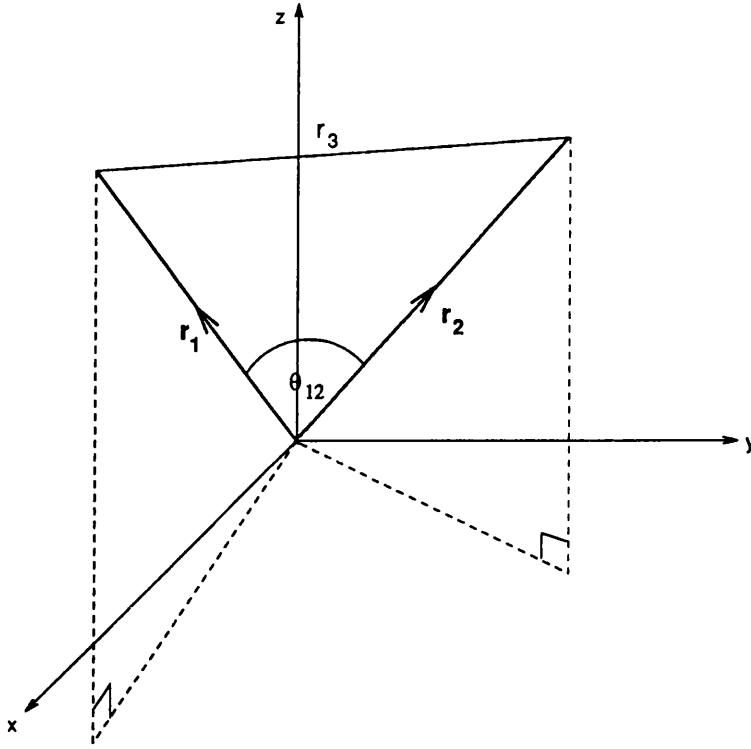
Figure 2.2: The internal variables of the positron-hydrogen system.

2.2.3 Angular Integration

Since the spherical harmonics, Y_{00}, have no azimuthal or polar dependence on the external angles which specify the orientation of the system, the angular integrations are very simple for s-wave scattering. The general form for an s-wave integral is

$$I = \int \int f(r_1, r_2, r_3) d\tau_1 d\tau_2, \tag{2.39}$$

where the integration is performed over all space for both the positron and electron. If spherical polar coordinates are used with the original set of axes for both integrations, the situation is complicated by the dependence of the integrand on the positron-electron separation, r_3. Taking the $\mathbf{r_1}$ vector as the z-axis for the $\mathbf{r_2}$ integration (or vice versa) simplifies things, however, since r_3 has no azimuthal dependence in this coordinate system (see figure 2.2). Performing this azimuthal integration to give 2π, and using the

37

original axes for the r_1 integration, the form of the integral becomes

$$I = 2\pi \int_0^\infty r_1^2 dr_1 \int_0^\pi \sin\theta_1 d\theta_1 \int_0^{2\pi} d\phi_1 \int_0^\infty r_2^2 dr_2 \int_0^\pi \sin\theta_{12} d\theta_{12} f(r_1, r_2, r_3), \quad (2.40)$$

where θ_{12} is the angle between the r_1 and r_2 vectors. The angular dependence for the r_1 integration is also trivial, yielding a further factor of 4π, whereupon the integral becomes

$$I = 8\pi^2 \int_0^\infty r_1^2 dr_1 \int_0^\infty r_2^2 dr_2 \int_0^\pi \sin\theta_{12} d\theta_{12} f(r_1, r_2, r_3), \quad (2.41)$$

and the remaining integration is over only the internal coordinates of the system. Since the integrand is expressed as a function of the three interparticle distances, it is appropriate to change variables so as to integrate over r_3 rather than θ_{12}. From the cosine rule we find that

$$r_3 dr_3 = r_1 r_2 \sin\theta_{12} d\theta_{12} \quad (2.42)$$

and hence

$$I = 8\pi^2 \int_0^\infty r_1 dr_1 \int_0^\infty r_2 dr_2 \int_{|r_1-r_2|}^{r_1+r_2} r_3 dr_3 f(r_1, r_2, r_3). \quad (2.43)$$

2.2.4   Numerical Integration

Because of the simplicity of the hydrogen $1s$ wavefunction and the zero-order spherical Bessel and Neumann functions, it is often convenient to evaluate the s-wave long-range–long-range elements analytically. For the remaining two categories it is much easier to use numerical integration techniques, such as Gauss-Laguerre quadrature. Here, the integral is reduced to a sum of weighted values of the integrand, evaluated at certain values of the integrating variable, such that

$$\int_0^\infty f(r) e^{-r} dr = \sum_{i=1}^n w_i f(r_i) \quad (2.44)$$

38

or, more generally,

$$\int_0^\infty f(r)e^{-\alpha r}dr = \frac{1}{\alpha}\sum_{i=1}^n w_i f\left(\frac{r_i}{\alpha}\right), \qquad (2.45)$$

where the weights, w_i, and abscissae, r_i, can be calculated, or obtained from library subroutines or books of tables. This procedure gives an exact result for the integration providing the function $f(r)$ is a polynomial of degree no higher than $2n - 1$, and can easily be generalised further to use for the multiple integrations required here.

Because the limits of the r_3 integration in (2.43) are dependent on the other two integrating variables, Gauss-Laguerre quadrature is not appropriate to this integral in its existing form. Instead, it is convenient to make a transformation of the variables r_1, r_2 and r_3 into a set of coordinates where the limits on the integrating variables are all independent of each other. The perimetric coordinates x, y and z are defined such that

$$x = r_1 + r_2 - r_3 \qquad (2.46)$$

$$y = r_2 + r_3 - r_1 \qquad (2.47)$$

$$z = r_3 + r_1 - r_2 \qquad (2.48)$$

and thus

$$r_1 = \tfrac{1}{2}(x+z) \qquad (2.49)$$

$$r_2 = \tfrac{1}{2}(y+x) \qquad (2.50)$$

$$r_3 = \tfrac{1}{2}(z+y). \qquad (2.51)$$

The Jacobian for the transformation is equal to $\tfrac{1}{4}$, so the integral (2.43) can be rewritten

$$I = \frac{8\pi^2}{4}\int_{x=0}^\infty \int_{y=0}^\infty \int_{z=0}^\infty f(r_1,r_2,r_3)r_1 r_2 r_3 dx dy dz, \qquad (2.52)$$

which is now in a form for which three-dimensional Gauss-Laguerre quadrature is appropriate.

39

Aside from the exponential factor, the short-range–short-range elements are purely polynomial in form, and can thus be evaluated exactly; the other types, being partly sinusoidal, cannot, but it is still possible to obtain a very accurate estimate of the exact value of the integral if a large enough number of weights and abscissae is used. Providing that this is the case, the limits on the accuracy of the final variational K-matrix elements are determined chiefly by the number of short-range linear parameters, N, and the suitability of the non-linear parameters α, β and γ.

The number of matrix elements to be computed increases as approximately $N(N + 1)$, so it is worthwhile to spend some time on optimising the non-linear parameters α, β and γ for a small N. The procedure for doing this is a matter of trial and error, to a large extent, it being very difficult to predict, especially where positronium formation is involved, what the exponential fall-off in each of the inter-particle coordinates is likely to be. In the case of s-wave positron-lithium scattering, an attempt was made, with some success, to devise a systematic method of optimisation and this is described more fully in chapter 5. For the new investigations of positron-hydrogen scattering, the values of α, β and γ have been set to those used for the earlier work.

2.2.5 Convergence Tests

In the case of positron-hydrogen scattering, where the formulation contains a complete description of the three-body system, there is no theoretical limit to the accuracy of the variational K-matrix, and it is possible to increase the number of linear parameters, obtaining continually better estimates, until the point where numerical precision leads to a breakdown in the calculation. In practice, however, considerations of time and expense involved in computation are also limiting factors, and therefore it is important to be able to determine how well converged the variational K-matrix is, in order to know whether it is worth increasing N further.

A systematic way of improving the trial functions Ψ_1 and Ψ_2 is arrived at by defining

a parameter ω, which is a non-negative integer, and then including all Hylleraas terms in the short-range expansions of (2.2) and (2.3) which satisfy the condition

$$k_i + l_i + m_i \leq \omega, \tag{2.53}$$

k_i, l_i and m_i also being non-negative integers. In this way, the highest power of any of the three inter-particle coordinates is equal to ω, and there is a relationship between ω and N,

$$N = 1 + \frac{11}{6}\omega + \omega^2 + \frac{1}{6}\omega^3 \tag{2.54}$$

such that $\omega = 0, 1, 2, 3, 4, 5, 6, \ldots$ corresponds to $N = 1, 4, 10, 20, 35, 56, 84, \ldots$.

In regions of the non-linear parameter space in which the diagonal elements of the variational K-matrix exhibit stability, they tend to converge upwards with respect to increasing ω, in accordance with the empirical lower bound principle. Even where Schwartz singularities intrude, it is usually still possible to see a convergence trend when Kohn and Inverse Kohn results are considered together, because in practice the Schwartz singularities only affect one or other of the results, but not both.

A useful procedure for assessing the level of convergence in this type of calculation is to plot K_{11}^v and K_{22}^v as a function of ω^{-n}, where n is chosen (positive) by a process of trial and error, such that the elements lie as close as possible to a straight line—the better the convergence, the higher the value of n required to provide such a fit. An estimate of their fully converged values, corresponding to $\omega = \infty$, can then be obtained by extrapolating back to the intercept of the straight line with the y-axis. This may be expressed mathematically as

$$K_{ii}(\omega) = K_{ii}(\infty) + \frac{c}{\omega^n}. \tag{2.55}$$

It is not really possible to evaluate fully converged cross sections using this method, since they depend on all of the K-matrix elements, including the off-diagonals for which no empirical bound principle exists. The value of the method is therefore in determining

41
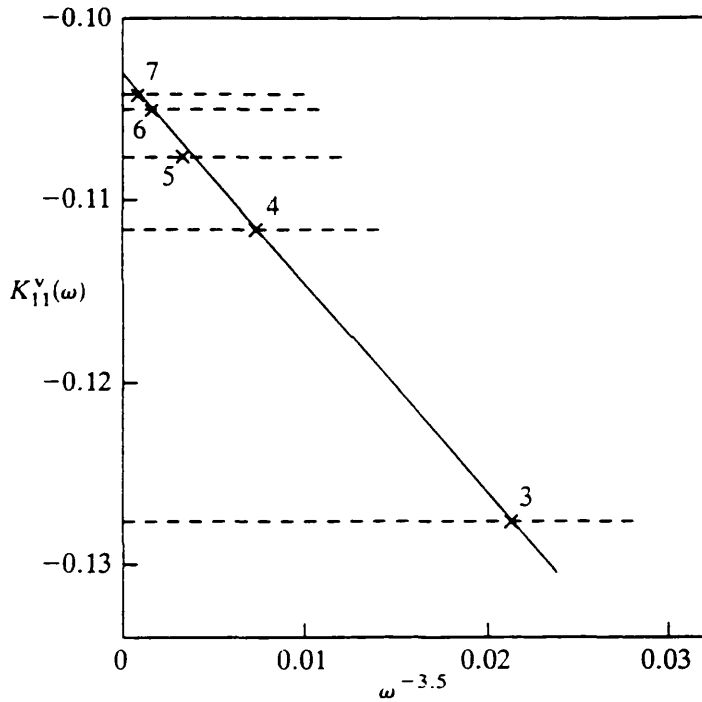
Figure 2.3: K_{11}^v plotted as a function of $\omega^{-3.5}$ at $k = 0.8$ for s-wave positron-hydrogen scattering. The numbers adjacent to the crosses are the values of ω. The fully converged value of K_{11}, obtained by extrapolating back to the y-axis, is estimated here at -0.103 ± 0.001.

the error margins within which the results lie, rather than in attempting to predict an exact result. An example of a typical convergence characteristic for s-wave positron-hydrogen scattering is illustrated in figure 2.3.

2.3 Extension to Higher Partial Waves

In the two channel case, where only elastic scattering and positronium formation are considered, the collision energy is not sufficient to result in an overall change in the orbital angular momentum of the target atom. Conservation of angular momentum therefore means that the incident and outgoing positron or positronium atom must have the same value of the orbital angular momentum quantum number, l. When considering higher partial waves, therefore, the asymptotic components of the scattering wavefunction are simply the appropriate higher order spherical Bessel and Neumann

functions.

At short-ranges, however, the extra total angular momentum is distributed between the positron and electron in a way which requires accounting for in the form of the Hylleraas expansion. In principal, there exists an infinite number of ways in which the individual angular momenta of the two particles, l_1 and l_2, can be combined to yield a given total angular momentum, l, but Schwartz (1961c) has shown that the summation over all possible couplings is actually greatly reducible, so that an eigenstate of the total orbital angular momentum may be expanded as

$$\Psi(\mathbf{r_1}, \mathbf{r_2}, l, m) = \sum_{l_1, l_2} \psi(l_1, l_2, l, m) F_{l_1 l_2}(r_1, r_2, r_3), \qquad (2.56)$$

where the summation only involves values of l_1 and l_2 such that

$$l_1 + l_2 = l. \qquad (2.57)$$

In general, $l + 1$ terms are required in the summation, so that $l + 1$ different symmetries of short-range term are needed in the Hylleraas expansion. For example, in considering p-wave scattering ($l = 1$), two types of short-range correlation term are required, corresponding to ($l_1 = 1, l_2 = 0$) and ($l_1 = 0, l_2 = 1$); in order that the correct boundary conditions are satisfied at the origin, it is also necessary that the wavefunction goes as $r_1^{l_1}$ and $r_2^{l_2}$ as $r_1, r_2 \rightarrow 0$. The function ψ is given by

$$\psi(l_1, l_2, l, m) = \sum_{m_1, m_2} Y_{l_1 m_1}(\theta_1, \phi_1) Y_{l_2 m_2}(\theta_2, \phi_2) < l_1 m_1 l_2 m_2 | l m >, \qquad (2.58)$$

where the summation is over all m_1, m_2 subject to the conditions

$$m_1 + m_2 = m \qquad (2.59)$$

and

$$-l_i \leq m_i \leq l_i. \qquad (2.60)$$

The terms $< l_1 m_1 l_2 m_2 | l m >$ are Clebsch-Gordan coefficients, the forms for which can easily be found in textbooks on angular momentum. It is a straightforward matter to

43

show that, for p-wave scattering with the z component of the total angular momentum set to zero, ψ reduces to one term for each of the l symmetries, since m_1 and m_2 can only take on the value zero. The Clebsch-Gordan coefficients are thus conveniently absorbed into the overall normalisation of the Hylleraas expansion,and need not be explicitly evaluated.

A suitable form for a two component trial function for positron-hydrogen p-wave scattering, and the one actually used, is thus

$$
\begin{aligned}
\Psi_1 \;=\; & \Phi_{\mathrm{H}}(r_2) Y_{10}(\theta_1, \phi_1)\sqrt{k}\left\{ j_1(kr_1) - K_{11}^t n_1(kr_1)\left[1 - \exp(-\lambda r_1)\right]^3 \right\} \\
& -\Phi_{\mathrm{Ps}}(r_3) Y_{10}(\theta_\rho, \phi_\rho)\sqrt{2\kappa}\, K_{21}^t n_1(\kappa\rho)\left[1 - \exp(-\mu\rho)\right]^6 \\
& +\Phi_{\mathrm{H}}(r_2)\exp\left[-(\alpha r_1 + \beta r_2 + \gamma r_3)\right]\left(Y_{10}(\theta_1, \phi_1) r_1 \sum_{i=1}^{N_1} a_i r_1^{k_i} r_2^{l_i} r_3^{m_i} \right. \\
& \left. +Y_{10}(\theta_2, \phi_2) r_2 \sum_{j=1}^{N_2} b_j r_1^{k_j} r_2^{l_j} r_3^{m_j} \right),
\end{aligned}
\tag{2.61}
$$

$$
\begin{aligned}
\Psi_2 \;=\; & \Phi_{\mathrm{Ps}}(r_3) Y_{10}(\theta_\rho, \phi_\rho)\sqrt{2\kappa}\left\{ j_1(\kappa\rho) - K_{22}^t n_1(\kappa\rho)\left[1 - \exp(-\mu\rho)\right]^6 \right\} \\
& -\Phi_{\mathrm{H}}(r_2) Y_{10}(\theta_1, \phi_1)\sqrt{k}\, K_{12}^t n_1(kr_1)\left[1 - \exp(-\lambda r_1)\right]^3 \\
& +\Phi_{\mathrm{H}}(r_2)\exp\left[-(\alpha r_1 + \beta r_2 + \gamma r_3)\right]\left(Y_{10}(\theta_1, \phi_1) r_1 \sum_{i=1}^{N_1} c_i r_1^{k_i} r_2^{l_i} r_3^{m_i} \right. \\
& \left. +Y_{10}(\theta_2, \phi_2) r_2 \sum_{j=1}^{N_2} d_j r_1^{k_j} r_2^{l_j} r_3^{m_j} \right).
\end{aligned}
\tag{2.62}
$$

The first order spherical Bessel and Neumann functions are now

$$
j_1(kr) \;=\; \frac{\sin kr}{(kr)^2} - \frac{\cos kr}{kr}
\tag{2.63}
$$

and

$$
n_1(kr) \;=\; -\frac{\cos kr}{(kr)^2} - \frac{\sin kr}{kr},
\tag{2.64}
$$

and the relevant spherical harmonics, Y_{10} are given by

$$
Y_{10}(\theta, \phi) \;=\; \sqrt{\frac{3}{4\pi}}\cos\theta.
\tag{2.65}
$$

In the case of d-wave ($l = 2$) scattering, three different symmetries of short-range term are necessary, corresponding to ($l_1 = 2, l_2 = 0$), ($l_1 = 1, l_2 = 1$) and ($l_1 = 0, l_2 = 2$). For the first and third cases, we can only have $m_1 = m_2 = 0$, so we have

$$\psi(2,0,2,0) = Y_{20}(\theta_1, \phi_1)Y_{00}(\theta_2, \phi_2) < 2,0,0,0|2,0 > \qquad (2.66)$$

$$\psi(0,2,2,0) = Y_{00}(\theta_1, \phi_1)Y_{20}(\theta_2, \phi_2) < 0,2,0,0|2,0 > . \qquad (2.67)$$

Again, the Clebsch-Gordan coefficients and the zero order spherical harmonics Y_{00}, which are independent of angle, are conveniently absorbed into the variational parameters in the Hylleraas expansion. The second order spherical harmonics are of the form

$$Y_{20}(\theta, \phi) = \sqrt{\frac{5}{4\pi}} \left(\frac{3}{2} \cos^2 \theta - \frac{1}{2} \right). \qquad (2.68)$$

For the second l symmetry ($l_1 = 1, l_2 = 1$) the situation is more complicated, as there are three sets of values of m which satisfy (2.59) and (2.60); we thus have

$$\psi(1,1,2,0) = Y_{1,-1}(\theta_1, \phi_1)Y_{1,+1}(\theta_2, \phi_2) < 1,1,-1,+1|2,0 >$$

$$+ Y_{1,0}(\theta_1, \phi_1)Y_{1,0}(\theta_2, \phi_2) < 1,1,0,0|2,0 >$$

$$+ Y_{1,+1}(\theta_1, \phi_1)Y_{1,-1}(\theta_2, \phi_2) < 1,1,+1,-1|2,0 > \qquad (2.69)$$

The Clebsch-Gordan coefficients required are

$$< 1,1,+1,-1 > = \frac{1}{\sqrt{6}} \qquad (2.70)$$

$$< 1,1,-1,+1 > = \frac{1}{\sqrt{6}} \qquad (2.71)$$

$$< 1,1,0,0 > = \frac{2}{\sqrt{6}}, \qquad (2.72)$$

and the three $l = 1$ spherical harmonics have the forms (2.65), for $m = 0$, plus

$$Y_{1,+1}(\theta, \phi) = -\sqrt{\frac{3}{8\pi}} \sin \theta e^{i\phi} \qquad (2.73)$$

$$Y_{1,-1}(\theta, \phi) = +\sqrt{\frac{3}{8\pi}} \sin \theta e^{-i\phi}. \qquad (2.74)$$

45

The form of ψ for the second symmetry can thus be shown to be

$$\psi(1,1,2,0) = \frac{3}{4\pi}\left(3\cos\theta_1\cos\theta_2 - \cos\theta_{12}\right)\left[\frac{1}{\sqrt{6}}\right]. \tag{2.75}$$

Since it is only necessary that the spherical harmonics are combined in the correct ratios, it is again simpler to absorb the common factor $\frac{1}{\sqrt{6}}$ into the normalisation of the linear variational parameters.

If, as in the s-wave case, the S and C notation is used for the Bessel and Neumann terms respectively, the stationary condition for the higher partial wave trial functions yields a matrix equation whose form is identical to (2.14). The short-range terms in the matrices A and B are most conveniently ordered as they appear in the trial functions, although this is quite arbitrary.

For partial waves higher than $l = 0$, a centrifugal $l(l+1)/r^2$ term arises from the action of the kinetic energy operator in the Hamiltonian on the angular functions $Y_{l0}(\theta, \phi)$ in the trial function, and this may be considered to represent an additional repulsive component in the interaction potential. Indeed, as we move to higher partial waves, this term becomes increasingly effective at keeping the positron away from the inner regions of the atom, lessening the importance of the short-range correlations, and making the Born approximation an increasingly good representation of the scattering process. In the previous work of Humberston on positron-hydrogen scattering, predictions of cross sections summed over all partial waves used the Born approximation for $l \geq 3$.

The greater complexity of the higher order spherical Bessel and Neumann functions makes analytic integration of any of the matrix elements impractical, and numerical techniques have been used throughout for partial waves higher than $l = 0$. The more complicated angular dependence of the spherical harmonics Y_{l0} makes integration over the external angles more complicated too, but this is still simple enough to perform analytically. The angular integration of a typical p-wave matrix element is described in detail in Appendix C.

46

Chapter 3

Threshold Effects in Positron-Hydrogen Scattering

3.1 Introduction

In the previous Kohn variational calculations of positron-hydrogen scattering cross sections, the whole of the energy region below the first excitation threshold of hydrogen ($E_{ex} = 10.2\text{eV}$) was investigated in some detail, but it remained for behaviour in the immediate vicinity of the positronium formation threshold ($E_{thr} = 6.8\text{eV}$) to be examined fully. This region is of particular interest, since it affords the opportunity of seeing the effect of the new Ps formation channel on the elastic and total cross sections, and of comparing results with the more general theories of threshold behaviour based on the R-matrix analyses of Wigner (1948).

In theoretical studies of other atomic and nuclear collision processes (e.g. electron-lithium scattering, see Norcross and Moores (1972)), cusps have been predicted to occur in the elastic cross section when an inelastic collision process becomes energetically viable, as a consequence of the inelastic cross section starting with an infinite slope with respect to the wavenumber or kinetic energy in the incident channel. This situation derives simply from the linear dependence of the s-wave inelastic cross section on the wavenumber in the outgoing rearrangement channel.

In positron-hydrogen scattering the wavenumbers of the positron, k, and positron-

ium, κ, are related by

$$\frac{k^2}{2} + E_H = \frac{\kappa^2}{4} + E_{Ps},$$ (3.1)

where E_H and E_{Ps} are the ground state energies of hydrogen and positronium respectively. Wigner's R-matrix threshold theory predicts that, for energies close to threshold, the inelastic cross section for a given partial wave l behaves like

$$\sigma_{Ps}^l \propto \kappa^{2l+1},$$ (3.2)

and therefore

$$\frac{d\sigma_{Ps}^l}{d\kappa} \propto (2l+1)\kappa^{2l}.$$ (3.3)

The gradient of the cross section with respect to k is

$$\frac{d\sigma_{Ps}^l}{dk} = \frac{d\sigma_{Ps}^l}{d\kappa}\frac{d\kappa}{dk},$$ (3.4)

and from (3.1) we have

$$\frac{d\kappa}{dk} = \frac{2k}{\kappa},$$ (3.5)

so consequently

$$\frac{d\sigma_{Ps}^l}{dk} \propto 2k(2l+1)\kappa^{2l-1}.$$ (3.6)

For s-wave scattering then, where $l = 0$, the linear dependence on κ of the inelastic cross section leads to an infinite derivative with respect to k as $\kappa \to 0$, although for all higher partial waves the slope is finite. The effect that the behaviour of the positronium formation cross section has on the elastic cross section is discussed later, in the context of the results obtained from these latest investigations.

Another stimulus to perform further calculations has been the recent experimental interest in threshold effects in positron-atom scattering. This follows an analysis of various e^+-He scattering measurements by Campeanu et $al.$ (1987), which suggested the possibility of a cusp-like structure in the elastic cross section at the positronium formation threshold. Coleman et $al.$ (1992) have since made measurements of elastic

cross sections for this system more directly, but failed to observe any such anomalous feature. The negative findings here were also borne out by the investigations of Moxom (1993), who measured Ps formation cross sections for the noble gases from He through to Xe. The results of these latter investigations were fitted using R-matrix threshold theory (Moxom *et al.*, 1994), the fits then being used to predict the energy dependence of the elastic cross sections for these atoms. Although no cusp was predicted for He by this analysis, such structure was predicted to develop for the heavier atoms, as a consequence of the increasing strength of the positron-atom interaction.

Further, more detailed theoretical investigations of positron-hydrogen scattering also seem pertinent, in view of recent experimental advances in the study of this system. Sperber *et al.* (1992) have now measured the total ionisation cross section, which, in the Öre gap, reduces to the Ps formation cross section. These results appear to be in reasonable accord with the theoretical predictions of Humberston (1986).

Positronium formation in positron-hydrogen scattering is possibly the simplest re-arrangement process which can be considered in atomic physics and, as such, is an ideal case for comparison with the predictions of threshold theory. In addition, the formulation of the Kohn calculation described in chapter 2 is essentially *ab initio*, containing a full description of the interactions between the three bodies comprising the system, and thus should be able to reproduce any of the qualitative features predicted by theory, providing sufficiently elaborate trial functions are used.

3.2 Results

Both the single- and two-channel versions of the Kohn formulation were used for calculating s-, p- and d-wave cross sections at very small energy intervals on either side of the Ps formation threshold. The non-linear parameters were set to the values used for previous work, and the e^+-H codes were used in essentially their original forms, although

49

changes were made to allow larger matrices to be generated from more flexible trial functions, this time containing up to 220 linear parameters of each symmetry ($\omega = 9$).

Because the formalism is not analytically continuous in going across the Ps formation threshold (since the two-channel approach does not define imaginary values of κ for energies below threshold), it is important to ensure that any anomalous behaviour which is observed to occur in the elastic cross section is not simply the result of differing levels of convergence for the two formulations. In all partial waves, in fact, some sort of step was observed in σ_{el}^l when changing from the single- to two-channel calculation. One factor which particularly has to be taken into account above threshold is the behaviour of the long-range functions S_2 and C_2 for very small values of κ. The spherical Bessel-type S_2 terms always decay to a finite value as $\kappa \to 0$, but the Neumann-type C_2 functions have a behaviour close to the origin given by

$$\lim_{\kappa\rho \to 0} n_l(\kappa\rho) \propto \frac{1}{(\kappa\rho)^l}, \tag{3.7}$$

and consequently become more singular as l increases. In the present formulation, a shielding factor is introduced into the C_2 terms to keep the wavefunction finite as $\rho \to 0$, but the problem remains of C_2 blowing up as $\kappa \to 0$ with resulting computational difficulties which grow more acute for the higher partial waves. Although it is a simple matter to introduce an energy dependent shielding factor which causes C_2 to vanish smoothly as $\kappa \to 0$, this amounts effectively to uncoupling the positronium channel at low Ps energies, and diminishes the accuracy of the representation. At the very low Ps energies encountered close to threshold, the range of the interaction also becomes long, and it is very likely that the short-range Hylleraas terms alone may be insufficient fully to represent the scattering process. For these reasons, convergence was studied carefully for values of k extremely close to threshold on either side.

Cross sections for the energy region close to threshold are illustrated for the s, p and d partial waves in figures 3.1, 3.2 and 3.3 respectively. In figures 3.4, 3.5 and

50
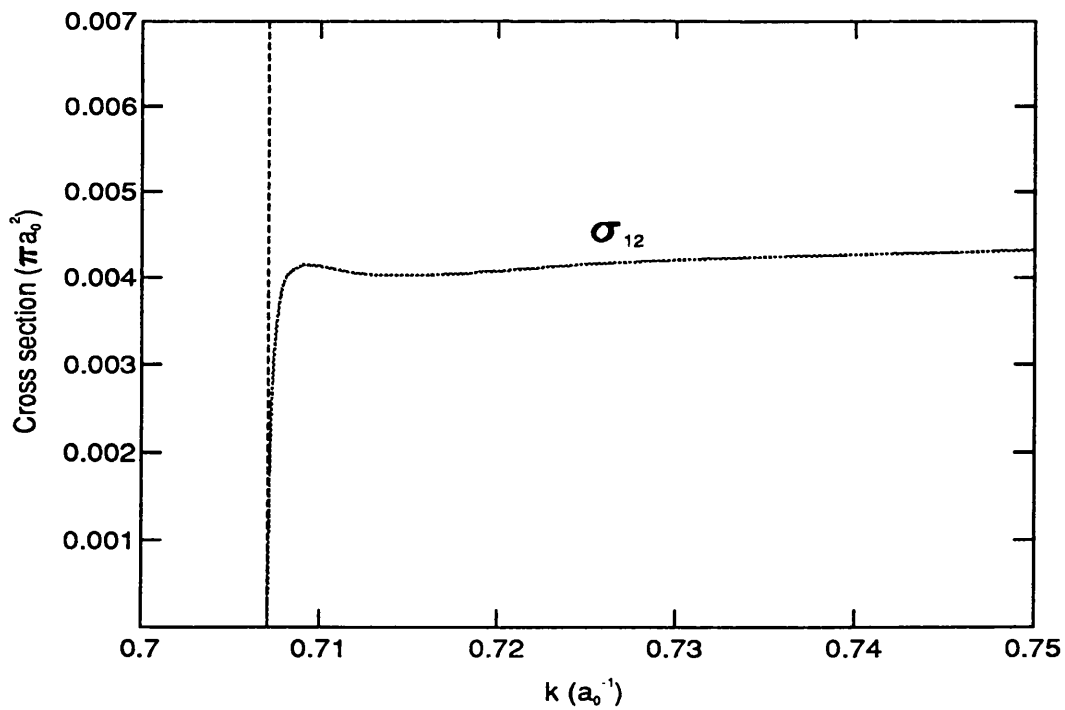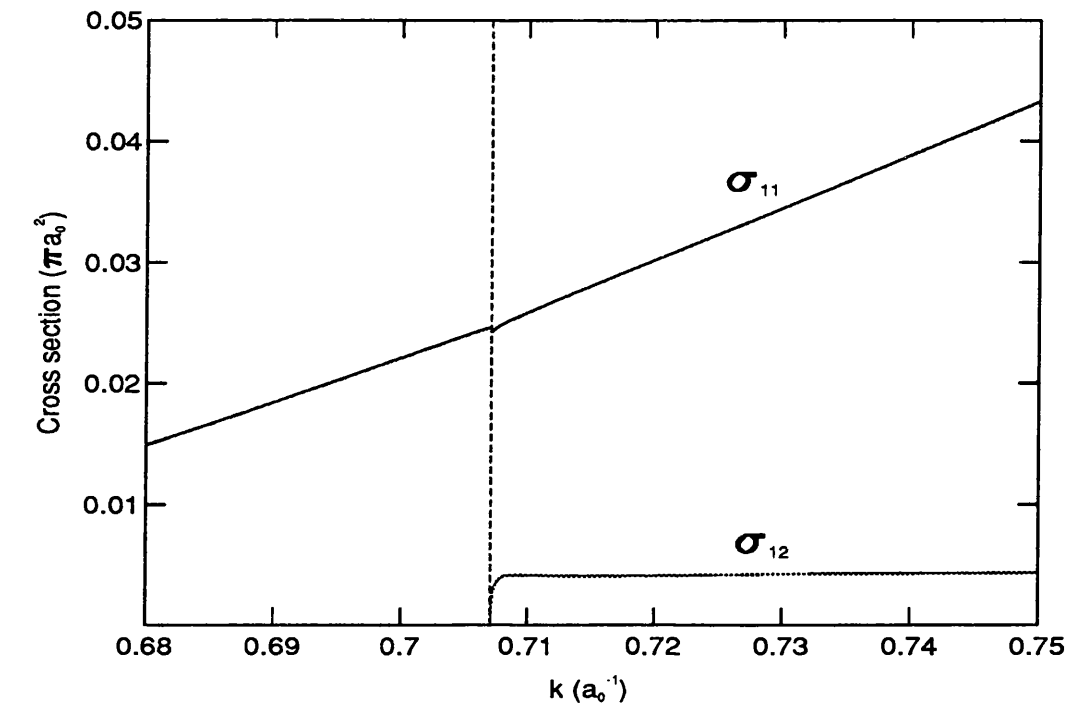
Figure 3.1: Cross sections for elastic scattering and positronium formation in positron-hydrogen s-wave scattering.
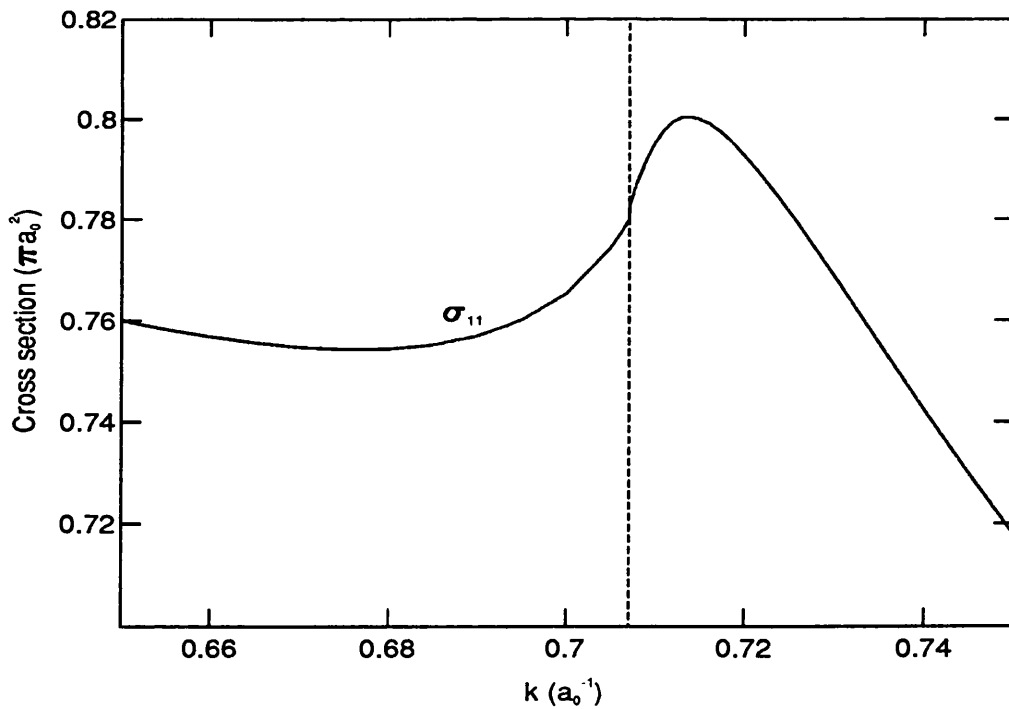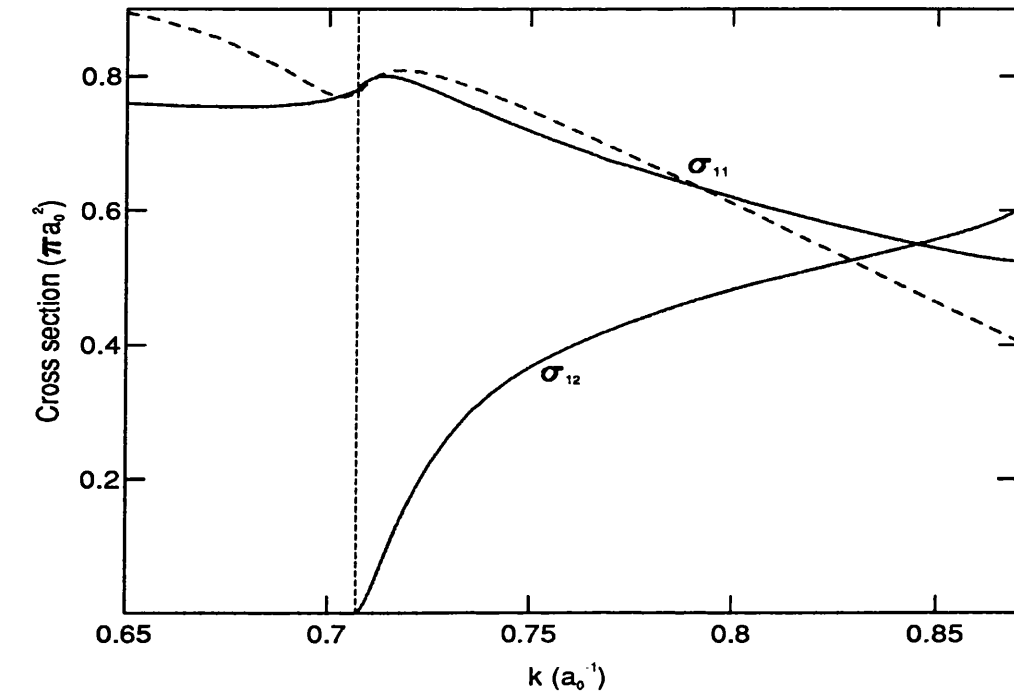
Figure 3.2: Cross sections for elastic scattering and positronium formation in positron-hydrogen p-wave scattering. Results obtained by Meyerhof (1994) using an R-matrix fitting procedure are included as the dashed line.
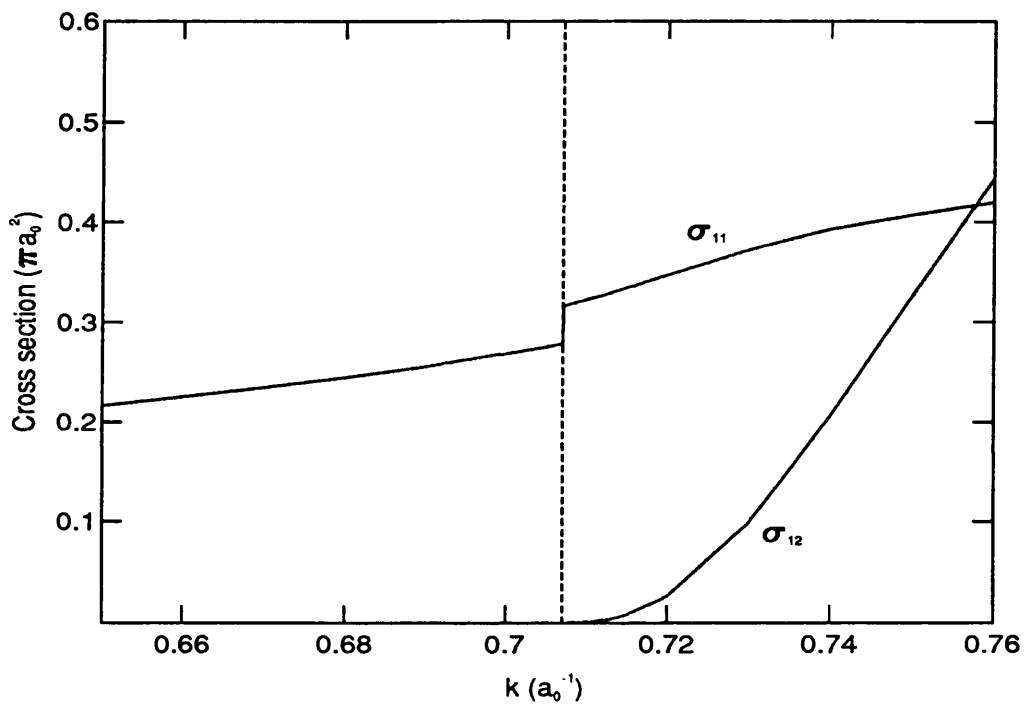
Figure 3.3: Cross sections for elastic scattering and positronium formation in positron-hydrogen d-wave scattering.
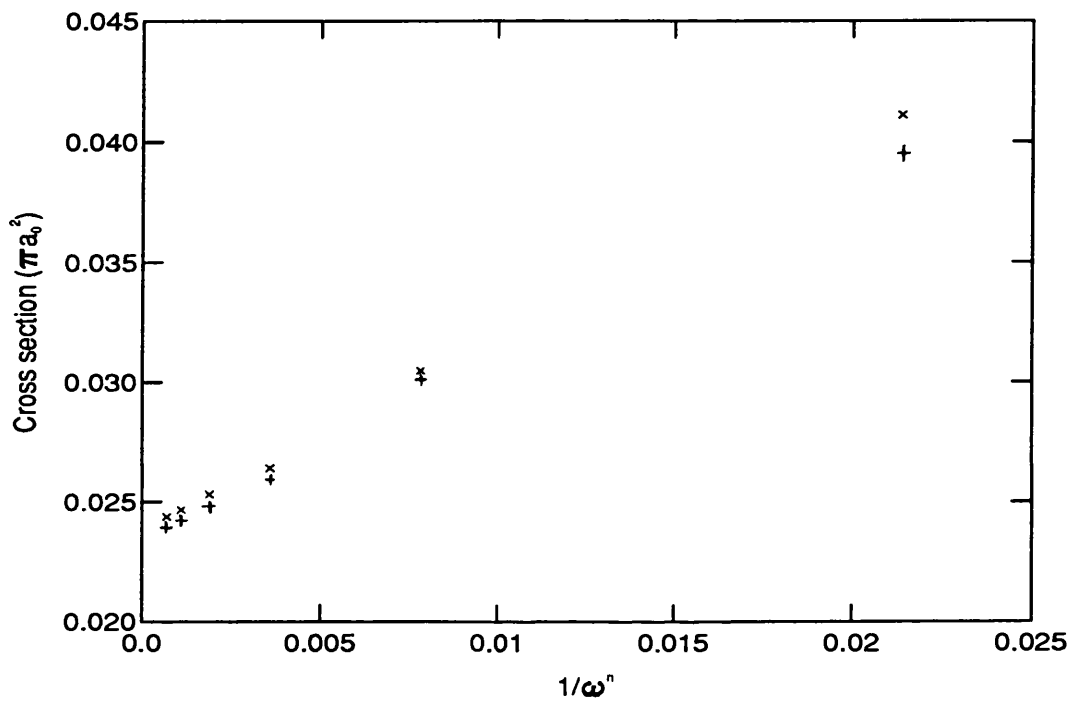
Figure 3.4: Convergence of the s-wave elastic cross section for energies just below $\left(k = 0.707106a_0^{-1}, \times\right)$ and above $\left(k = 0.707107a_0^{-1}, +\right)$ the Ps formation threshold for positron-hydrogen scattering. For both plots, $n = 3.5$.
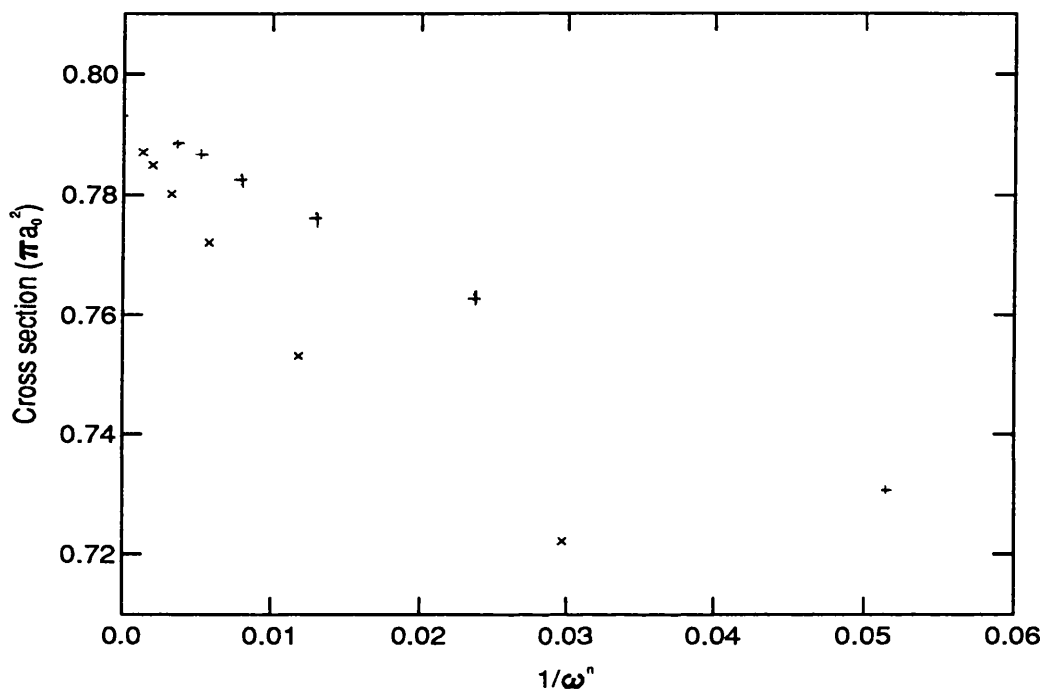
Figure 3.5: Convergence of the p-wave elastic cross section for energies just below ($\times$) and above ($+$) the Ps formation threshold for positron-hydrogen scattering. The values of n are 3.2 and 2.7, below and above threshold respectively.
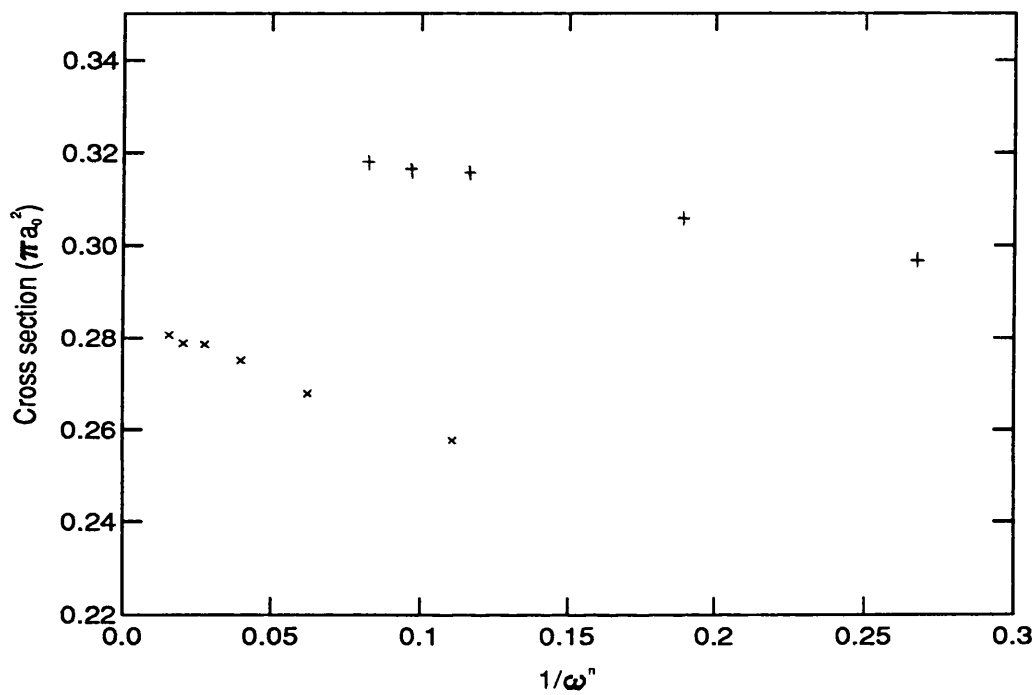
Figure 3.6: Convergence of the d-wave elastic cross section for energies just below ($\times$) and above ($+$) the Ps formation threshold for positron-hydrogen scattering. The values of n are 2.0 and 1.2, below and above threshold respectively.

3.6, convergence of the cross sections is illustrated as a function of an inverse power of ω, using the method described in section 2.2.5. Below threshold the convergence corresponds to $k = 0.707106a_0^{-1}$, and above threshold $k = 0.707107a_0^{-1}$ has been used. It was believed justifiable to extrapolate the elastic cross sections in this way, rather than just the diagonal K-matrix elements, since K_{11} does not change sign in any partial wave when the number of linear parameters is increased, and thus the cross sections converge monotonically. Above threshold, it is true that K_{12} and K_{22} contribute to the elastic cross section but, being extremely small, they have very little effect on the convergence trend.

3.3 Threshold Theory

In considering the effect of the newly opened inelastic channel on the elastic cross section, we follow Meyerhof (1962,1963) and work with the S-matrix, in terms of which the partial wave cross sections are given by

$$\sigma_{el}^l = \frac{\pi}{k^2}(2l+1)|1 - S_{11}^l|^2, \tag{3.8}$$

$$\sigma_{Ps}^l = \frac{\pi}{k^2}(2l+1)|S_{12}^l|^2. \tag{3.9}$$

Conservation of flux requires that

$$|S_{11}^l|^2 + |S_{12}^l|^2 = 1, \tag{3.10}$$

so the expression for the positronium formation cross section may alternatively be written

$$\sigma_{Ps}^l = \frac{\pi}{k^2}(2l+1)(1 - |S_{11}^l|^2), \tag{3.11}$$

whereupon the total cross section in a given partial wave is easily shown to be given by

$$\sigma_{tot}^l = \sigma_{el}^l + \sigma_{Ps}^l = \frac{\pi}{k^2}(2l+1)2(1 - Re S_{11}^l). \tag{3.12}$$

57

So long as we take care to keep the different partial waves separate, it avoids unnecessary algebraic complexity to work in units of cross section $\frac{\pi}{k^2}(2l+1)$. Rearranging (3.11), we thus have

$$|S_{11}^l|^2 = 1 - \sigma_{Ps}^l \tag{3.13}$$

and hence

$$S_{11}^l = e^{2i\theta_l}(1 - \sigma_{Ps}^l)^{\frac{1}{2}}. \tag{3.14}$$

At energies very close to threshold, where σ_{Ps}^l is still very small, we get a good approximation by using a binomial expansion on (3.14) and neglecting terms of second order and higher, so that

$$S_{11}^l \simeq e^{2i\theta_l}\left(1 - \frac{1}{2}\sigma_{Ps}^l\right). \tag{3.15}$$

We make no assumptions yet about θ_l, except to note that at threshold, where $\sigma_{Ps} = 0$, the S-matrix is defined by

$$S_{11}^l = \exp 2i\theta_l, \tag{3.16}$$

which means that when $E = E_{thr}$, θ_l is simply the scattering phaseshift in the lth partial wave. The expression for S_{11}^l, equation (3.15), can be made to apply below threshold, as well as above, by replacing σ_{Ps}^l by a purely imaginary quantity, $\varrho^l(\kappa)$, which is arrived at by considering Wigner's threshold relation (3.2) for $E < E_{thr}$. In this energy region we have $\kappa = i|\kappa|$, so if the constant of proportionality in (3.2) is C, we can write

$$\begin{aligned}
\varrho^l(\kappa) &= C\kappa^{2l+1} \\
&= Ci^{2l+1}|\kappa|^{2l+1} \\
&= i(-1)^l\sigma_{Ps}^l(|\kappa|). \tag{3.17}
\end{aligned}$$

It should be noted, however, that, since this attempt to find a quantity which is an appropriate continuation of σ_{Ps} below threshold already makes use of Wigner's threshold

58

relation, it can only be taken to be strictly valid immediately below threshold. If we now take σ_{Ps}^l always to mean $\sigma_{Ps}^l(|\kappa|)$, then a suitable expression for S_{11}^l, which is continuous across threshold, is

$$S_{11}^l = e^{2i\theta_l}\left(1 - \frac{1}{2}\sigma_{Ps}^l\left\{\begin{matrix} 1 \\ i(-1)^l \end{matrix}\right.\right),\tag{3.18}$$

where the upper line refers to positron energies $E \geq E_{thr}$, and the lower line to $E < E_{thr}$. If we abbreviate the term in brackets as F_l, then from (3.8) the elastic cross section is given by

$$\begin{aligned} \sigma_{el}^l &= \left|1 - F_l e^{2i\theta_l}\right|^2 \\ &= \left(1 - F_l e^{2i\theta_l}\right)\left(1 - F_l^* e^{-2i\theta_l}\right) \\ &= 1 - F_l e^{2i\theta_l} - F_l^* e^{-2i\theta_l} + |F_l|^2 \end{aligned}\tag{3.19}$$

Above threshold, where F_l is real, this becomes

$$\begin{aligned} \sigma_{el}^l &= 1 - 2F_l \cos 2\theta_l + F_l^2 \\ &= 1 - 2F_l(1 - 2\sin^2\theta_l) + F_l^2, \end{aligned}\tag{3.20}$$

and it is soon found, substituting in the explicit expression for F_l and dropping the second order term in σ_{Ps}^l, that

$$\sigma_{el}^l = 4\sin^2\theta_l - 2\sin^2\theta_l\sigma_{Ps}^l.\tag{3.21}$$

Below threshold, on the other hand, we find that if we again ignore the term of second order in σ_{Ps}^l, then

$$\begin{aligned} \sigma_{el}^l &= 1 - (\cos 2\theta_l + i\sin 2\theta_l)\left(1 - \frac{1}{2}\sigma_{Ps}^l i(-1)^l\right) \\ &\quad - (\cos 2\theta_l - i\sin 2\theta_l)\left(1 + \frac{1}{2}\sigma_{Ps}^l i(-1)^l\right) + 1 \\ &= 2 - 2\cos 2\theta_l - \sigma_{Ps}^l(-1)^l \sin 2\theta_l \\ &= 2 - 2(1 - 2\sin^2\theta_l) - \sigma_{Ps}^l(-1)^l \sin 2\theta_l, \\ &= 4\sin^2\theta_l - \sigma_{Ps}^l(-1)^l \sin 2\theta_l.\end{aligned}\tag{3.22}$$

Combining (3.21) and (3.22), and reintroducing the factor $\frac{\pi}{k^2}(2l+1)$, we thus get

$$\sigma_{el}^l = \frac{4\pi}{k^2}(2l+1)\sin^2\theta_l - \sigma_{Ps}^l \begin{cases} 2\sin^2\theta_l & E \geq E_{thr} \\ (-1)^l\sin 2\theta_l & E < E_{thr}. \end{cases} \qquad (3.23)$$

3.4 Discussion

Predictions about the physical behaviour close to threshold based on (3.23) clearly depend on the interpretation of the parameter θ_l. At $E = E_{thr}$ we have

$$\sigma_{el}^l = \frac{4\pi}{k^2}(2l+1)\sin^2\theta_l, \qquad (3.24)$$

which is consistent with taking it to be the scattering phaseshift. Away from threshold, however, the above derivation leaves θ_l with a somewhat arbitrary energy dependence. If we assume it to vary slowly enough with energy that it can be considered to remain constant over the region close to threshold, then the energy dependence of the first term in (3.23) is restricted to the k^{-2} factor, and the second term can be interpreted as essentially a correction to the elastic cross section at threshold. It is immediately obvious that such an interpretation requires σ_{el}^l to fall away immediately above threshold for all partial waves, with the behaviour below threshold dependent upon the value of the phaseshift at threshold and whether l is odd or even.

The elastic cross sections for the s, p and d partial waves in positron-hydrogen scattering (figures 3.1–3.3), however, all appear to violate these predictions, by rising immediately above threshold, and it therefore appears necessary to take account of the energy dependence of θ_l, even for the purpose of making qualitative predictions. A more rigorous derivation from R-matrix theory defines a phase parameter δ_l, in terms of which the S-matrix is shown to be given by

$$S_{11}^l = e^{2i\delta_l}\left(1 - \frac{1}{2}\sigma_{Ps}^l \begin{Bmatrix} 1 \\ i \end{Bmatrix}\right), \qquad (3.25)$$

for $l = 0$, and

$$S_{11}^l = e^{2i\delta_l}\left(1 + iB_l - \frac{1}{2}\sigma_{Ps}^l \begin{Bmatrix} 1 \\ i(-1)^l \end{Bmatrix}\right), \qquad (3.26)$$

60

for $l \geq 1$. The B_l term is due to Breit (1957), and is given by

$$B_l = \frac{R^{1-2l}\sigma_{\mathrm{Ps}}^l}{2^{l+1}\left[l!/(2l!)^2\right](2l-1)} \left\{ \begin{array}{c} 1 \\ -1 \end{array} \right. , \qquad (3.27)$$

where

$$R = \kappa a, \qquad (3.28)$$

a being the radius of the R-matrix sphere, which defines the region of interaction outside which the wavefunction is taken to assume its asymptotic form. Within the R-matrix formalism, δ_l is defined to be the phaseshift with the inelastic channel uncoupled, which, in the case of positron-hydrogen scattering, means a phase which has no component corresponding to positronium formation, either real or virtual. This definition holds for energies both above and below E_{thr}, and hence δ_l varies smoothly across threshold. Since the S-matrix reduces to $\exp 2i\delta_l$ at threshold, we also have the result that, at this particular energy, the uncoupled and fully coupled phases coincide.

In the Kohn formulation, it is impossible to calculate the uncoupled phase of the R-matrix formalism, because the presence of virtual positronium is implicit in the form of the total Hamiltonian for the system, and the trial functions will always attempt to represent Ps, where it makes a contribution to the scattering process. Above threshold, it is possible to uncouple the real outgoing positronium channel, as described in chapter 5, but this does not suppress all reference to virtual Ps, as required by R-matrix theory. In the absence of accurate R-matrix data for the quantity δ_l in the case of positron-hydrogen scattering, we assume that at threshold it takes on the value of our fully coupled estimate of the phaseshift, and varies only slowly with k.

For s-wave scattering, there is no Breit term, and thus the phase parameter δ_l of equation (3.25) is equal to θ_l in equation (3.18)—hence the form of (3.23), which gives the threshold effect in the elastic cross section, is unaltered. Since the positronium formation cross section varies with infinite slope at threshold, and δ_0 is assumed only to vary slowly, we therefore expect the elastic cross section also to be varying with an

infinite derivative. According to R-matrix theory, then, the s-wave elastic cross section *must* fall immediately above threshold. If δ_0 lies in the first or third quadrant, so that $\sin 2\delta_0$ is positive, then we also expect σ^0_{el} to be falling below threshold, as we move towards lower positron energies, giving rise to a distinct 'Wigner cusp'. Otherwise, if δ_0 lies in the second or fourth quadrants, σ^0_{el} rises below threshold.

In the Kohn variational investigations, we find that the s-wave phaseshift just below threshold lies in the fourth quadrant (at $k = 0.7071$, for $\omega = 6$ we have $\delta_0 = -0.055\text{rads}$), and so we would expect a rise in σ^0_{el} with decreasing k below threshold, rather than a fall. Referring to figure 3.1, we see that in the vicinity of the threshold σ^0_{Ps} reaches a maximum of approximately $0.004\pi a_0^2$, and hence the threshold effect in the elastic cross section for $E \leq E_{thr}$, which is proportional to $\sigma^0_{Ps} \sin 2\delta_0$, is of the order of $4 \times 10^{-4}\pi a_0^2$. Above threshold, the drop in σ^0_{el} as a consequence of the onset of the new channel is expected to be an order of magnitude smaller still ($\sigma^0_{Ps} \sin^2 \delta_0 \simeq 10^{-5}\pi a_0^2$). Such effects are much too small to be resolved within the accuracy of the present calculation, and certainly likely to remain unobserved experimentally.

The slight structure in the s-wave Ps formation cross section, in the form of a rounded maximum, had not been observed in the previous Kohn variational investigations of positron-hydrogen scattering. More structure has been noted in this energy region in calculations using the reactive scattering method by Archer *et al.* (1990), although they calculate σ^0_{Ps} to be approximately 15% smaller. Recent investigations by Carbonell (1994) using the Fadeev technique, however, yield an s-wave Ps formation cross section which is in excellent agreement with the present results for energy in the Öre gap, suggesting that the Kohn results are probably very reliable.

The variationally calculated s-wave elastic cross section illustrated in figure 3.1 does exhibit a small downward step in going across threshold, which corresponds to the change from the single- to the two-channel Kohn formulation, but this is not believed to

be a real physical feature. The sense in which σ_{el}^0 converges, as illustrated in figure 3.4, indicates that the results above threshold are rather more accurate than those obtained below. This is probably because the presence of the positronium terms in the trial function in the two-channel formulation allows a better representation of the long-range interaction to be attained than do the Hylleraas terms alone.

For partial waves higher than $l = 0$, it is possible for the Breit term to be absorbed into the phase factor θ_l of (3.18), so that (3.23) may still be used to obtain the threshold effects, but it is easier to see how it affects the elastic cross section by using (3.26) as it stands. It is then found that the appropriate expressions for the elastic cross section above and below threshold are given by

$$\sigma_{el}^l = \frac{4\pi}{k^2}(2l+1)\sin^2\delta_l + 2B_l\sin 2\delta_l - \sigma_{Ps}^l \begin{cases} 2\sin^2\delta_l \\ (-1)^l\sin 2\delta_l \end{cases}. \qquad (3.29)$$

For the partial waves of interest, the Breit term is given by

$$B_1 = \frac{\sigma_{Ps}^1}{\kappa a} \begin{cases} 1 \\ -1 \end{cases} \qquad (3.30)$$

$$B_2 = \frac{\sigma_{Ps}^2}{3(\kappa a)^3} \begin{cases} 1 \\ -1 \end{cases}. \qquad (3.31)$$

Since σ_{Ps}^l is proportional to κ^{2l+1} close to threshold, the Breit term is always proportional to κ^2, making it the dominant correction term in the immediate vicinity of threshold. The energy range over which it dominates the third term is governed, for a given partial wave, by the size of the R-matrix radius, a. The sign of the correction is then given by the phase factor, δ_l—if δ_l lies in the first or the third quadrant, then the Breit term makes a positive contribution to the elastic cross section above threshold, and a negative contribution below. Otherwise, the reverse is true.

Assuming δ_l to remain constant in the region close to threshold allows a qualitative matching of R-matrix theory with calculation. In the Kohn results for positron-hydrogen p-wave scattering, the phaseshift lies well within the first quadrant for energies close to threshold (at $k = 0.7071$ and $\omega = 6$, the phaseshift is 0.181rads), and thus the

Breit term is expected to cause a rise in the elastic scattering cross section for $E > E_{thr}$ and a fall when $E < E_{thr}$. When $|\kappa|$ becomes sufficiently large, the third term in (3.29), which is of the opposite sign both above and below threshold for $l = 1$, overwhelms the Breit term's influence, and the trend ought to reverse. Both of these characteristics seem to be borne out by the present investigations, as is illustrated well in figure 3.2. The convergence plots in figure 3.5 show that the small discontinuity observed in going across threshold is almost certainly the result of differing levels of convergence, with results above threshold being marginally better converged. The small magnitude of these differences, however, would appear to indicate that the non-linear parameters in the wavefunction are well optimised.

Meyerhof (1994) has attempted to fit the above R-matrix theory to the present Kohn elastic scattering data, and some of the results of his analysis are included in figure 3.2. This fit has used an energy-independent R-matrix sphere radius, fixed at $a = 1.95a_0$. The energy dependence for the uncoupled phase, δ_l, has been estimated from a fuller R-matrix treatment, which Meyerhof has used to investigate the influence of the positronium formation channel over a wider energy range than is considered here. By definition, δ_l is made to coincide with the Kohn estimate of the phaseshift at $E = E_{thr}$. It can be seen that above threshold the R-matrix theory fits the Kohn data quite well, reproducing the distinctive hump in the elastic cross section, which is also, incidentally, a feature of the recent positron-hydrogen calculations of Higgins and Burke (1993). Below threshold, the trends of the Kohn and R-matrix data are in qualitative agreement, but the energy dependences of the cross sections are very different. This may be due to the fact that the form for the quantity ϱ^l, which replaces the Ps formation cross section below threshold (given by equation (3.17)), is only appropriate over a very small energy range. The indications are, therefore, that the theory discussed above, for a quantitative analysis, requires some modification for energies $E < E_{thr}$.

64

In the case of d-wave scattering, the phaseshift again lies comfortably within the first quadrant (0.0835radians at $k = 0.7071$ and $\omega = 6$, converging upwards), suggesting that the sign of the Breit term's contribution to σ_{el}^2 should be the same as for the $l = 1$ partial wave. Below threshold, however, the third term in (3.29), for $l = 2$, acts to reduce σ_{el}^2, reinforcing rather than cancelling the effect of the Breit term. Again assuming δ_2 to be approximately constant in the threshold region, the present results seem to be in accord with these predictions.

Doubt must be cast, though, on the reliability of the Kohn d-wave results below threshold by the unphysical step which appears in the elastic cross section in going from the one- to the two-channel formulation. Although the convergence characteristics illustrated in figure 3.6 individually appear quite respectable, the above and below threshold cross sections seem to be converging to markedly different values. The scatter of the lower energy cross sections, however, makes a reliable extrapolation rather difficult. The inverse power of ω here is selected so that all the results lie as close as possible to a straight line, whereas it may be that the results for the higher values of ω should be given more weight. Taking the points corresponding to the three highest values of ω below threshold, for example, would enable an extrapolation to a value closer to our estimate of the cross section just above threshold.

A comparison with other work (for example, Register and Poe (1975)) shows that the present results are indeed rather poorly converged below threshold, suggesting that the non-linear parameters in the trial function are not very well optimised. Above threshold, on the other hand, results are well in accord with those of recent hyperspherical close-coupling investigations by both Zhou and Lin (1994) and Igarashi and Toshima (1994), despite the fact that the same non-linear parameters have been used as in the one-channel problem.

The reason for the inferior convergence is likely to be the same as for s-wave scat-

tering, namely that the positronium terms are able better to represent the long-range interaction than are the Hylleraas terms alone. The fact that the p-wave results are in much better agreement above and below threshold, however, would seem to indicate that the existing forms of trial function, with more suitably chosen non-linear parameters, would be capable of improving convergence, and further study is clearly warranted.

Chapter 4

The Lithium Model Atom

4.1 Introduction

One of the major differences between the variational treatments of positron-hydrogen and positron-lithium scattering is the use, in the latter case, of a model to describe the system under investigation. In the positron-hydrogen work, the simplicity of the situation makes an essentially complete representation possible—here there are three distinguishable particles, and thus three inter-particle interactions to consider, where the nature of the interactive forces is known completely. The distinguishability of the electron, proton and positron means that no allowance is necessary for exchange effects brought about by the Pauli exclusion principle, and the limits on the accuracy of the final cross sections are governed by the flexibility and form of the trial functions and, to some extent, computational precision.

In view of the completeness of the representation used for calculations of positron-hydrogen scattering, assessments of the accuracy of the theoretical cross sections are made on the basis of agreement between different techniques, and stability of results. Experimental investigations of the positron-hydrogen system have not yet reached a level of sophistication where a detailed comparison of low energy partial cross sections is possible, although measurements of cross sections are now becoming available (for example, Sperber *et al.* (1992), Zhou *et al.* (1994)). The theoretical results obtained

67

using the Kohn method are very well converged and, below the Ps formation threshold, agree to high precision with those of Bhatia *et al.* (1971,1974), thought to be the most accurate available. Above threshold, the cross sections for both elastic scattering and positronium formation are also very stable and, as discussed in chapter 3, are seen to agree qualitatively with R-matrix threshold theory.

The complexity and number of inter-particle interactions associated with the positron-atom system obviously increase as we move along the periodic table to higher atomic numbers. For the second simplest atom, helium, a complete representation of the scattering problem needs to account for six inter-particle interactions (treating the nucleus as a point charge) with the further complication of exchange effects between the two electrons. The results of positron-helium calculations so far using the Kohn method (Humberston 1973, 1979 and Campeanu, 1977) have utilised the 'method of models' approach for the calculation of elastic scattering cross sections below the Ps formation threshold. Here, an accurate, but not exact, target wavefunction was generated from a Rayleigh-Ritz variational calculation, and then assumed to be an eigenfunction of a very good approximation to the target Hamiltonian. Subsequently expressing all components of the scattering trial function as products of this model target wavefunction with appropriate other functions, simplified the formulation of the problem considerably, enabling the nature of the electron-nucleus and electron-electron interactions to be disregarded. (Further information on the method of models is contained in Appendix A.)

The excellent agreement of experimental and theoretical data for elastic scattering cross sections for the positron-helium system indicates the strength of this approach for the one channel case. The treatment of Ps formation for energies above threshold, however, necessitates the abandonment of the method of models if the resulting He^+ ion is to be considered as having structure. Work is currently under way to investigate

this more complicated problem.

A full representation of the positron-lithium system, effectively a five-body problem, would require the consideration of ten inter-particle interactions, but the lithium atom's physical structure makes it particularly amenable to treatment as a hydrogenic atom, and this is the approach which has been adopted. The tightly bound inner $1s$ shell shields two units of nuclear charge very effectively from the $2s$ valence electron which is consequently very loosely bound. Exchange forces between the two shells are thus rendered very small, and a very good approximation to the real situation is obtained by making the assumption of a point core in the field of which the valence electron moves. The small influence of exchange effects is also convenient in that it allows the further assumption that the various components of the positron-core potential have the same form as for the electron.

4.2   The Lithium Model Potential

The potential used to represent the interaction between the electron and core is based on a phenomenological one developed by Peach et $al.$ (1988). The full form of the Peach potential is

$$V(r) = -\frac{1}{r} - \frac{2e^{-\gamma r}}{r}\left(1 + \delta r + \delta' r^2\right) - \frac{\alpha_d}{2r^4}\omega_2(\beta r), \qquad (4.1)$$

where

$$\omega_2(x) = [\chi_2(x)]^2, \quad \chi_2(x) = 1 - e^{-x}\sum_{n=0}^{2}\frac{x^n}{n!}.$$

The first two terms represent the static component of the potential, and the third arises due to the polarizability of the inner shell electrons, α_d being the dipole polarizability of the core which has a value of $0.1925a_0^3$. The parameters γ, δ and δ' are chosen so as to provide a close fit to the observed energy spectrum of the lithium atom. Two different sets of values have been found to yield excellent agreement with experiment, and both

have been used for the scattering calculations. The one on which most attention has been concentrated produces a $2s$ state, of the correct nodal structure, corresponding to the ground state of the real atom, and energies for the first three s and p states which are within 1% of experimental estimates. Inevitably, however, it also gives rise to a very tightly bound $1s$ state which, of course, has no real existence. It has been assumed that the very large energy separation of the $1s$ and $2s$ states of this potential ($E_{1s} = -51.5\text{eV}$), in comparison with the collision energies under investigation, renders the former's influence very small in the scattering problem.

As a check on this assumption, the second set of parameters causes the introduction of a short-range repulsive component into the electron-core potential, which prevents the formation of the tightly bound $1s$ pseudo-state, but instead produces a $1s$ state whose energy is in good agreement with experimental estimates of the lithium ground state. Although the energies of the higher eigenstates of this potential also correspond well with experiment, it has a drawback when considering scattering in that the structure of its eigenfunctions is unrealistic, since each has one less node than that which it is supposed to represent physically. Even so, except at short ranges, the ground-state eigenfunctions for the two different electron-core potentials seem to agree well, and it was felt that both models could be plausible representations of the atom, although the first type was clearly the more appealing. Henceforth, the two potentials are referred to as A and B respectively. Their short range forms are shown graphically in figure 4.1. The parameter values are given in Appendix D.

For the reasons mentioned above, exchange forces between the $2s$ valence electron and the electrons in the $1s$ shell are taken to be very small. If this is the case, then it is reasonable to assume that very little allowance is made for these effects in the parameters of the model potential, and a very good approximation to the positron-core interaction can be obtained simply by reversing the sign of the static terms, the
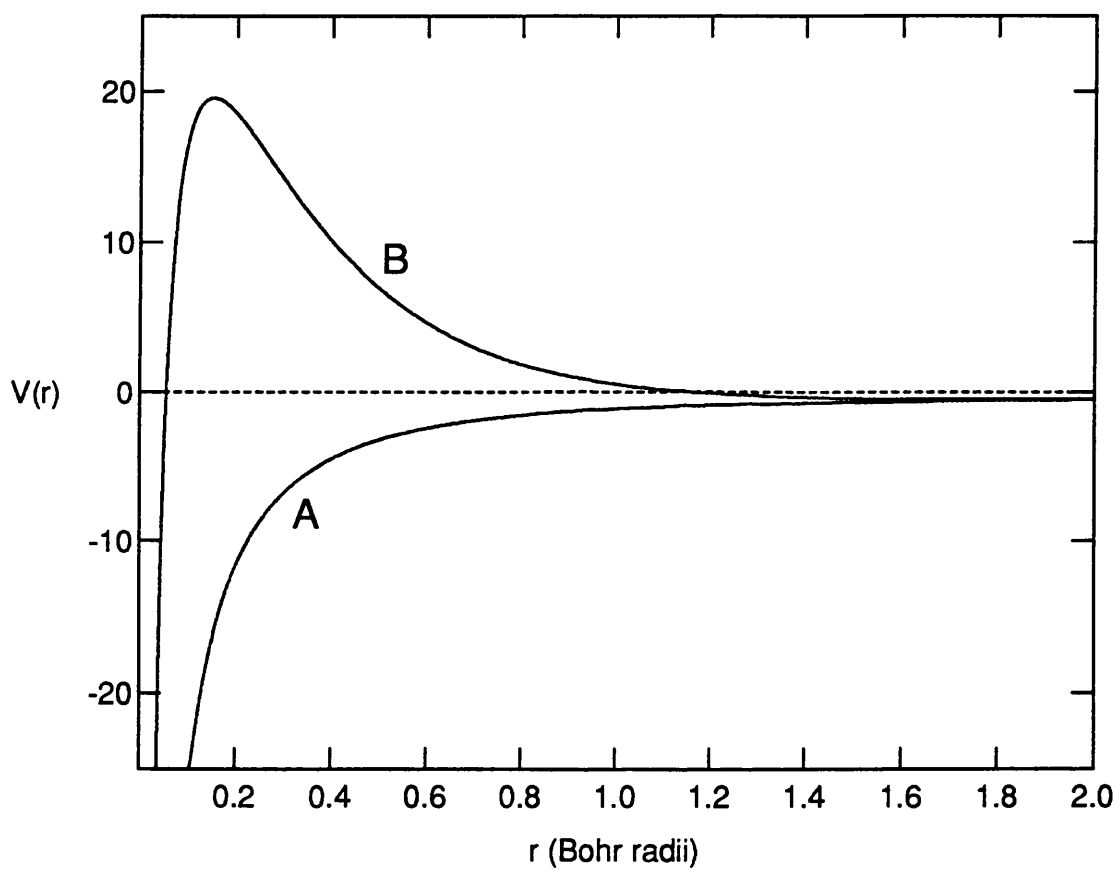
Figure 4.1: The electron-core model potentials A and B.

core polarization term remaining attractive. In doing this, the short-range repulsive component of potential B becomes an attractive well for the positron, thus introducing the possibility of unphysical positron-core bound states. At the low positron energies considered here, however, tunnelling into this region is unlikely to exert much of an influence on the scattering process, although it provides another reason to consider potential A the more reliable of the two.

In the scattering problem the inclusion of the core polarization component in the potential generates a slight complication, since the polarization of the core brought about by the presence of the electron alters the effect experienced by the positron, and vice versa; thus, for a full treatment, the problem requires the introduction of a three-body term into the total interaction potential of the form

$$V'(r_1, r_2) \quad = \quad \frac{\alpha_d}{r_1^2 r_2^2} \cos \theta_{12} \sqrt{\omega(\beta r_1)\omega(\beta r_2)}, \tag{4.2}$$

where r_1 and r_2 are the radial coordinates of the positron and electron respectively, and θ_{12} the inter-particle angle at the origin. In addition to increasing the complexity of the problem, the introduction of a term in the potential which is of the same sign for both electron and positron destroys certain symmetry arguments which prove very useful in checking on the numerical accuracy of the scattering calculation. The very small polarizability of the lithium core, however, suggested that this complication might be an avoidable one, and it was therefore decided to assess the effects on the energy level structure and polarizability of dropping the core polarization term altogether.

4.3 The Energy Spectra of the Lithium Models

A Rayleigh-Ritz calculation was performed for both electron-core potentials, with and without the core polarization term, using lithium wavefunctions of the form

$$\phi_{\text{Li}} \quad = \quad \frac{1}{\sqrt{4\pi}} \sum_{i=0}^{N-1} c_i r^i e^{-\alpha r}. \tag{4.3}$$

The stationary condition yields the set of N linear simultaneous equations

$$\sum_{j=0}^{N-1} c_j \left(< \phi_i|H|\phi_j > -E < \phi_i|\phi_j > \right) = 0 \qquad (4.4)$$

where

$$H = -\tfrac{1}{2}\nabla^2 + V(r) \qquad (4.5)$$

and

$$\phi_i = \frac{1}{\sqrt{4\pi}} r^i e^{-\alpha r}. \qquad (4.6)$$

The calculation thus reduces to the matrix eigenvalue problem

$$(A - \lambda B)C = 0, \qquad (4.7)$$

the solutions to which can be obtained using any one of a number of 'black box' subroutines. In this case, one of the Numerical Algorithms Group (NAG) Library routines, F02AEF, was used for the purpose—this routine returns both the N solutions for the eigenvalues E, and the corresponding sets of eigenvectors c_j.

The eigenvalues and eigenvectors corresponding to the different energy levels of the model atom were calculated for various N, and convergence was studied. The exponential parameter α was varied separately in order to obtain the lowest possible value for the ground state energy, E_0. Figures 4.2 and 4.3 show how the energy eigenvalues for the $2s$ and $3s$ states of potential A converge with respect to increasing N. It is interesting to note the pairing of the curves in these diagrams—in calculating the energy of the $2s$ eigenvalue, for example, it is found that at the optimum value of α for an even N, the variational estimate is hardly improved at all by the inclusion of an extra term in the expansion. Studying the eigenvectors of the expansion shows that the stationary condition seems to force the last c_i to be zero, if i is even, although the other eigenvectors with even i are non-zero. A similar situation arises in the calculation of the $3s$ state, but here it is the final terms corresponding to odd i that are killed off.
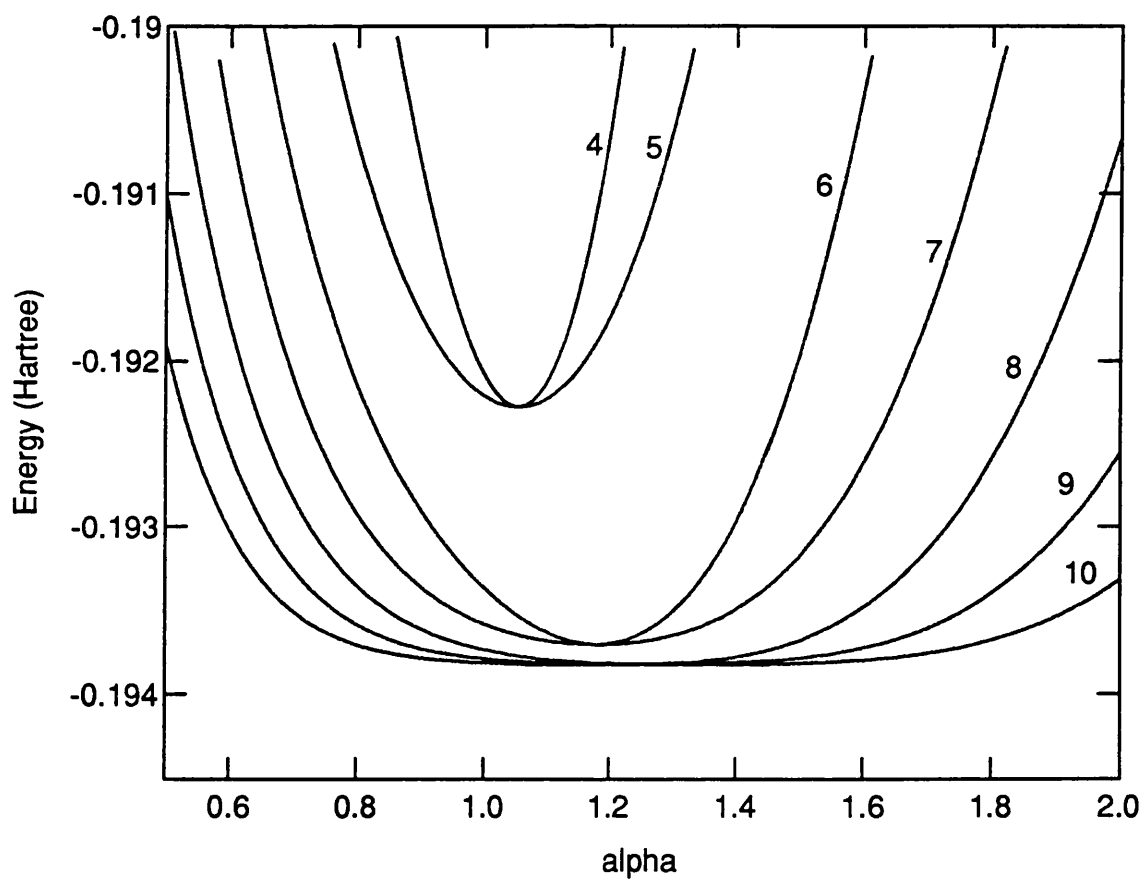
73

Figure 4.2: Convergence of the 2s state of potential A with respect to increasing N.
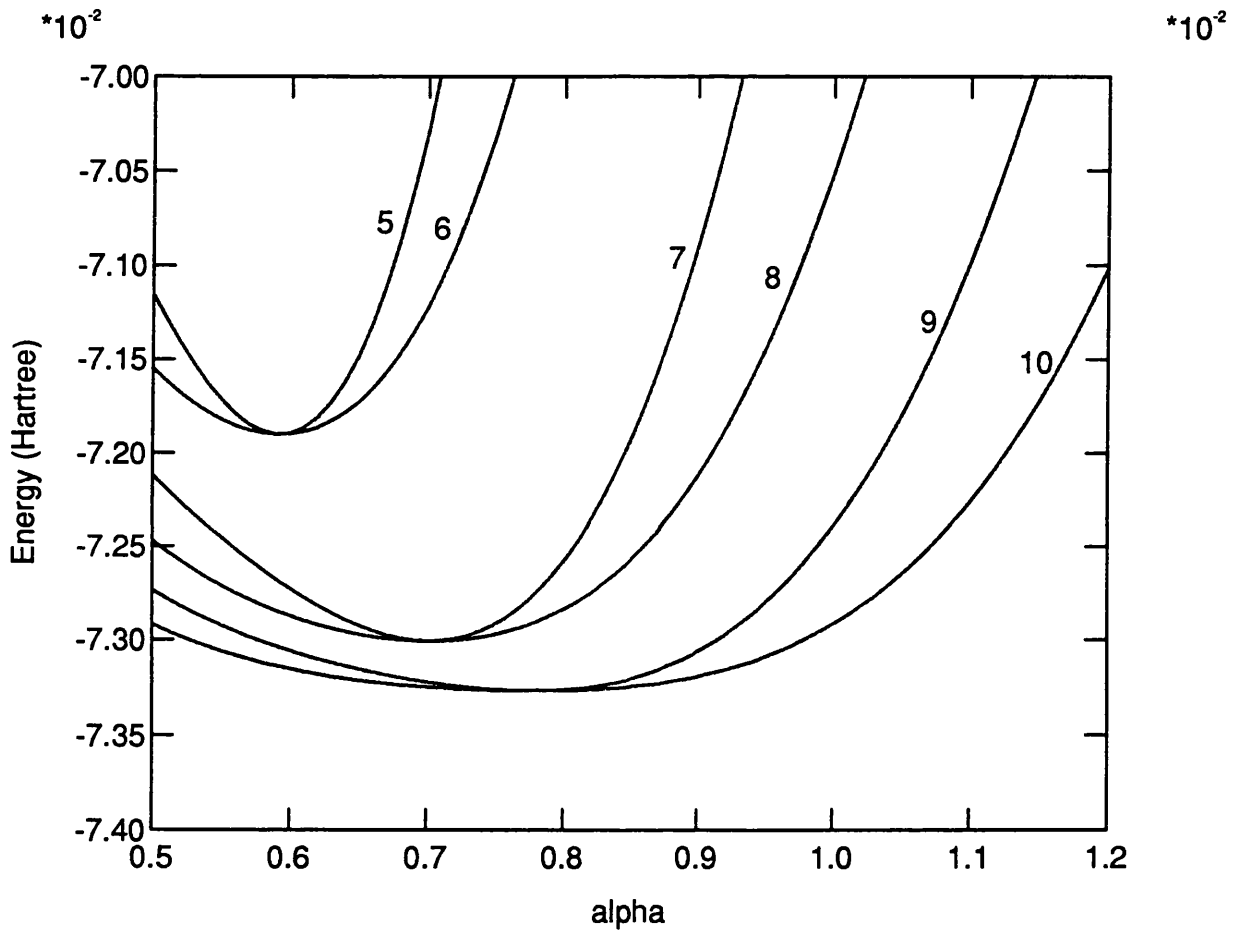
Figure 4.3: Convergence of the 3s state of potential A with respect to increasing N.

Potential A						
N	2s		3s		4s	
	a	b	a	b	a	b
5	−0.189401	−0.184340	−0.056594	−0.054657	0.012296	0.014753
7	−0.197227	−0.192986	−0.071986	−0.070905	−0.031969	−0.031264
9	−0.197902	−0.193767	−0.073993	−0.073064	−0.037651	−0.037235
11	−0.197950	−0.193823	−0.074206	−0.073301	−0.038501	−0.038148
13	−0.197952	−0.193826	−0.074223	−0.073320	−0.038619	−0.038279
15	−0.197952	−0.193826	−0.074224	−0.073322	−0.038636	−0.038300
17	−0.197952	−0.193826	−0.074224	−0.073322	−0.038639	−0.038304
19	−0.197952	−0.193826	−0.074224	−0.073322	−0.038640	−0.038304
Exptl.	−0.198158		−0.074188		−0.038618	

Table 4.1: Convergence of $l = 0$ states of the lithium model atom. The columns labelled a include the core polarization term. Those labelled b exclude it. All energies are in Hartree.

Potential A						
N	2p		3p		4p	
	a	b	a	b	a	b
5	−0.121288	−0.118409	−0.056240	−0.055540	−0.005833	−0.004352
7	−0.128669	−0.126337	−0.057169	−0.056518	−0.026850	−0.026288
9	−0.129984	−0.127787	−0.057232	−0.056581	−0.031031	−0.030686
11	−0.130187	−0.128019	−0.057240	−0.056588	−0.031839	−0.031549
13	−0.130214	−0.128051	−0.057241	−0.056590	−0.031963	−0.031686
15	−0.130218	−0.128055	−0.057242	−0.056591	−0.031978	−0.031703
17	−0.130218	−0.128056	−0.057242	−0.056591	−0.031979	−0.031704
19	−0.130218	−0.128056	−0.057242	−0.056591	−0.031979	−0.031704
Exptl.	−0.130245		−0.057239		−0.031976	

Table 4.2: Convergence of $l = 1$ states of the lithium model atom.

Potential B						
N	1s		2s		3s	
	a	b	a	b	a	b
5	−0.189486	−0.186568	−0.051279	−0.050150	−0.001962	−0.000942
7	−0.197402	−0.194904	−0.071531	−0.070901	−0.033673	−0.033312
9	−0.198110	−0.195665	−0.073929	−0.073390	−0.037949	−0.037720
11	−0.198155	−0.195715	−0.074170	−0.073645	−0.038541	−0.038342
13	−0.198158	−0.195717	−0.074187	−0.073664	−0.038607	−0.038413
15	−0.198158	−0.195718	−0.074188	−0.073665	−0.038615	−0.038422
17	−0.198158	−0.195718	−0.074188	−0.073665	−0.038617	−0.038424
19	−0.198158	−0.195718	−0.074188	−0.073665	−0.038618	−0.038424
Exptl.	−0.198158 (2s)		−0.074188 (3s)		−0.038618 (4s)	

Table 4.3: Convergence of $l = 0$ states of the lithium model atom.

Potential B						
N	2p		3p		4p	
	a	b	a	b	a	b
5	−0.097917	−0.096854	−0.050430	−0.050177	0.010914	0.011395
7	−0.111117	−0.110351	−0.051898	−0.051698	−0.021466	−0.021272
9	−0.113944	−0.113262	−0.051996	−0.051802	−0.027960	−0.027844
11	−0.114498	−0.113837	−0.052008	−0.051815	−0.029373	−0.029281
13	−0.114592	−0.113936	−0.052012	−0.051819	−0.029638	−0.029553
15	−0.114607	−0.113951	−0.052014	−0.051821	−0.029676	−0.029593
17	−0.114608	−0.113953	−0.052015	−0.051821	−0.029680	−0.029597
19	−0.114609	−0.113954	−0.052015	−0.051821	−0.029680	−0.029598
Exptl.	−0.130245		−0.057239		−0.031976	

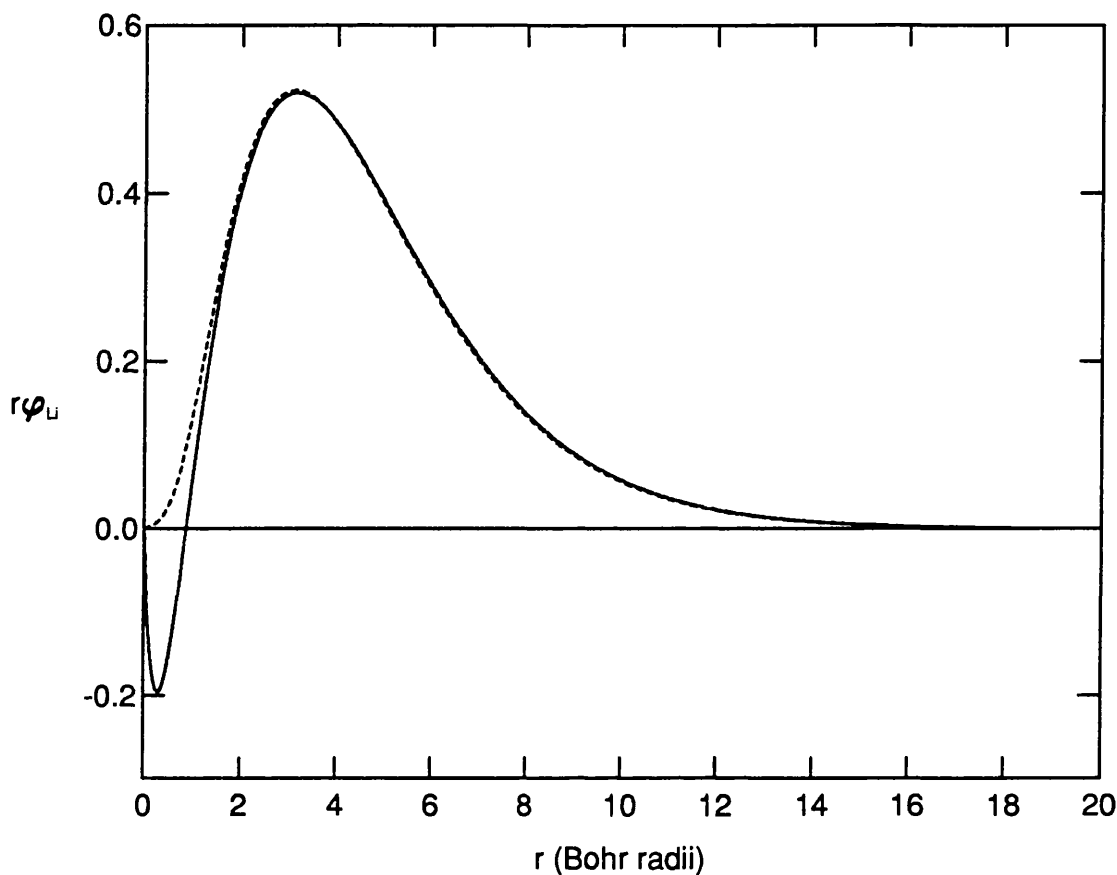Table 4.4: Convergence of $l = 1$ states of the lithium model atom.

Figure 4.4: The 'ground' state eigenfunctions of potentials A (solid) and B (dashed).

The Rayleigh-Ritz calculations of the energies of the first three s and p states of each model, as shown in tables 4.1-4.4, yielded six figure accuracy for $N = 19$ and a suitable choice of the non-linear parameter, α. For the ground states a value of $N = 15$ proved adequate for obtaining this level of convergence. Figure 4.4 shows the forms of the ground state eigenfunctions for both potentials. Figure 4.5 indicates the extent to which the form of the $2s$ eigenfunction of potential A is affected by the exclusion of the core polarization term. Both sets of data, for the full form of the Peach potential, and also that excluding the core polarization term, are seen to agree well with the experimental estimates quoted, which are those of Johansson (1958). The exclusion
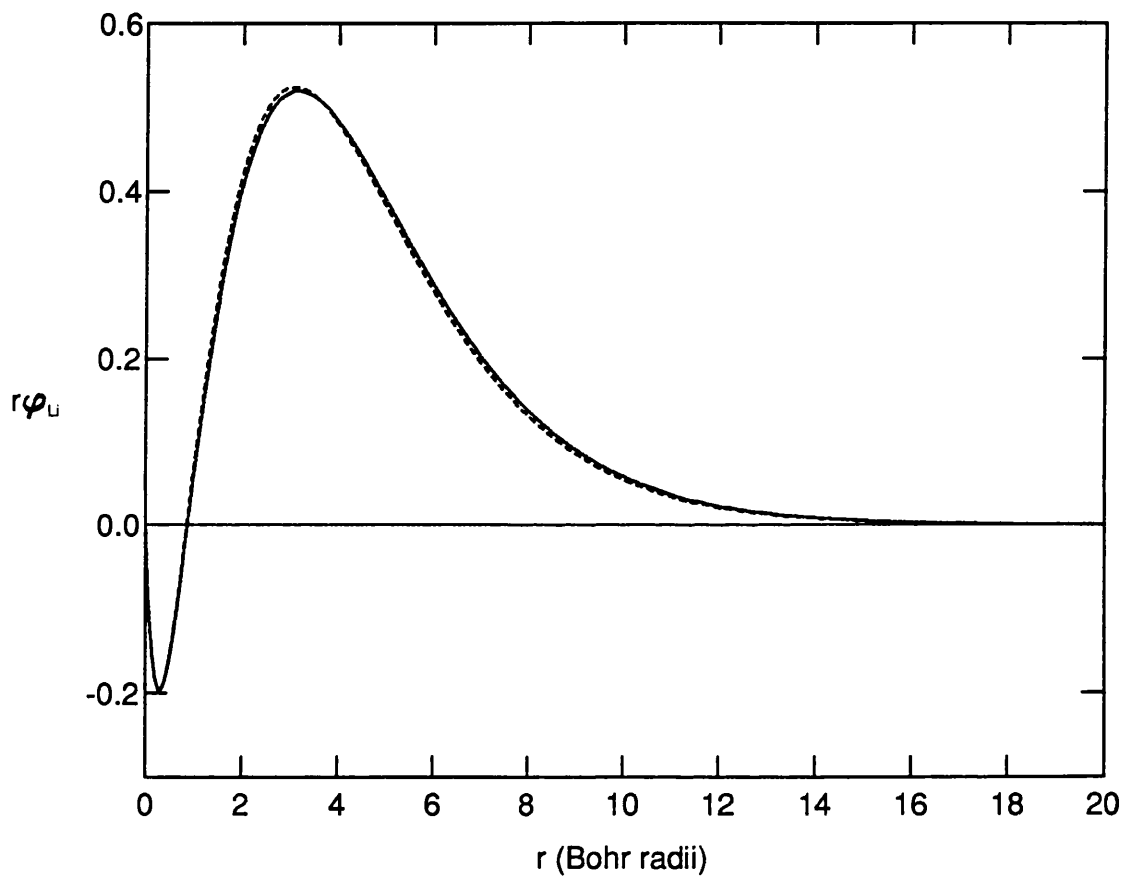
Figure 4.5: The 2s eigenfunctions of potential A with (solid) and without (dashed) the core polarization term.

of the term has the effect of shifting the energy of the ground state of potential A by about 2%, with its influence becoming smaller for higher states, as would be expected.

4.4 Determination of Polarizabilities

In addition to generating an energy spectrum which is in good agreement with experiment, a further desirable property of the lithium core-electron model potentials is that they should yield suitable values of the dipole polarizability, α_d, for their respective ground states. In order to determine α_d, it is necessary to consider the atom situated in a uniform electric field, ε, so that the Hamiltonian for the system becomes

$$H = -\tfrac{1}{2}\nabla^2 + V(r) - \varepsilon r \cos\theta, \qquad (4.8)$$

the electric field being chosen, without loss of generality, to lie along the z-axis. Perturbation theory shows that there is no first order correction to the unperturbed eigenvalues of the atomic spectrum as a consequence of the presence of the field, but that second order effects are important, so that for weak fields the correction, ΔE, is quadratic in ε, and is such as always to make the energies more negative. The dipole polarizability is then given by

$$\alpha_d = -\frac{2\Delta E}{\varepsilon^2}. \qquad (4.9)$$

To compute the perturbed energy spectrum of the lithium models in the presence of a polarizing field, a further Rayleigh-Ritz calculation was performed using the Hamiltonian (4.8), and a new form of trial function. Since the electric field destroys the spherical symmetry of the system, it is necessary to introduce an angular dependence, in the form of a p-state character, into the polarized wavefunction. A suitable form for the new trial function is thus

$$\phi_{Pol} = e^{-\alpha r}\left[\sum_{i=0}^{N-1} a_i r^i + \sum_{j=0}^{M-1} b_j r^j \cos\theta\right]. \qquad (4.10)$$

Potential A				Potential B		
M	Dipole polarizability, α_d			M	Dipole polarizability, α_d	
	a	b			a	b
5	160.91	171.86		5	120.05	124.28
6	164.75	176.50		6	133.38	138.91
7	165.16	177.07		7	136.93	142.91
8	165.29	177.23		8	138.16	144.30
9	165.29	177.24		9	138.38	144.56
10	165.29	177.24		10	138.44	144.63
11	165.29	177.24		11	138.45	144.65
12	165.29	177.24		12	138.45	144.65
Exptl.	163.98			Exptl.	163.98	

Table 4.5: Convergence of polarizabilities of the lithium models, in a_0^3, with respect to increasing the flexibility of the polarized wavefunction. Again, the columns a and b refer to the core polarization term being included and excluded respectively.

With the number of 's-type' terms fixed at $N = 15$, and the electric field strength set to $\varepsilon = 0.0001$au, convergence of the polarizabilities of the 2s state of potential A and the 1s state of potential B was studied with respect to increasing M, the number of 'p-type' terms. The results of these investigations are shown in table 4.5.

The experimental estimate for the dipole polarizability of lithium, quoted in the tables, is that of Miller and Bederson (1977). In comparison with this, the Rayleigh-Ritz estimate for the full form of potential A is in very good agreement, being rather less than 1% larger. Removing the core polarization term does have quite a pronounced effect, however, and increases the overall polarizability, making the error on the experimental estimate nearer to 8%.

Using potential B, the agreement between variational and experimental estimates is much poorer, which is not surprising in view of the relatively poor representation of the lithium p-states produced by this potential. With the full form, the Rayleigh-Ritz value is too small by approximately 16%, although removal of the core polarization term does have the effect of improving the agreement somewhat, yielding a value which

is in error by about 12%.

On the strength of the variational calculations of the energies and polarizabilities of the two lithium models, it was felt justifiable to proceed with the scattering calculation omitting the core polarization term. Its exclusion in the forms for the electron- and positron-core potentials, as mentioned earlier, simplifies the formulation of the scattering problem by preserving certain symmetry arguments, and dispensing with the need for the inclusion of a further three-body interaction term. The discrepancy between the theoretical and experimental estimates of α_d, arising as a consequence of ignoring the polarization of the core, is likely to affect very low energy scattering most markedly, since polarization effects are at their most important here, and this has to be borne in mind when assessing the accuracy of the scattering cross sections.

Chapter 5

Positron-Lithium Scattering

5.1 Introduction

As mentioned previously, the alkalis are unusual in positron-atom scattering in that the positronium formation channel is open for all energies of the incident positron; thus, in considering positron-lithium collisions at any energy, there are at least two scattering processes to be considered. In the investigations reported here, studies have been confined to the energy region below the $2p$ excitation threshold of the lithium atom (1.844eV), where only elastic scattering and Ps formation are possible, i.e.

$$e^+ + \text{Li} \rightarrow e^+ + \text{Li} \qquad \text{elastic scattering}$$

$$\rightarrow \text{Ps} + \text{Li}^+ \qquad \text{positronium formation.}$$
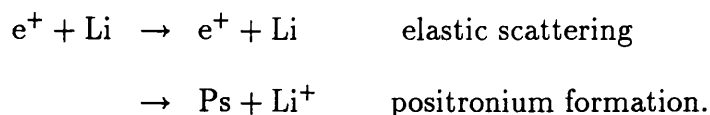
An extension of the two channel Kohn method, used previously for the hydrogen problem, is thus appropriate for the energy range considered here for positron-lithium scattering, and the basic structures of the existing e^+-H codes have been used as the starting point for the present calculations.

For systems where an inelastic channel is open from zero energy, as is the case here, Wigner's threshold theory can be used to predict the k dependence of the cross section for this process at very low energies. At zero positron energy, we are at the threshold

for the endothermic process

$$Ps + Li^+ \rightarrow e^+ + Li. \tag{5.1}$$
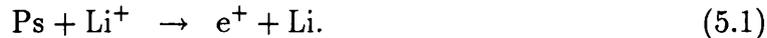
If we denote the partial cross sections for this reaction by σ_{21}^l, then, from equation (3.2), we can express σ_{21}^l in terms of the outgoing positron wavenumber as

$$\lim_{k \to 0} \sigma_{21}^l \propto k^{2l+1}. \tag{5.2}$$

The positronium formation cross section, σ_{12}^l, is easily expressible in terms of σ_{21}^l. In terms of the S-matrix we have

$$\sigma_{12}^l = \frac{\pi}{k^2}(2l+1)\left|S_{12}^l\right|^2 \tag{5.3}$$

and

$$\sigma_{21}^l = \frac{\pi}{\kappa^2}(2l+1)\left|S_{21}^l\right|^2, \tag{5.4}$$

but since $S_{12}^l = S_{21}^l$, we find

$$\sigma_{12}^l = \frac{\kappa^2}{k^2}\sigma_{21}^l \tag{5.5}$$

and thus, from (5.2)

$$\lim_{k \to 0} \sigma_{12}^l \propto \kappa^2 k^{2l-1}. \tag{5.6}$$

For s-wave scattering, therefore, we have the result that the positronium formation cross section becomes inversely proportional to k at very low positron energies, and is infinite at $k = 0$. For the higher partial waves, σ_{Ps}^l ($= \sigma_{12}^l$) is zero when the incident positron energy is zero. These features should be reproducible in the Kohn calculation.

In considering e^+-Li scattering in the context of e^+-H interactions, one of the major differences to be noted is that between the dipole polarizabilities of the two targets: for atomic hydrogen, $\alpha_d = 4.5a_0^3$, as compared with $163.98a_0^3$ for lithium. The very high polarizability of the lithium atom inevitably puts great demands on the scattering trial functions, particularly at low energies, since the valence electron is very easily

drawn away from the core by the field of the positron. For this reason, it is important that these wavefunctions be sufficiently flexible in form to allow for the complicated interactions which arise when the particles are close to one another. The best test of the suitability of the forms is the rate at which results converge with respect to systematic improvements in flexibility, and two slightly different forms of short-range function have been used in an effort to find the most satisfactory convergence.

5.2 Positron-Lithium s-wave Scattering

5.2.1 Old Form of Trial Function

The original forms which were used for the lithium s-wave trial functions are identical to those used for hydrogen, (2.2) and (2.3), but with the hydrogen wavefunction $\phi_{\mathrm{H}}(r_2)$ replaced by the lithium target function $\phi_{\mathrm{Li}}(r_2)$, calculated in chapter 4, thus

$$
\begin{aligned}
\Psi_1 &= Y_{00}(\theta_1, \phi_1)\Phi_{\mathrm{Li}}(r_2)\sqrt{k}\left\{j_0(kr_1) - K_{11}^t n_0(kr_1)\left[1 - \exp(-\lambda r_1)\right]\right\} \\
&\quad - Y_{00}(\theta_\rho, \phi_\rho)\Phi_{\mathrm{Ps}}(r_3)\sqrt{2\kappa}K_{21}^t\left[n_0(\kappa\rho) + \exp(-\mu\rho)(1 + a\rho + b\rho^2)/\kappa\rho\right] \\
&\quad + Y_{00}(\theta_1, \phi_1)\Phi_{\mathrm{Li}}(r_2)\exp\left(-(\alpha r_1 + \beta r_2 + \gamma r_3)\right)\sum_{i=1}^{N} c_i r_1^{k_i} r_2^{l_i} r_3^{m_i} \qquad (5.7) \\
\Psi_2 &= Y_{00}(\theta_\rho, \phi_\rho)\Phi_{\mathrm{Ps}}(r_3)\sqrt{2\kappa}\left\{j_0(\kappa\rho) - K_{22}^t\left[n_0(\kappa\rho) + \exp(-\mu\rho)(1 + a\rho + b\rho^2)/\kappa\rho\right]\right\} \\
&\quad - Y_{00}(\theta_1, \phi_1)\Phi_{\mathrm{Li}}(r_2)\sqrt{k}K_{12}^t n_0(kr_1)\left[1 - \exp(-\lambda r_1)\right] \\
&\quad + Y_{00}(\theta_1, \phi_1)\Phi_{\mathrm{Li}}(r_2)\exp\left(-(\alpha r_1 + \beta r_2 + \gamma r_3)\right)\sum_{j=1}^{N} d_j r_1^{k_j} r_2^{l_j} r_3^{m_j}. \qquad (5.8)
\end{aligned}
$$

The formulation then proceeds on the assumption that the lithium eigenfunction evaluated in the Rayleigh-Ritz calculation of chapter 4 is an exact eigenfunction of the model Hamiltonian, so that the expressions for L operating on the various terms in the trial function have the same forms as those derived for hydrogen in chapter 2.

The elements of the matrices A, B and (S, LS) of equation (2.14) are built up using numerical integration methods throughout, since the presence of $\phi_{\mathrm{Li}}(r_2)$ in all components of the scattering wavefunction makes analytic integration impractical, even for

the simpler long-range–long-range terms. Once these matrices have been generated, however, the operations performed to evaluate the variational K-matrix and cross sections are the same for lithium as for hydrogen. The major modifications made to the hydrogen codes are thus the incorporation of the lithium model potentials in place of the pure Coulombic form, and the inclusion of the ground state wavefunctions of the new target.

5.2.2   Choice of Non-linear Parameters

At first sight, it would appear that the choice of the non-linear parameters α, β and γ in (5.7) and (5.8) would not be of great importance, provided they were selected so as to suppress the Hylleraas terms in the wavefunction effectively at ranges greater than a few atomic radii. However, whilst it is true that a large enough basis set can compensate for a poor choice of non-linear parameters, it is also the case that rates of convergence can be improved greatly by selecting a suitable set of values of these parameters. In fact, it was found in earlier work on positron-hydrogen scattering that, particularly for the higher partial waves, results are actually very sensitive to the values of the non-linear parameters. This situation arises because of the necessity for the wavefunction to represent all possible scattering processes, real and virtual, which might take place; for the higher partial waves in hydrogen ($l \geq 1$), the positronium formation and elastic scattering cross sections are comparable in magnitude, and the choice of α, β and γ has to suit the two different channels simultaneously. It is to be expected, therefore, that in positron-lithium scattering, results and rates of convergence will be very much dependent on a suitable set of values for these exponential parameters, particularly since we know, in the s-wave case, that positronium formation is the dominant channel close to zero energy.

The parameters α, β and γ determine the exponential fall off in the positron-core, electron-core and electron-positron coordinates respectively. Without knowing very

much, however, about the relative importance of the two possible scattering processes over most of the energy range considered, it is difficult to predict suitable values for them in advance. Broadly speaking, one might suppose that, since the positron will tend to attract the outer electron away from the core, the wavefunction will be stretched out in the r_2 coordinate more than the lithium target function is, making a negative value for β appropriate. Since, also, the ground state positronium eigenfunction has a simple $e^{-\frac{1}{2}r_3}$ dependence, it might be assumed that a value of γ greater than 0.5 would be physically unrealistic.

Although these considerations provide a very general guide to the choice of parameters, they are rather too simplistic to be of very much use. When the exponential factor is multiplied by the polynomial expansion in the three inter-particle coordinates, r_1, r_2 and r_3, the resulting rate of decay of the short-range wavefunction changes, particularly as higher powers are included, in a way which is very difficult to predict. Problems are compounded by the fact that the optimum values of the non-linear parameters are likely to alter with respect to the number of Hylleraas terms, and also to be energy dependent although, from the point of view of studying convergence and deriving cross sections which vary continuously with energy, it is desirable to have a single set of exponential parameters with which to work.

The inclusion of a loop structure within the positron-lithium code, allowing one non-linear parameter to be varied, keeping the others fixed, enabled the dependence of the K-matrix on the non-linear parameters to be studied for a given energy and a small number of linear parameters, typically 20 ($\omega = 3$). With α and γ fixed, β could be varied to find a region where the diagonal K-matrix elements displayed either a local maximum, or at least reasonable stability, for both Kohn and Inverse Kohn methods. With β fixed at this stable value, one of the other parameters could then be varied, followed by the remaining one. The cycle was repeated in an attempt to find a region
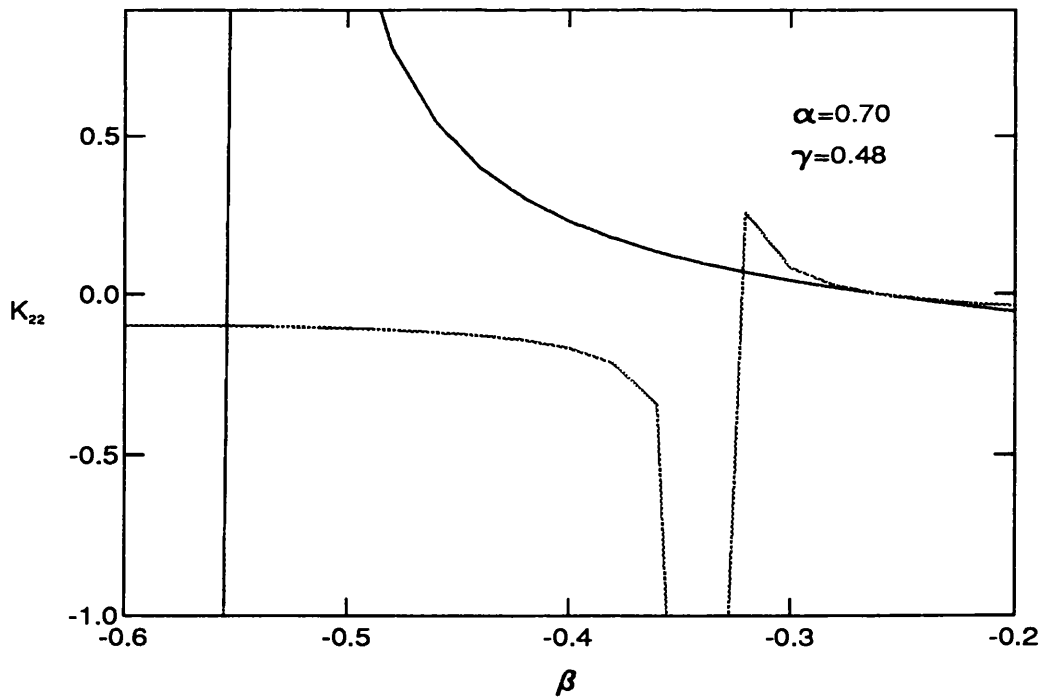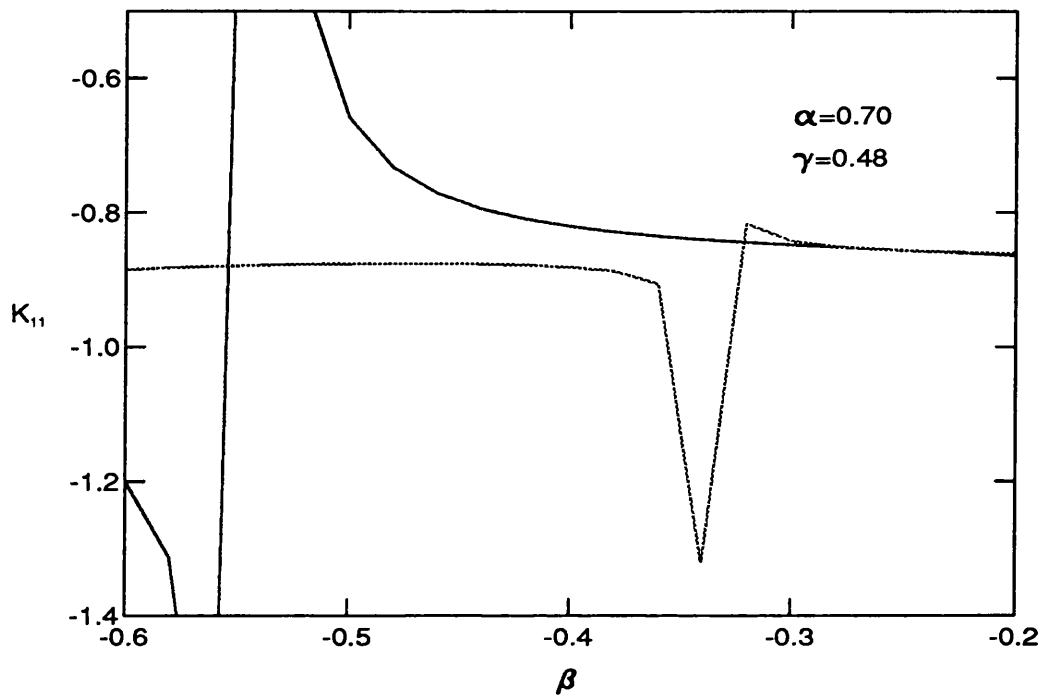
Figure 5.1: Variation of K-matrix with respect to β for positron-lithium s-wave scattering, with the old style of wavefunction, where $k = 0.1$ and $\omega = 3$. The solid and dashed lines correspond to Kohn and Inverse Kohn results respectively.
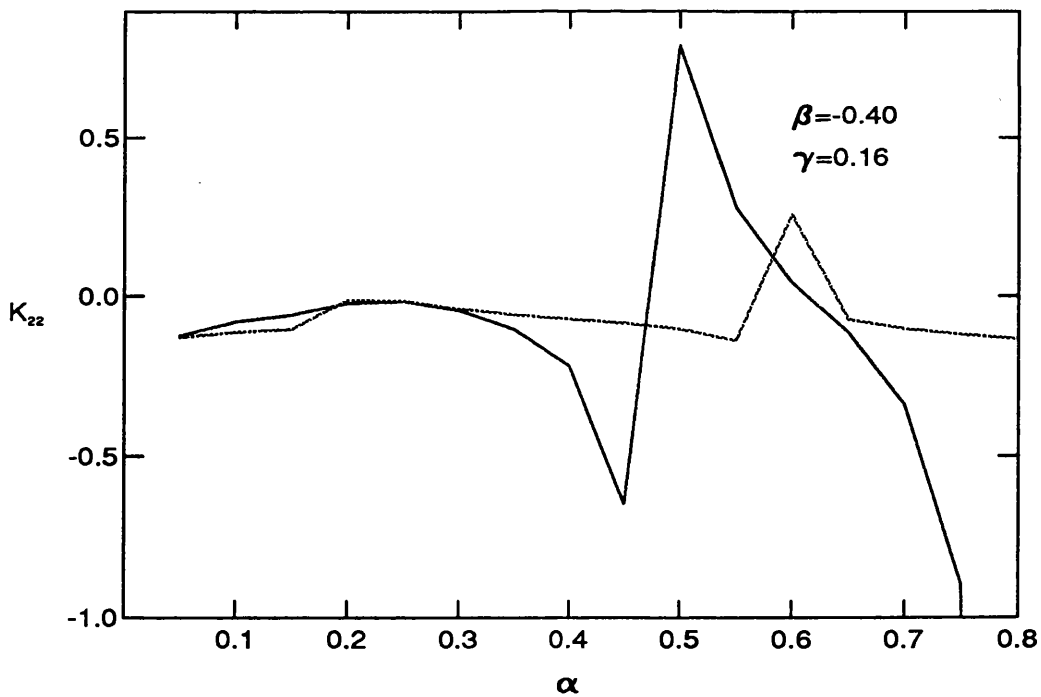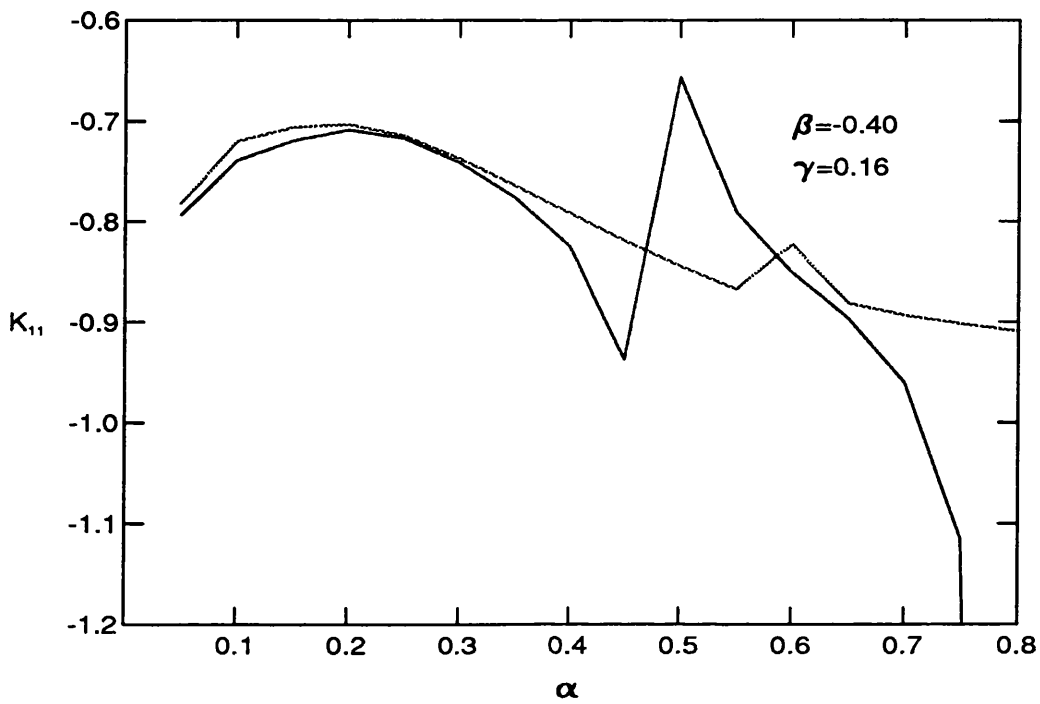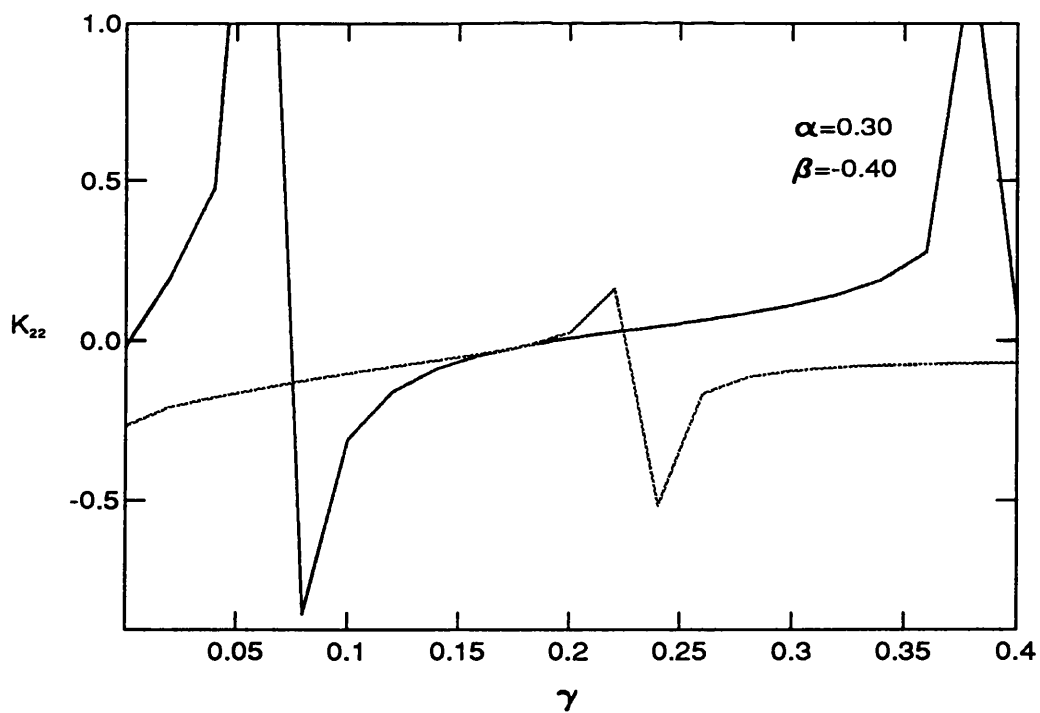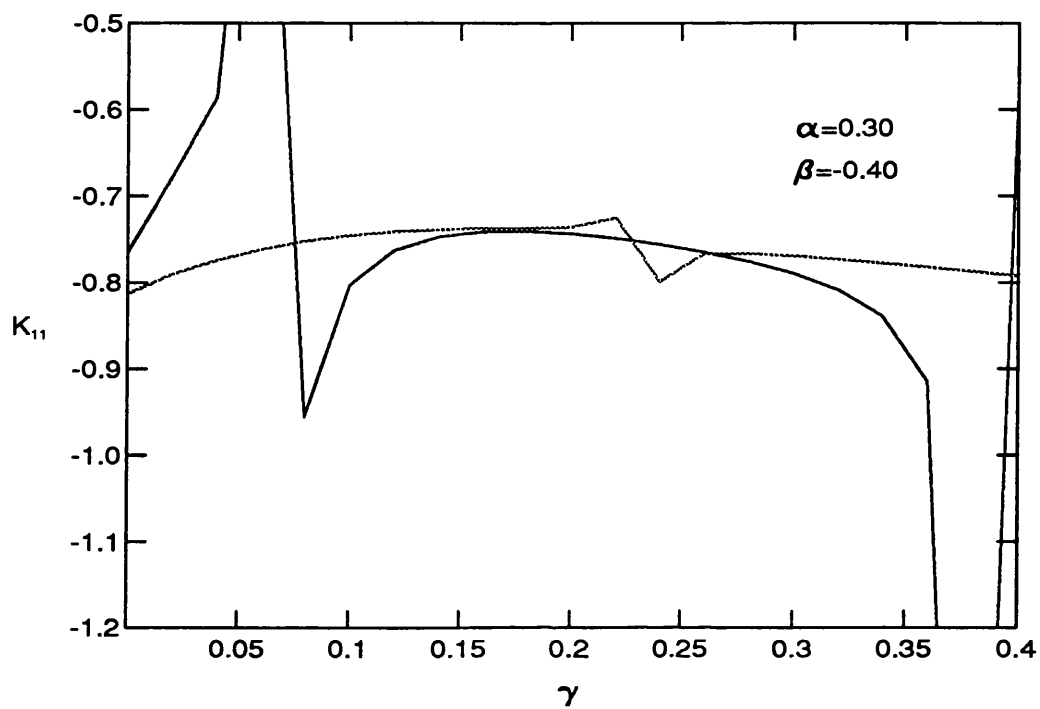
Figure 5.2: Variation of K-matrix with respect to α for positron-lithium s-wave scattering, with the old style of wavefunction, where $k = 0.1$ and $\omega = 3$. The solid and dashed lines correspond to Kohn and Inverse Kohn results respectively.

Figure 5.3: Variation of K-matrix with respect to γ for positron-lithium s-wave scattering, with the old style of wavefunction, where $k = 0.1$ and $\omega = 3$. The solid and dashed lines correspond to Kohn and Inverse Kohn results respectively.

of the non-linear parameter space which was stable with respect to variations in all three parameters. Extensive searches were carried out in this way for an energy which was intermediate in the range considered; a sample of the graphical output from this procedure is contained in figures 5.1-5.3.

Although this method provided some useful information, the search for suitable values for α, β and γ proved problematical because of their strong interdependence, at least for a low ω. The method could conceivably be used for a larger number of linear parameters, but would obviously be considerably more time consuming. The values eventually settled on for the original form of s-wave trial function were $\alpha = 0.17$, $\beta = -0.40$ and $\gamma = 0.20$.

5.2.3 Results Using Old Form of Trial Function

With this original type of wavefunction, calculations were performed using up to 165 linear parameters ($\omega = 8$), for wavenumbers of the incident positron ranging from $k = 0.01a_0^{-1}$ up to $k = 0.36a_0^{-1}$, the first excitation threshold of potential A. A reasonably smooth set of results was obtained for the elastic scattering cross section, with good agreement between the Kohn and Inverse Kohn calculations, but the positronium formation cross sections were generally not in such good agreement, although a trend could be observed which seemed to support Wigner's predictions close to zero energy. Convergence of the K-matrix at low energies was also found to be rather poor, as illustrated in figure 5.4. Rather better convergence was obtained at intermediate energies, as in figure 5.5, where the positronium formation cross section was small in comparison to that for elastic scattering.

5.2.4 New Form of Trial Function

Bearing in mind the large distortions that an atom as polarizable as lithium is likely to undergo when experiencing the field of the incoming positron, it is evident that the
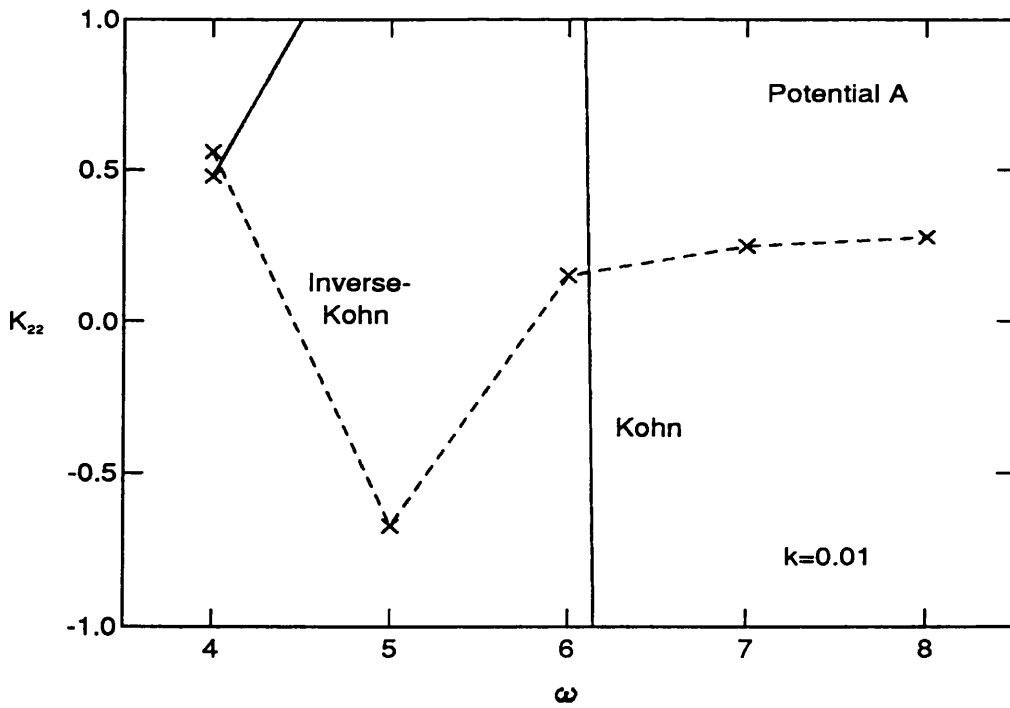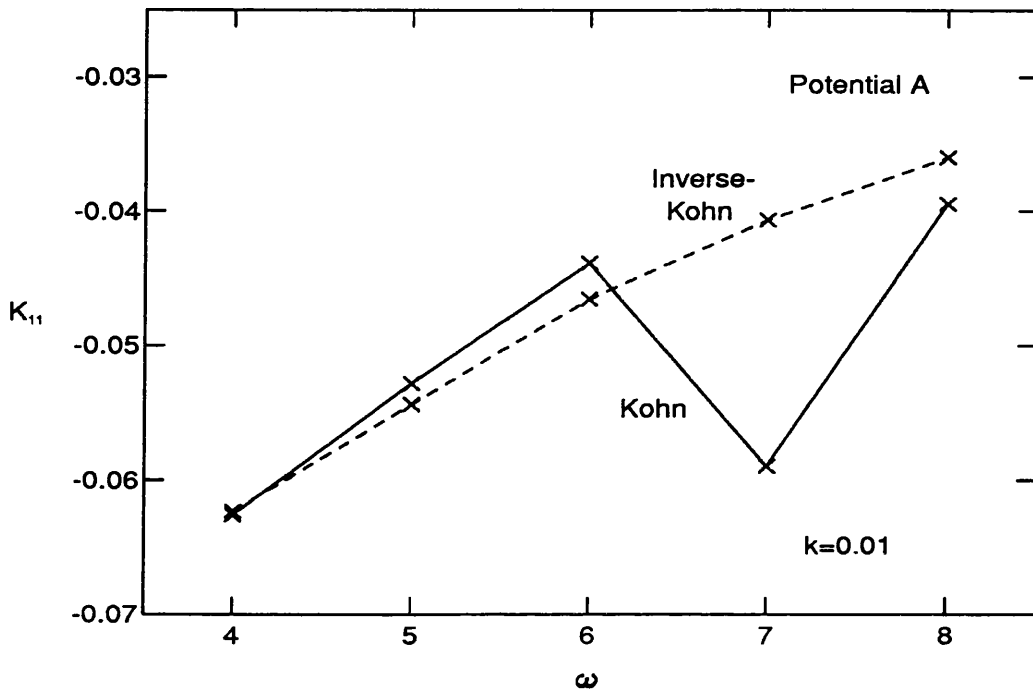
Figure 5.4: Positron-lithium s-wave scattering, potential A. Convergence of the diagonal K-matrix elements for the old style of wavefunction. $k = 0.01$
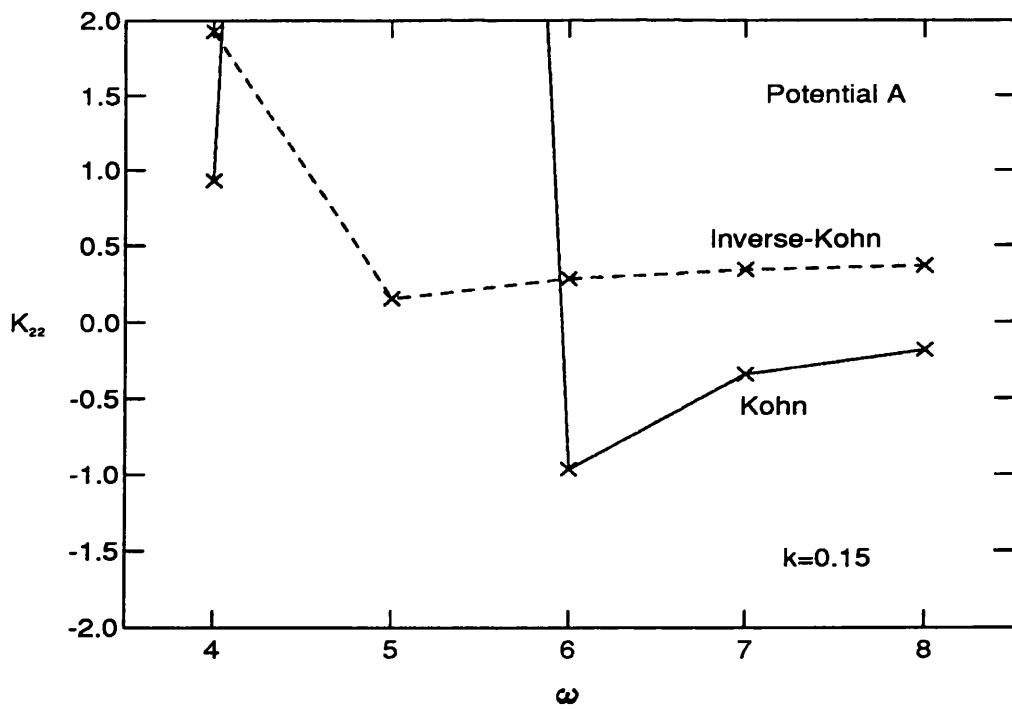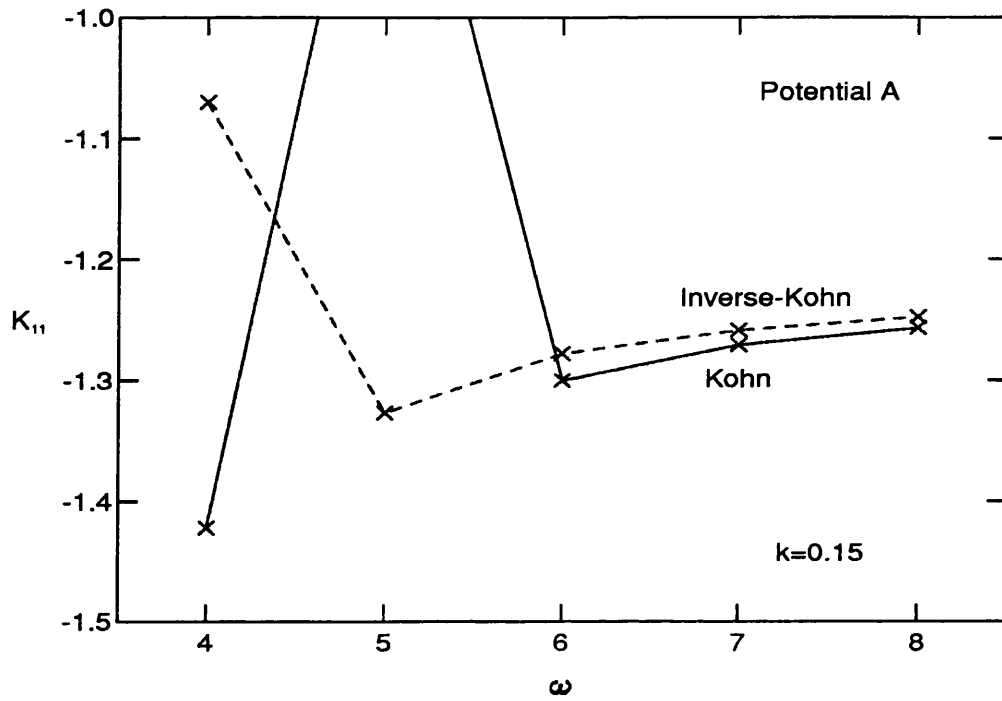
Figure 5.5: Positron-lithium s-wave scattering, potential A. Convergence of the diagonal K-matrix elements for the old style of wavefunction. $k = 0.15$

main drawback with the original style of wavefunction is the restrictive nature of the product form of short-range component. By multiplying every term in the Hylleraas expansion by the lithium target function, a form for the scattering wavefunction is suggested which may not be appropriate when the particles are in close proximity to one another, especially where positronium formation eventually results. For potential A, in particular, the node in the $2s$ eigenfunction forces a node in the scattering wavefunction at the same value of the r_2 coordinate, which is an inappropriate restriction. Although the inclusion of enough Hylleraas terms should ensure a reasonably good result, the convergence rate will be much worse if the overall form of trial function is unsuitable. In the positron-hydrogen calculation, this problem does not really arise in the same way, because of the simple exponential form of the nodeless target wavefunction. Any constraint that the product form of short-range function imposes here can be compensated by an appropriate choice of the non-linear parameter β, which governs the exponential fall-off in r_2.

It was therefore felt that convergence was likely to be improved substantially by removing all reference to $\phi_{\text{Li}}(r_2)$ in the short-range correlation terms, thus giving more freedom to the form of scattering wavefunction.

The new trial functions thus take the form

$$
\begin{aligned}
\Psi_1 \; = \; & Y_{00}(\theta_1, \phi_1)\Phi_{\text{Li}}(r_2)\sqrt{k}\left\{j_0(kr_1) - K_{11}^t n_0(kr_1)\left[1 - \exp(-\lambda r_1)\right]\right\} \\
& -Y_{00}(\theta_\rho, \phi_\rho)\Phi_{\text{Ps}}(r_3)\sqrt{2\kappa}K_{21}^t\left[n_0(\kappa\rho) + \exp(-\mu\rho)(1 + a\rho + b\rho^2)/\kappa\rho\right] \\
& +Y_{00}(\theta_1, \phi_1)\exp\left(-(\alpha r_1 + \beta r_2 + \gamma r_3)\right)\sum_{i=1}^{N} c_i r_1^{k_i} r_2^{l_i} r_3^{m_i} \qquad\qquad (5.9)
\end{aligned}
$$

$$
\begin{aligned}
\Psi_2 \; = \; & Y_{00}(\theta_\rho, \phi_\rho)\Phi_{\text{Ps}}(r_3)\sqrt{2\kappa}\left\{j_0(\kappa\rho) - K_{22}^t\left[n_0(\kappa\rho) + \exp(-\mu\rho)(1 + a\rho + b\rho^2)/\kappa\rho\right]\right\} \\
& -Y_{00}(\theta_1, \phi_1)\Phi_{\text{Li}}(r_2)\sqrt{k}K_{12}^t n_0(kr_1)\left[1 - \exp(-\lambda r_1)\right] \\
& +Y_{00}(\theta_1, \phi_1)\exp\left(-(\alpha r_1 + \beta r_2 + \gamma r_3)\right)\sum_{j=1}^{N} d_j r_1^{k_j} r_2^{l_j} r_3^{m_j}, \qquad\qquad (5.10)
\end{aligned}
$$

the product forms of the long-range terms being retained, in order that the correct

asymptotic conditions are satisfied.

Because there is no reference to the lithium target function in the short-range terms, it is necessary to change the way in which the short-range–short-range terms in the matrix A of (2.15) are evaluated. Thus, where the operator $L = 2(H - E)$ operates on the functions ϕ_i, explicit reference is now made to the electron-core interaction and the ground state energy of the target model atom. The form of a short-range–short-range matrix element for the new style of trial function is

$$(\phi_i, L\phi_j) = \int \phi_i \left(-\nabla_1^2 - \nabla_2^2 + 2V^+(r_1) + 2V^-(r_2) - \frac{2}{r_3} - k^2 - 2E_0 \right) \phi_j d\tau \quad (5.11)$$

where

$$\phi_i = Y_{00}(\theta_1, \phi_1) r_1^{k_i} r_2^{l_i} r_3^{m_i} \exp[-(\alpha r_1 + \beta r_2 + \gamma r_3)]. \quad (5.12)$$

Integrating by parts, as we did for the hydrogen short-range elements, we find

$$(\phi_i, L\phi_j) = \int \left\{ [\nabla_1 \phi_i \cdot \nabla_1 \phi_j + \nabla_2 \phi_i \cdot \nabla_2 \phi_j] \right.$$
$$\left. + \left(2V^+ + 2V^- - \frac{2}{r_3} - k^2 - 2E_0 \right) \phi_i \phi_j \right\} d\tau, \quad (5.13)$$

which is the same in form as (2.38) for the product type of short-range term, but contains no reference to the target atom wavefunction, whilst including the full form of the interaction potential.

A further search of the non-linear parameter space showed that the optimum values of the parameters α and γ were not greatly affected by the change in form of the trial function. With the removal of the lithium target function, however, and the exponential dependence on r_2 contained therein, it was necessary to adjust the value of β considerably to compensate. The most suitable values found for s-wave scattering with the new style of wavefunction were $\alpha = 0.13$, $\beta = 0.74$ and $\gamma = 0.17$.

5.2.5 Results for *s*-wave Scattering

Both of the lithium model potentials were used with the new style of wavefunction to perform calculations over the energy range from close to zero, up to the slightly differing excitation thresholds of the two potentials. As with the original form of trial function, a maximum of 165 linear parameters, corresponding to $\omega = 8$, was used. The non-linear parameters used were the same for both potentials.

It was immediately apparent that agreement between the Kohn and Inverse Kohn results for positronium formation was much improved, as were rates of convergence of the diagonal K-matrix elements, as shown in figures 5.6-5.9. In nearly all cases, the values of K_{11} and K_{22} obtained with the new type of trial function were more positive, and hence probably more accurate (according to the empirical lower bound), than corresponding results using the old style.

Tables 5.1-5.4 show the most accurate estimates obtained, for both potentials, of the variational K-matrix and cross sections at four energies across the range considered. Figures 5.10 and 5.11 show plots of the variation of the elastic scattering and positronium formation cross sections with k; the results here are sampled from both the Kohn and Inverse Kohn calculations, in order to circumvent the problem of Schwartz singularities. The cross sections obtained using the ordinary Kohn functional are used as the starting point, with Inverse Kohn results being substituted wherever irregular behaviour is encountered. Also included in figures 5.10 and 5.11, for comparison, are the results of McAlinden, Kernoghan and Walters (1994a), who have performed the most sophisticated close-coupling calculation to date of positron-lithium scattering, using up to nine states/pseudostates of Ps, and up to five states of Li; these results supersede those of Hewitt *et al.* (1992) who use fewer states in their close-coupling calculation. The curves included on these graphs use the expansion Ps($1s,2s,\overline{3s},\overline{4s},2p,\overline{3p},\overline{4p},\overline{3d},\overline{4d}$) plus Li($2s,2p,3s,3p,3d$), where the Ps pseudostates are appropriately scaled versions of

96

the hydrogen pseudostates of Fon *et al.* (1981), and the lithium states are taken from Weiss (1963). Figure 5.12 shows how fast the close-coupling results change (particularly the Ps formation cross section) as more states are included. The full legend for these plots is:

5 state: $Ps(1s,2s,2p) + Li(2s,2p)$

8 state: $Ps(1s,2s,2p) + Li(2s,2p,3s,3p,3d)$

11 state: $Ps(1s,2s,\overline{3s},\overline{4s},2p,\overline{3p}, \overline{4p}, \overline{3d},\overline{4d}) + Li(2s,2p)$

14 state: $Ps(1s,2s,\overline{3s},\overline{4s},2p,\overline{3p}, \overline{4p}, \overline{3d},\overline{4d}) + Li(2s,2p,3s,3p,3d)$,

where the 5 and 8 state results are those published in McAlinden *et al.* (1994b). Note that results shown for σ_{Ps} obtained using only three states of Ps are scaled down by a factor of one thousand.

In figure 5.13, the elastic cross section is again plotted as a function of k, but here the positronium channel is suppressed. This amounts to removing all the matrix elements in equation (3.16) which contain reference to the long-range positronium terms, S_2 and C_2. Although virtual positronium formation may still be represented through the short-range Hylleraas terms, this formulation artificially forces all scattering to take place via the elastic channel. Thus, in regions where the positronium formation cross section is normally of large magnitude, it is to be expected that the trial function will be under considerable strain to represent the scattering process. Though physically unrealistic, it is interesting to see the effect of preventing scattering into a channel which is energetically viable, particularly since several of the earlier close-coupling calculations of positron-alkali scattering ignored Ps formation (e.g. McEachran *et al.* (1990)). It should be noted, however, that uncoupling the Ps channel in a Kohn variational calculation is somewhat different from excluding states of Ps in the close-coupling formalism, since in the latter case virtual Ps formation is also suppressed.
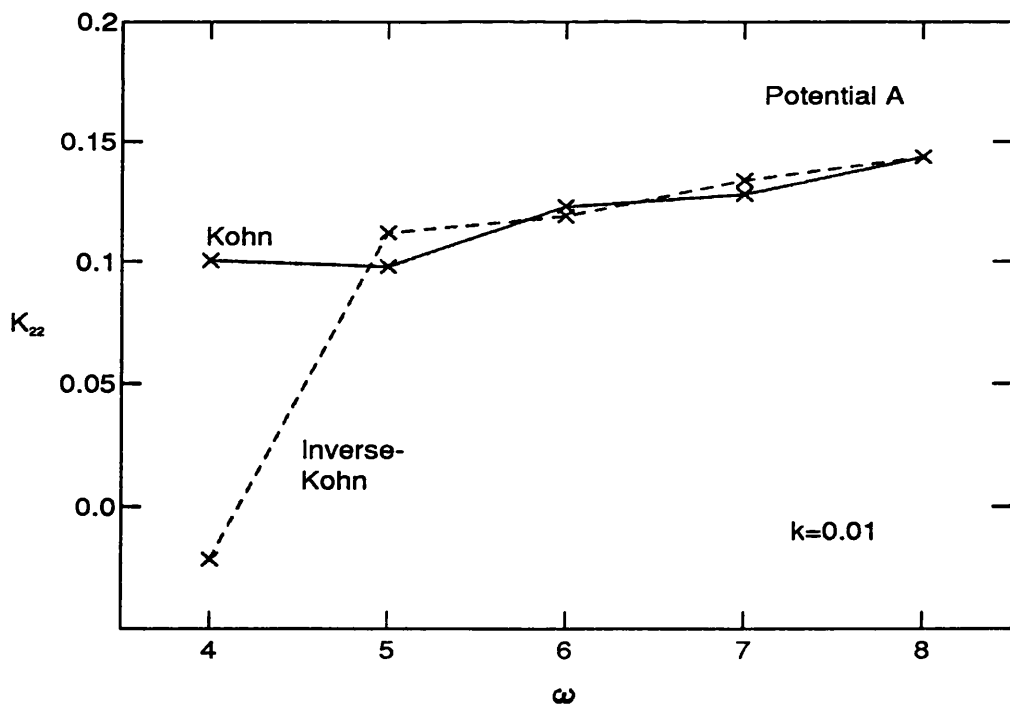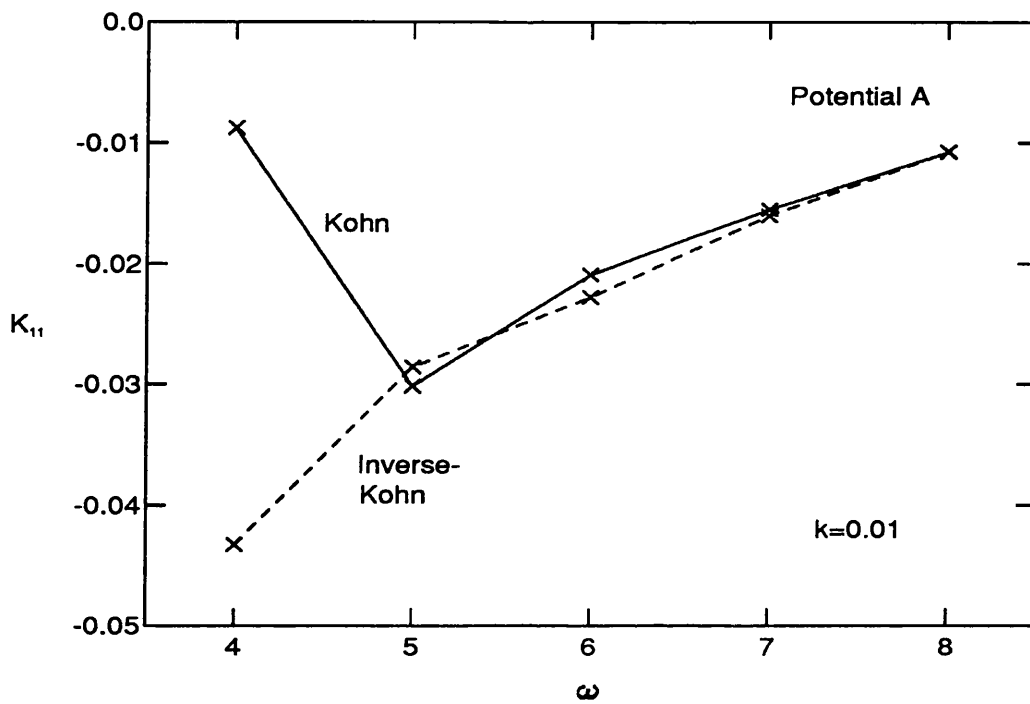
Figure 5.6: Positron-lithium s-wave scattering, potential A. Convergence of the diagonal K-matrix elements for the new style of wavefunction. $k = 0.01$
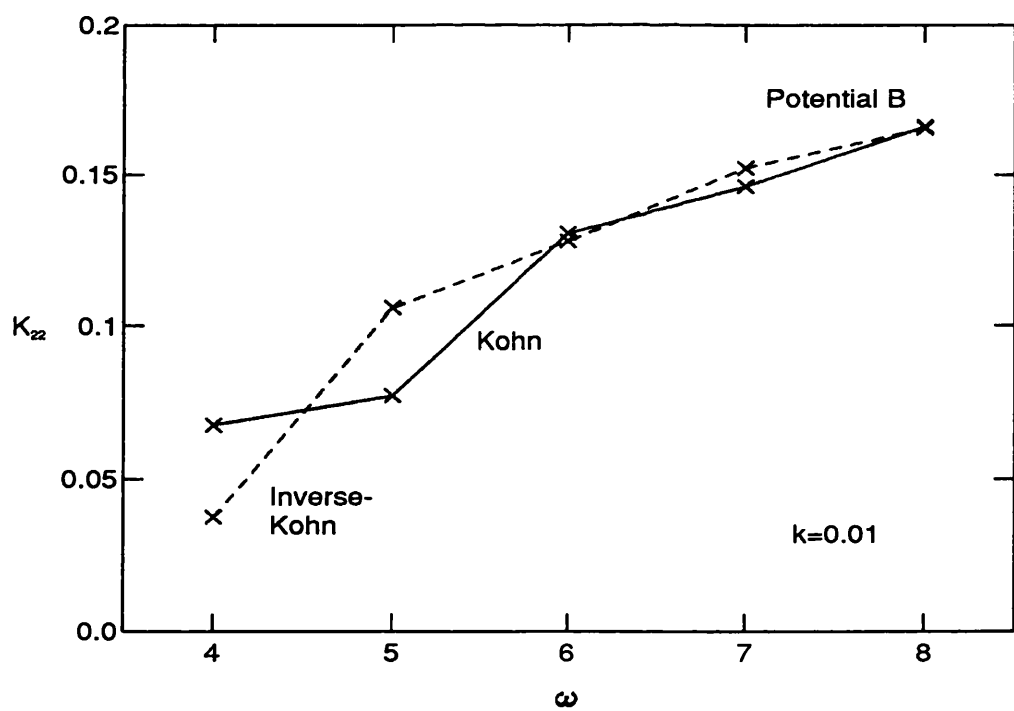
Figure 5.7: Positron-lithium s-wave scattering, potential B. Convergence of the diagonal K-matrix elements for the new style of wavefunction. $k = 0.01$

Figure 5.8: Positron-lithium s-wave scattering, potential A. Convergence of the diagonal K-matrix elements for the new style of wavefunction. $k = 0.15$
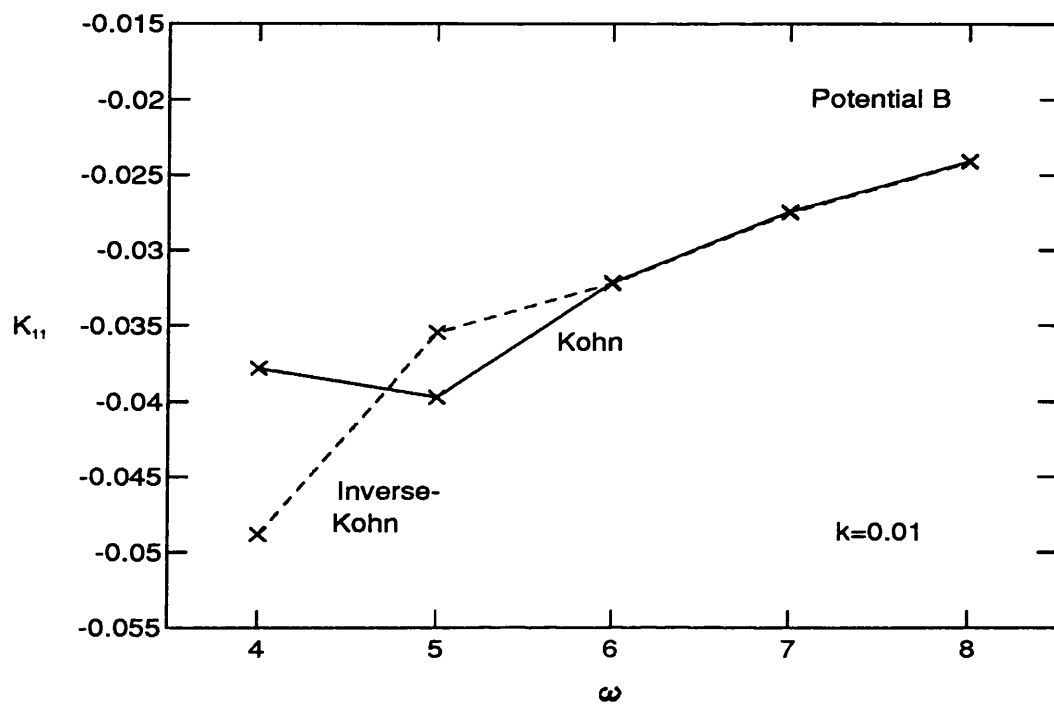
Figure 5.9: Positron-lithium s-wave scattering, potential B. Convergence of the diagonal K-matrix elements for the new style of wavefunction. $k = 0.15$
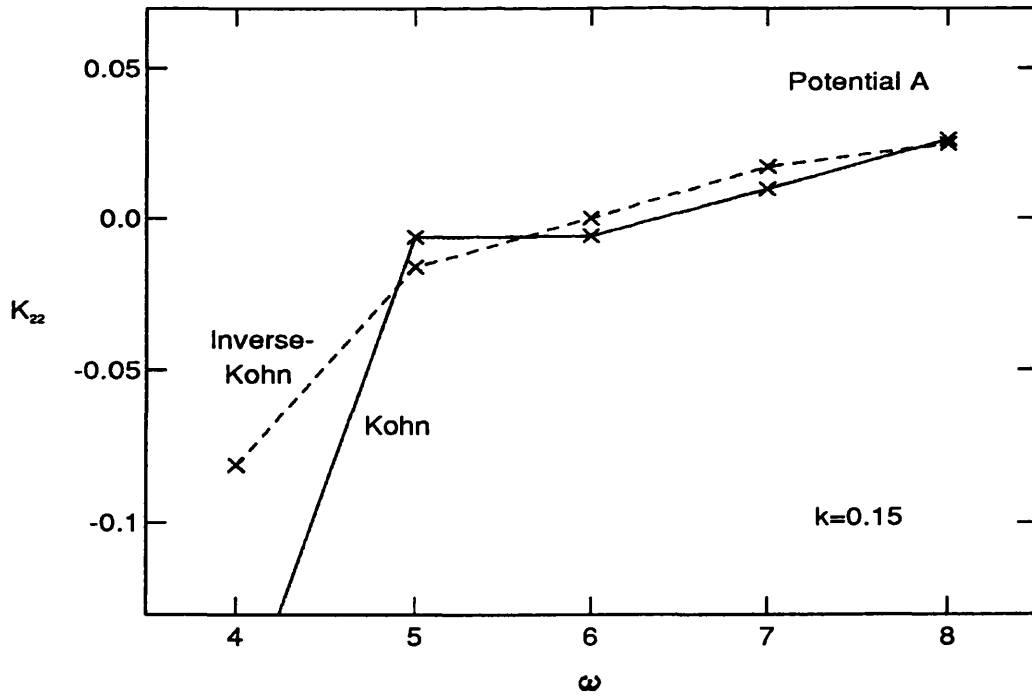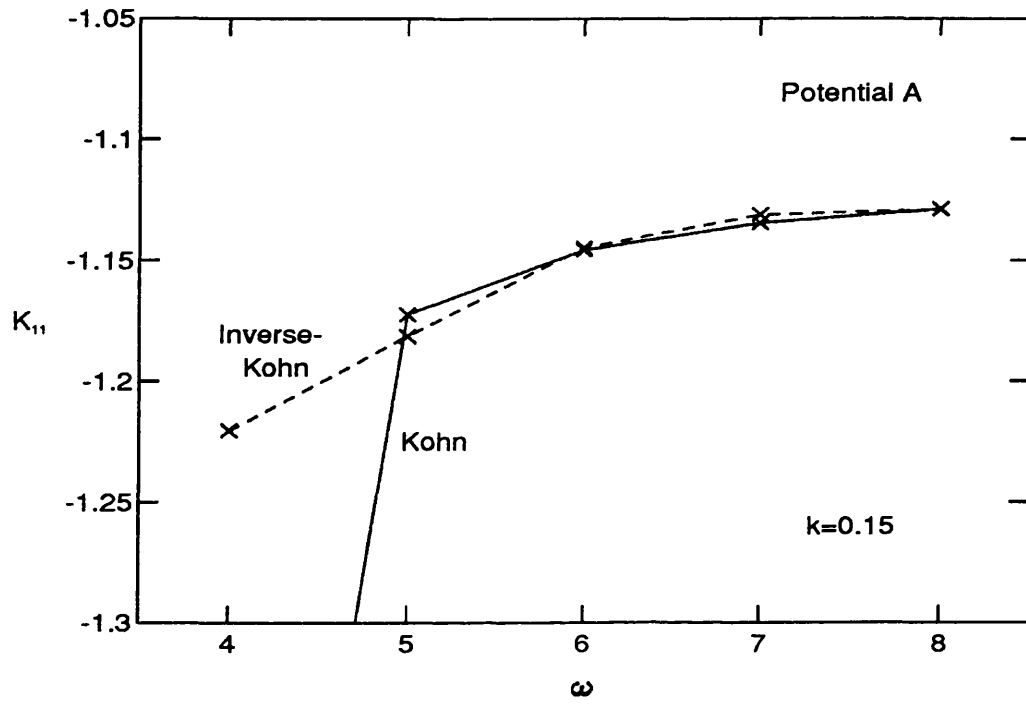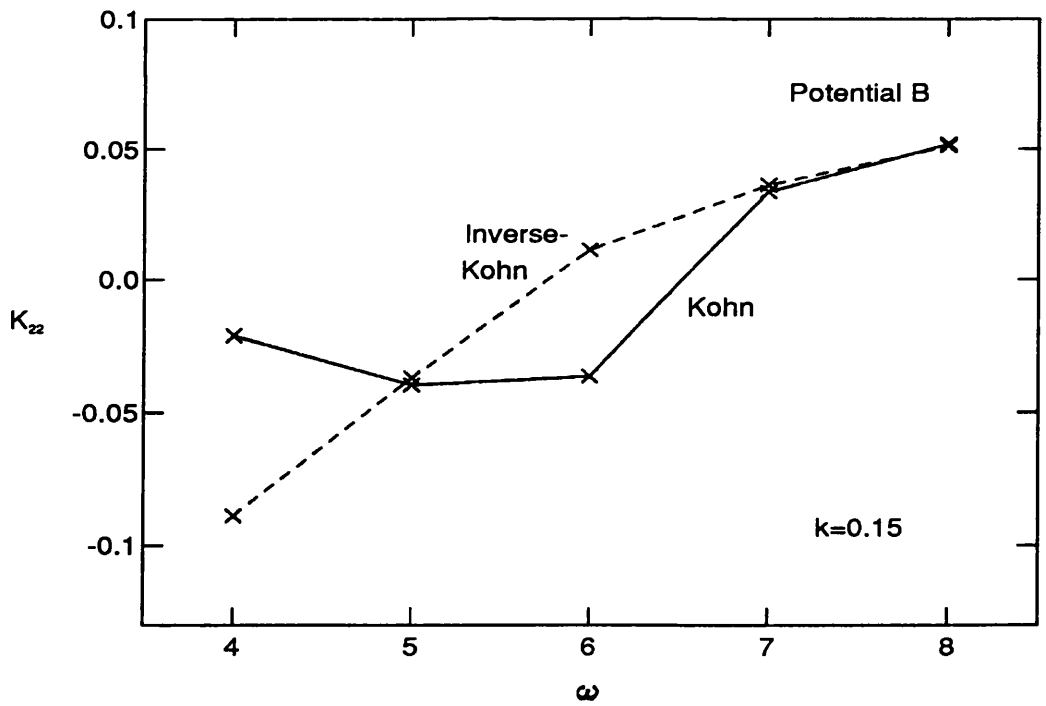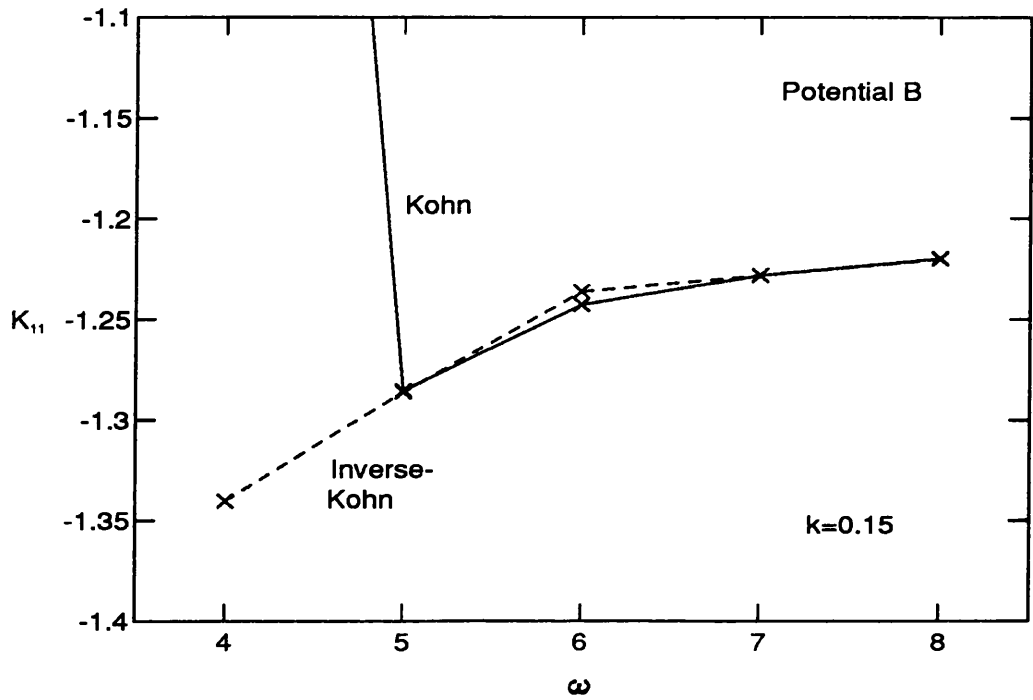
101

$k(a_0^{-1})$	K_{11}	K_{12}	K_{21}	K_{22}
0.01	−0.010755	−0.000550	−0.000473	0.143458
	−0.010726	−0.000558	−0.000481	0.143436
0.10	−0.547425	0.001483	0.001629	0.088526
	−0.547824	0.000861	0.000996	0.087628
0.20	−2.357052	0.012639	0.012535	−0.049412
	−2.253357	0.028032	0.028160	−0.052214
0.30	6.460034	−0.016368	−0.016329	−0.243272
	6.428105	−0.013708	−0.013622	−0.237123

Table 5.1: K-matrix elements for positron-lithium s-wave scattering, potential A, $\omega = 8$.

$k(a_0^{-1})$	σ_{11}	σ_{12}	σ_{21}	σ_{22}
0.01	4.62613	0.00877	0.00001	0.35866
	4.60165	0.00905	0.00001	0.35855
0.10	92.23037	0.00081	0.00003	0.12712
	92.33377	0.00030	0.00001	0.12457
0.20	84.74191	0.00239	0.00032	0.03190
	83.52405	0.01301	0.00169	0.03529
0.30	43.40388	0.00026	0.00006	0.55243
	43.39391	0.00018	0.00004	0.52628

Table 5.2: Cross sections for positron-lithium s-wave scattering, potential A in πa_0^2, $\omega = 8$.

$k(a_0^{-1})$	K_{11}	K_{12}	K_{21}	K_{22}
0.01	−0.024090	0.006667	0.006564	0.165976
	−0.024140	0.006670	0.006598	0.165530
0.10	−0.603130	0.018357	0.018413	0.111300
	−0.602429	0.018366	0.018241	0.111595
0.20	−2.604381	0.039487	0.040442	−0.022295
	−2.606428	0.039676	0.039798	−0.024424
0.30	5.576508	−0.075100	−0.075524	−0.195969
	5.462990	−0.081625	−0.080084	−0.193386

Table 5.3: K-matrix elements for positron-lithium s-wave scattering, potential B, $\omega = 8$.

$k(a_0^{-1})$	σ_{11}	σ_{12}	σ_{21}	σ_{22}
0.01	23.21046	1.67615	0.00080	0.49340
	23.30766	1.69390	0.00080	0.49082
0.10	106.65199	0.09817	0.00411	0.20685
	106.47054	0.09640	0.00412	0.20793
0.20	87.11512	0.02100	0.00269	0.00637
	87.13312	0.02030	0.00272	0.00768
0.30	43.04564	0.00760	0.00170	0.37599
	42.98658	0.00890	0.00210	0.36716

Table 5.4: Cross sections for positron-lithium s-wave scattering, potential B in πa_0^2, $\omega = 8$.
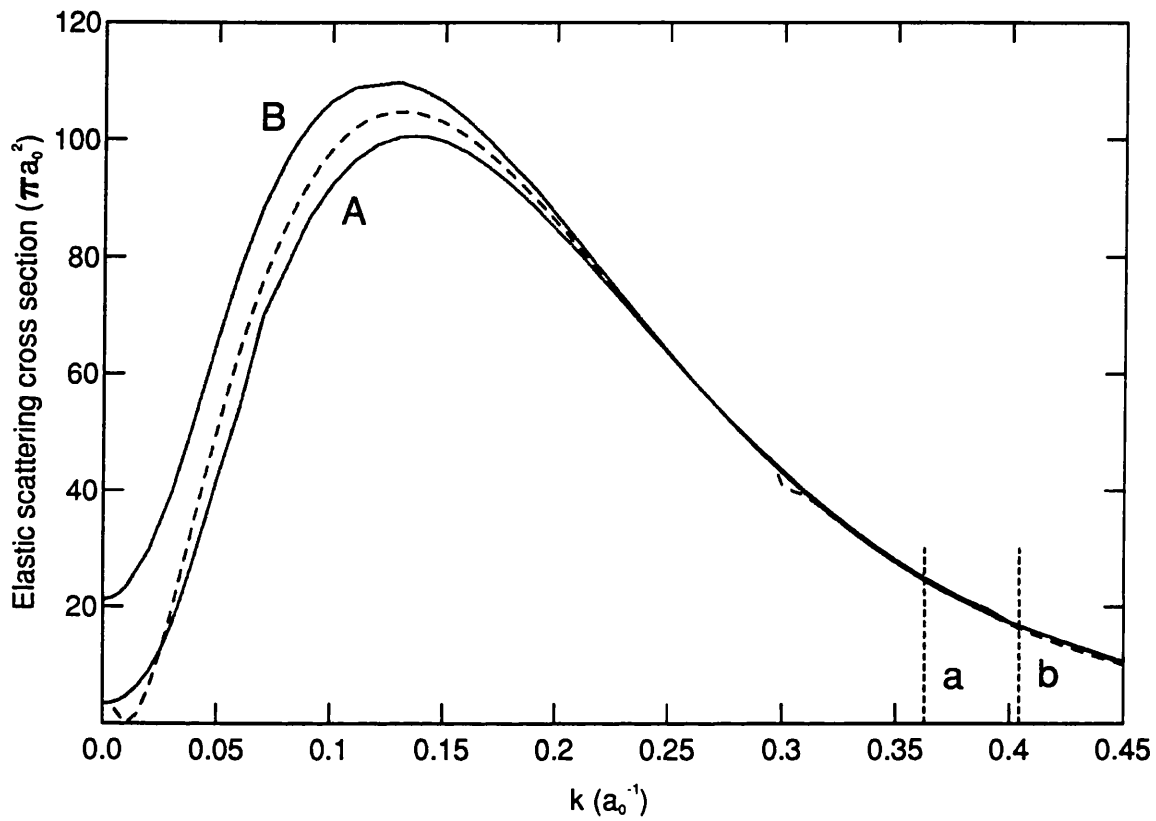
Figure 5.10: Variation of the s-wave positron-lithium elastic scattering cross section with respect to wavenumber k for potentials A and B. The first excitation thresholds of the two potentials are labelled a and b. The 14 state close-coupling results of McAlinden et al. (1994a) are included as the dashed line.
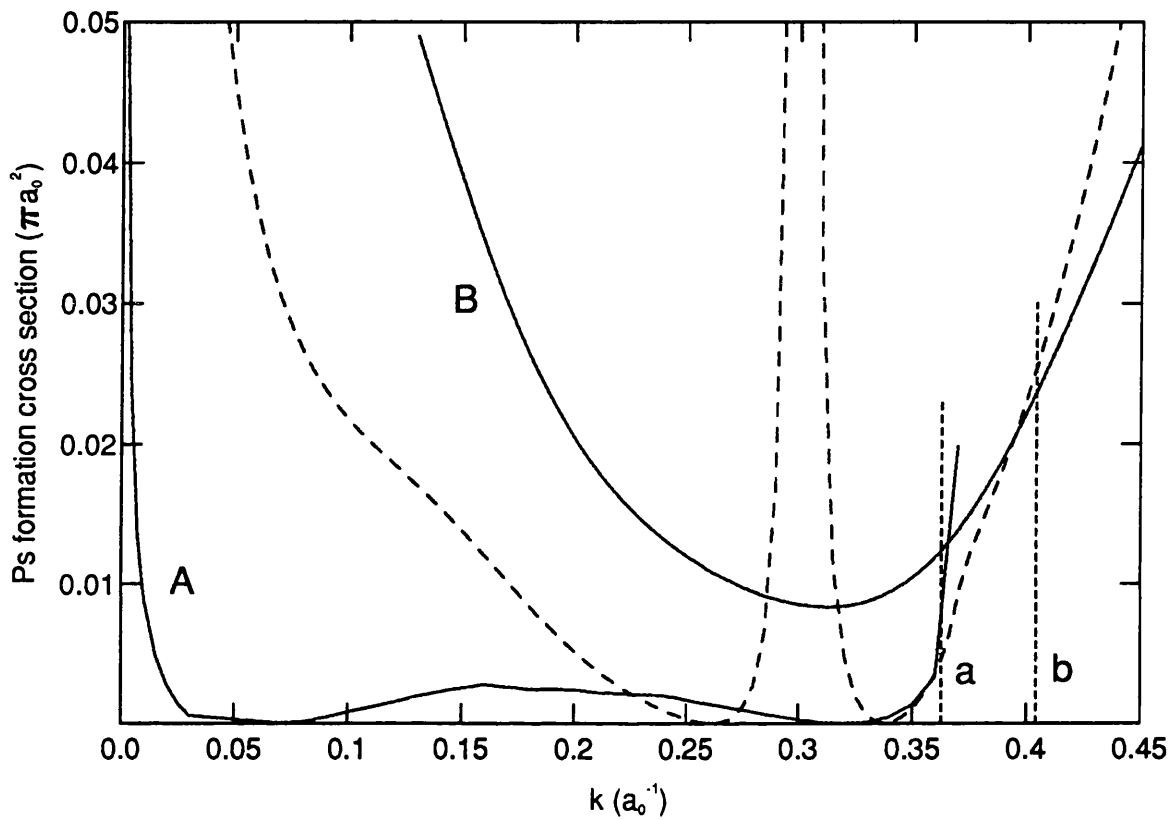
Figure 5.11: Variation of the s-wave positron-lithium positronium formation cross section with respect to wavenumber k for potentials A and B. The first excitation thresholds of the two potentials are labelled a and b. The 14 state close-coupling results of McAlinden et $al.$ (1994a) are included as the dashed line.
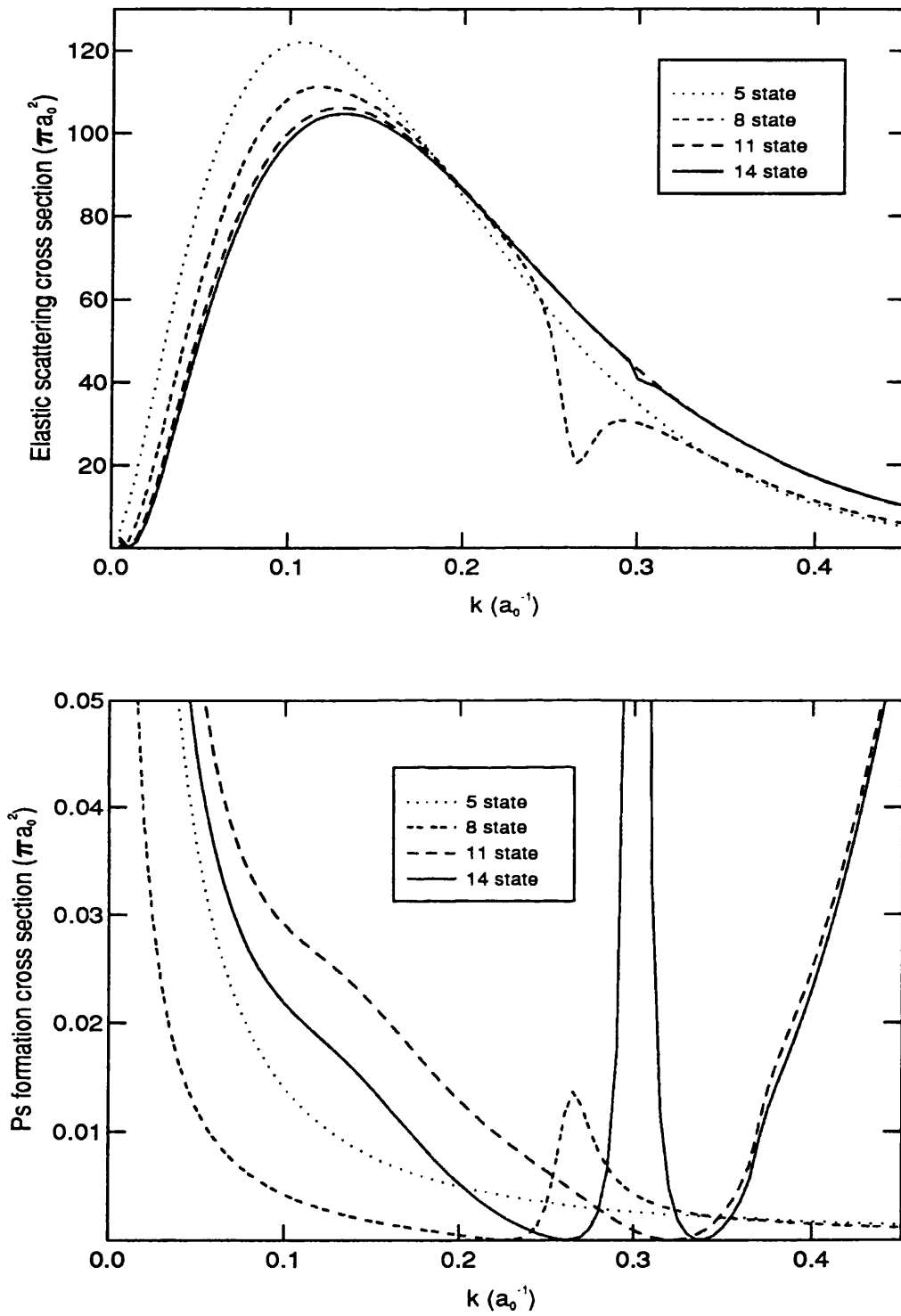
Figure 5.12: Close-coupling results of McAlinden *et al.* (1994a,b) for positron-lithium *s*-wave scattering, showing elastic scattering (top) and positronium formation (bottom) cross sections. Note that the 5 and 8 state positronium formation cross sections are scaled down by a factor of 1000.
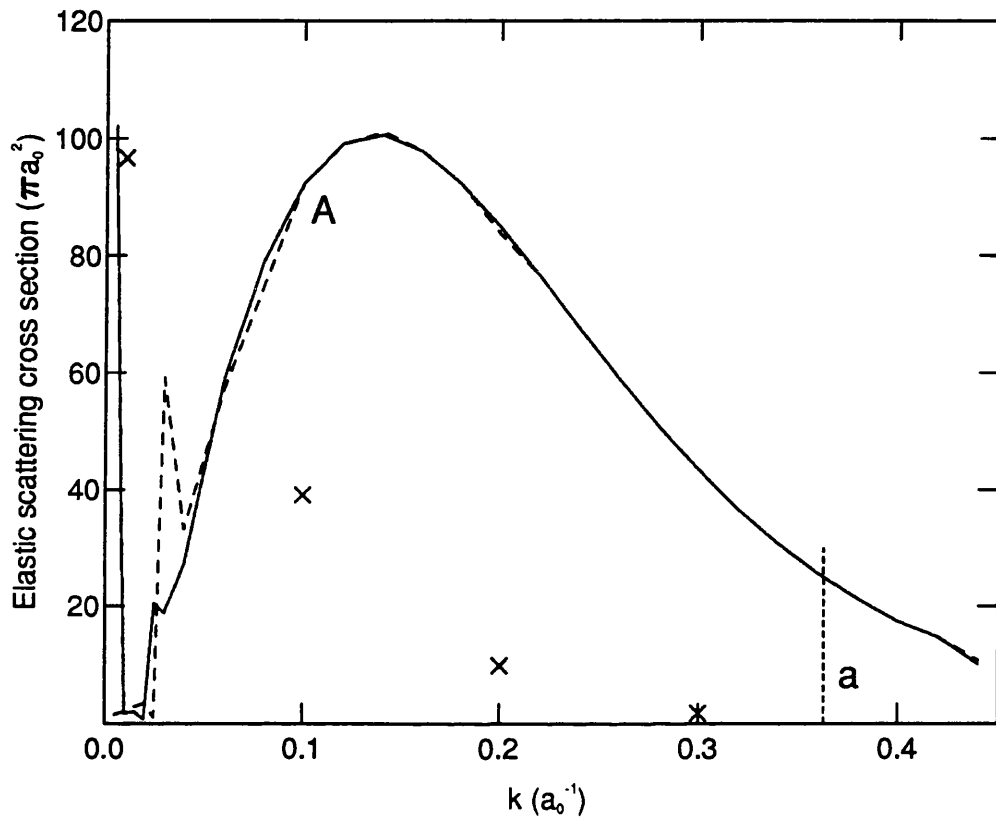
Figure 5.13: Variation of the s-wave positron-lithium elastic scattering cross section with respect to k for potential A, but with the positronium channel uncoupled. The solid and dashed lines correspond to Kohn and Inverse-Kohn results respectively. The crosses correspond to results obtained from McEachran (1992) using eight states of lithium in a close-coupling expansion. These latter cross sections are scaled down by a factor of ten.

5.2.6 Conclusions for s-wave Scattering

Using the new style of trial function, without the product form of short-range correlation term, satisfactory elastic scattering and positronium formation cross sections were calculated across the energy range from zero up to the first excitation threshold of lithium, although convergence at very low energies was not completely ideal. Here, the correlations and distortions of the highly polarizable system are really too complicated to be represented by the present form of trial function, and a more accurate investigation close to $k = 0$ would require the introduction of medium range polarization terms into the wavefunction, of the type used in previous studies of very low energy e^+-H and e^+-He scattering (Humberston and Wallace (1972), Humberston (1973)). For intermediate energies, results were good enough for the convergence of K_{11} to be fitted as an inverse power of ω, in the way described in section 2.2.5. Graphs of such fits are shown for $k = 0.15$ in figure 5.14.

The positronium formation cross sections obtained close to zero energy are in accordance with Wigner's prediction of a k^{-1} dependence, falling very sharply, with increasing energy, from infinity to values negligibly small in comparison with the elastic cross section across most of the range considered. There are significant discrepancies between σ_{Ps} for the two different potentials, with that for potential B falling away much more slowly than for potential A. Of the two characteristics, the latter is likely to be more reliable since the short-range form of potential A is more physically realistic. For s-wave scattering, this is particularly significant since the $l(l+1)/r^2$ centrifugal barrier is zero, allowing the positron to penetrate the regions close to the core to a greater extent than for the higher partial waves. It is interesting to note that the Ps formation cross section for each of the two potentials displays a definite upturn as the first excitation threshold is approached.

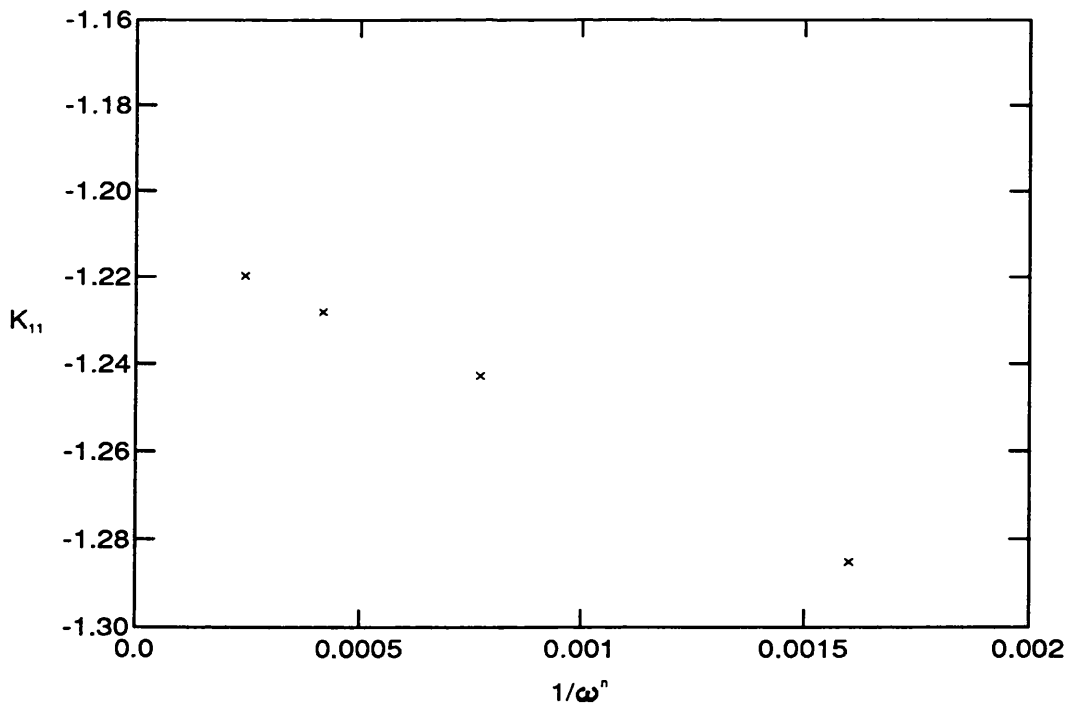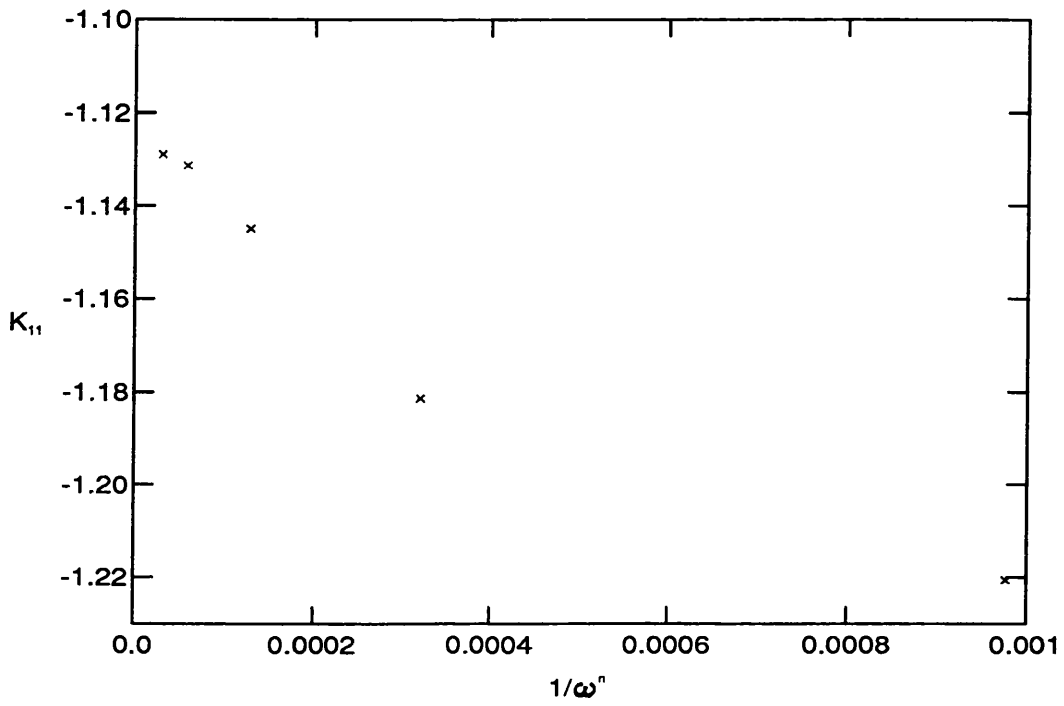The elastic cross sections appear to be converging downwards with increasing ω, as

Figure 5.14: Positron-lithium s-wave scattering. K_{11} fitted as a function of ω^{-n} for $k = 0.15$. For Potential A (top), $n = 5$, and for Potential B (bottom), $n = 4$.

K_{11} becomes less negative, but it is possible that this convergence trend may actually reverse at low energies if the latter matrix element eventually passes through zero. This would almost certainly give rise to a minimum in the elastic cross section, close to zero energies, which would be compatible with that illustrated in the 14 state close-coupling results. It should be noted that the infinite value of σ_{Ps} at $k = 0$ does not imply a zero elastic scattering cross section here, since the Ps formation rate, proportional to $k\sigma_{Ps}$, is always finite.

The elastic cross sections for both potentials reach a maximum of approximately $100\pi a_0^2$ at $k \simeq 0.15a_0^{-1}$. For $k < 0.23a_0^{-1}$ the results for potential B yield a larger value of σ_{el} than they do for potential A—again, the latter set is probably more reliable. Above this energy, the two potentials provide good agreement for elastic scattering.

The close-coupling results of McAlinden et $al.$, in their most sophisticated approximation, agree very favourably with the Kohn variational results, particularly for elastic scattering and, in the way that they appear to be converging, lend weight to the assumption that potential A provides the more accurate representation of the electron- and positron-core interactions. The effect that the inclusion of more states of Ps has on the magnitude of the close-coupling Ps formation cross section is very striking, and indicates well the complicated nature of the scattering process. It seems highly likely that the inclusion of further states in the expansion would result in a further reduction in this cross section, yielding even better agreement with σ_{Ps} as calculated variationally using potential A.

Close-coupling calculations have the advantage that cross sections can be calculated for scattering into any of the states explicitly incorporated into the scattering wavefunction, making the technique applicable over a wide energy range, but they also have a drawback in that these states also represent the only allowed virtual transitions in the scattering process. The Kohn method, whilst only strictly applicable over an energy

range where asymptotic components are specified for all channels, allows implicitly for any important virtual transitions, providing the Hylleraas expansion is flexible enough. Thus, where convergence is satisfactory, as it is here except at very low energies, the Kohn positronium formation cross sections for potential A can probably be taken to be more accurate than the close coupling results obtained so far.

At energies where the Ps formation cross section is very much smaller than the elastic cross section, uncoupling the positronium channel has a negligible effect on the elastic cross section for potential A. At very low energies, however, the calculation clearly breaks down, as the trial function attempts to represent a scattering channel whose cross section is tending towards infinity, but which is disallowed by the formalism.

5.3 Positron-Lithium p-wave Scattering

5.3.1 Trial Function

The modifications which require making to the positron-lithium s-wave codes to treat the $l = 1$ partial wave are basically analogous to those for hydrogen which were described in section 2.3. Again, two different symmetries are required for the short-range correlation terms, so that the two components of the trial function for p-wave positron-lithium scattering have the form

$$
\begin{aligned}
\Psi_1 \;=\; & \Phi_{\text{Li}}(r_2)Y_{10}(\theta_1,\phi_1)\sqrt{k}\left\{j_1(kr_1) - K_{11}^t n_1(kr_1)\left[1 - \exp(-\lambda r_1)\right]^3\right\} \\
& -\Phi_{\text{Ps}}(r_3)Y_{10}(\theta_\rho,\phi_\rho)\sqrt{2\kappa}K_{21}^t n_1(\kappa\rho)\left[1 - \exp(-\mu\rho)\right]^6 \\
& +\exp\left[-\left(\alpha r_1 + \beta r_2 + \gamma r_3\right)\right]\left(Y_{10}(\theta_1,\phi_1)r_1\sum_{i=1}^{N_1}a_i r_1^{k_i}r_2^{l_i}r_3^{m_i}\right. \\
& \left. +Y_{10}(\theta_2,\phi_2)r_2\sum_{j=1}^{N_2}b_j r_1^{k_j}r_2^{l_j}r_3^{m_j}\right), \quad (5.14)
\end{aligned}
$$

$$
\begin{aligned}
\Psi_2 \;=\; & \Phi_{\text{Ps}}(r_3)Y_{10}(\theta_\rho,\phi_\rho)\sqrt{2\kappa}\left\{j_1(\kappa\rho) - K_{22}^t n_1(\kappa\rho)\left[1 - \exp(-\mu\rho)\right]^6\right\} \\
& -\Phi_{\text{Li}}(r_2)Y_{10}(\theta_1,\phi_1)\sqrt{k}K_{12}^t n_1(kr_1)\left[1 - \exp(-\lambda r_1)\right]^3 \\
& +\exp\left[-(\alpha r_1 + \beta r_2 + \gamma r_3)\right]\left(Y_{10}(\theta_1,\phi_1)r_1\sum_{i=1}^{N_1}c_i r_1^{k_i}r_2^{l_i}r_3^{m_i}\right. \\
& \left. +Y_{10}(\theta_2,\phi_2)r_2\sum_{j=1}^{N_2}d_j r_1^{k_j}r_2^{l_j}r_3^{m_j}\right). \quad (5.15)
\end{aligned}
$$

The angular dependence of the p-wave scattering functions is given by the the spherical harmonics, Y_{10}, given by

$$
Y_{10}(\theta,\phi) \;=\; \sqrt{\frac{3}{4\pi}}\cos\theta, \quad (5.16)
$$

which again makes the angular integrations more complicated than for s-wave, although no more complicated than for positron-hydrogen scattering. The procedure for performing them is decribed in Appendix C.

Although it arises from the kinetic energy part of the Hamiltonian, the $l(l + 1)/r^2$ term, which becomes non-zero for partial waves higher than s-wave, effectively adds a

repulsive component to the positron-core potential, which tends to keep the positron away from the inner regions of the atom. Whilst this probably makes the short-range distortions less complicated than in s-wave scattering, the previous studies of hydrogen indicated that it was likely that a much larger contribution to positronium formation could be expected in p-wave scattering, making it necessary still to retain maximum flexibility in the trial functions. For this reason, no attempt was made to include the lithium target function in the Hylleraas expansions, as in the original forms of the s-wave trial functions.

5.3.2 Results for p-wave Scattering

A similar procedure to that used for s-wave scattering was adopted to attempt to locate the optimum values of the non-linear parameters, α, β and γ, in the scattering wavefunction. The best set of values found was $\alpha = 0.2$, $\beta = 0.7$ and $\gamma = 0.2$. These values gave rise to quite good convergence for each potential, at both low and intermediate energies in the range under study, as shown in figures 5.15–5.18.

Using 165 terms in the Hylleraas expansion for each of the two angular momentum symmetries, calculations were performed for both potentials over the same energy range as for s-wave scattering. For four energies, K-matrix elements and cross sections are presented numerically in tables 5.5–5.8, and cross sections are plotted as a function of k in figures 5.19 and 5.20, where results are again compared with the close-coupling data of McAlinden *et al.* Figure 5.21 illustrates the convergence of these p-wave close-coupling results with respect to the inclusion of more states in the close-coupling expansion. In figure 5.22 the elastic cross section for both potentials is plotted as a function of k with the positronium channel uncoupled.

Figure 5.15: Potential A. Convergence of the diagonal K-matrix elements for p-wave positron-lithium scattering. $k = 0.01$

Figure 5.16: Potential A. Convergence of the diagonal K-matrix elements for p-wave positron-lithium scattering. $k = 0.25$
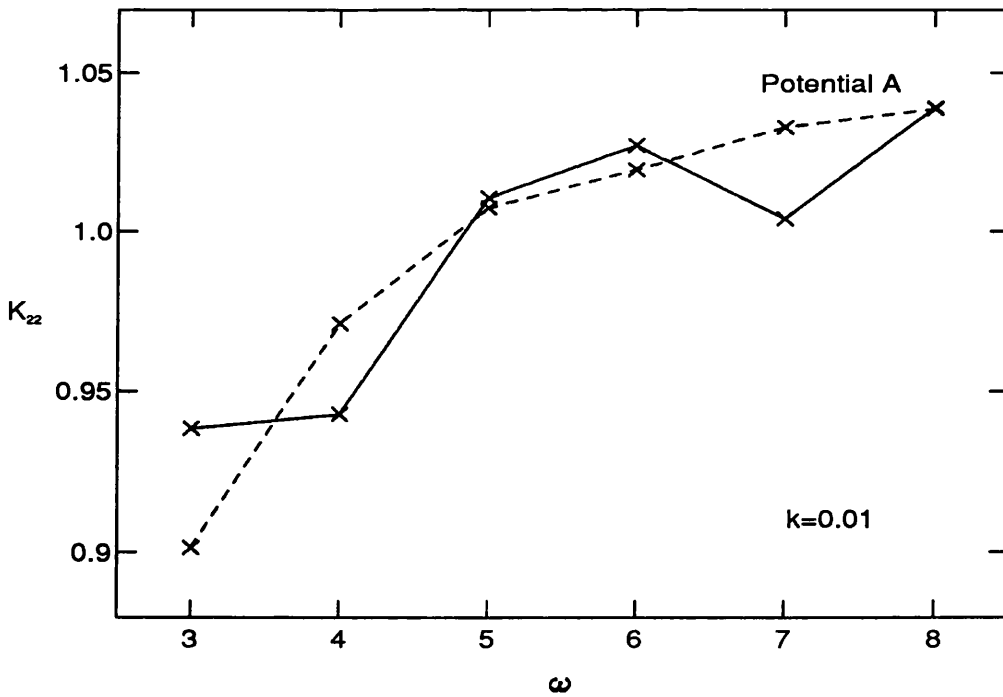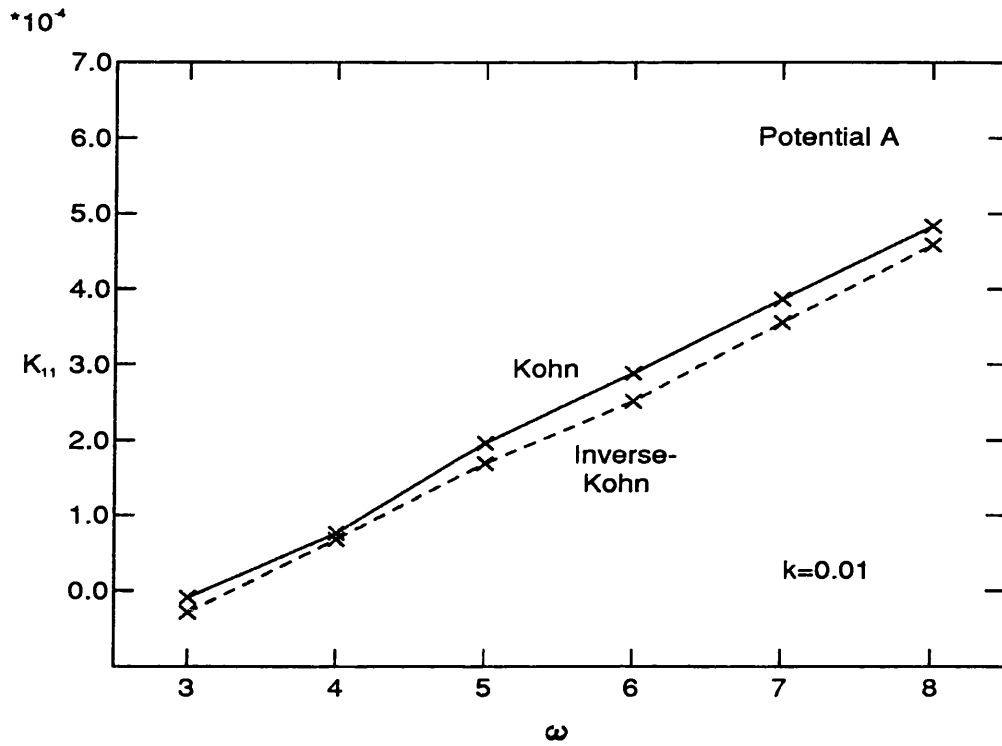
Figure 5.17: Potential B. Convergence of the diagonal K-matrix elements for p-wave positron-lithium scattering. $k = 0.01$
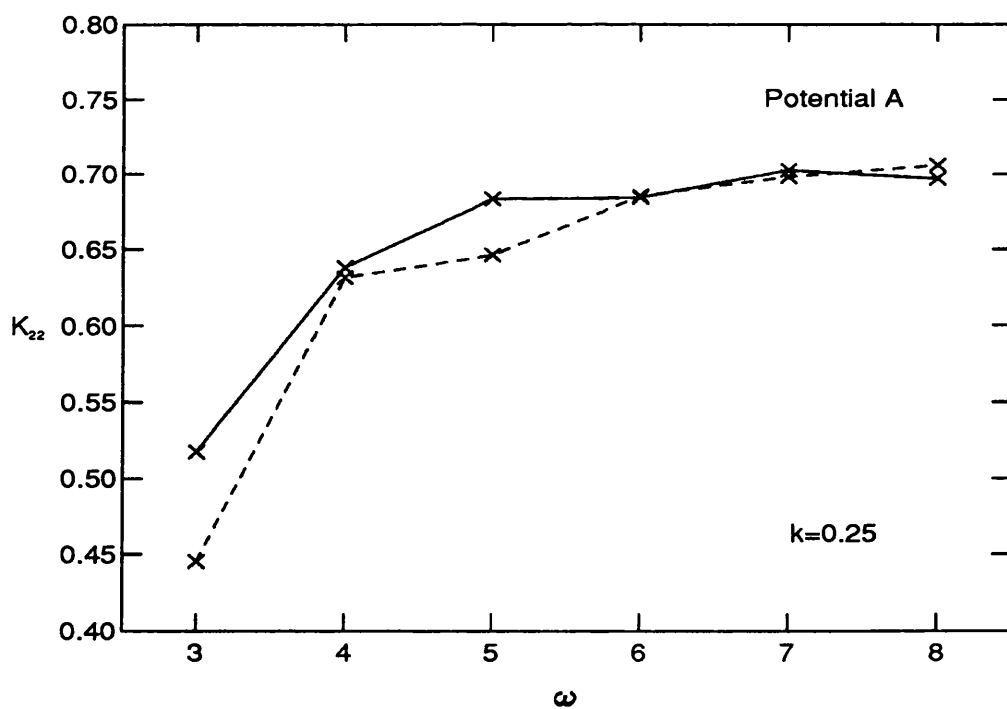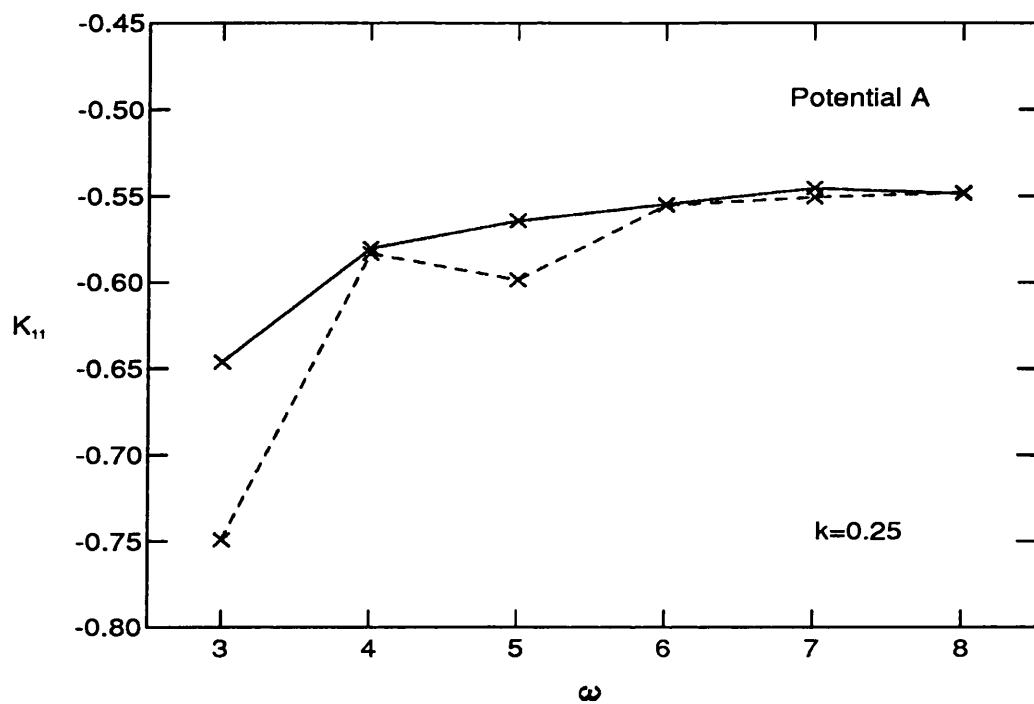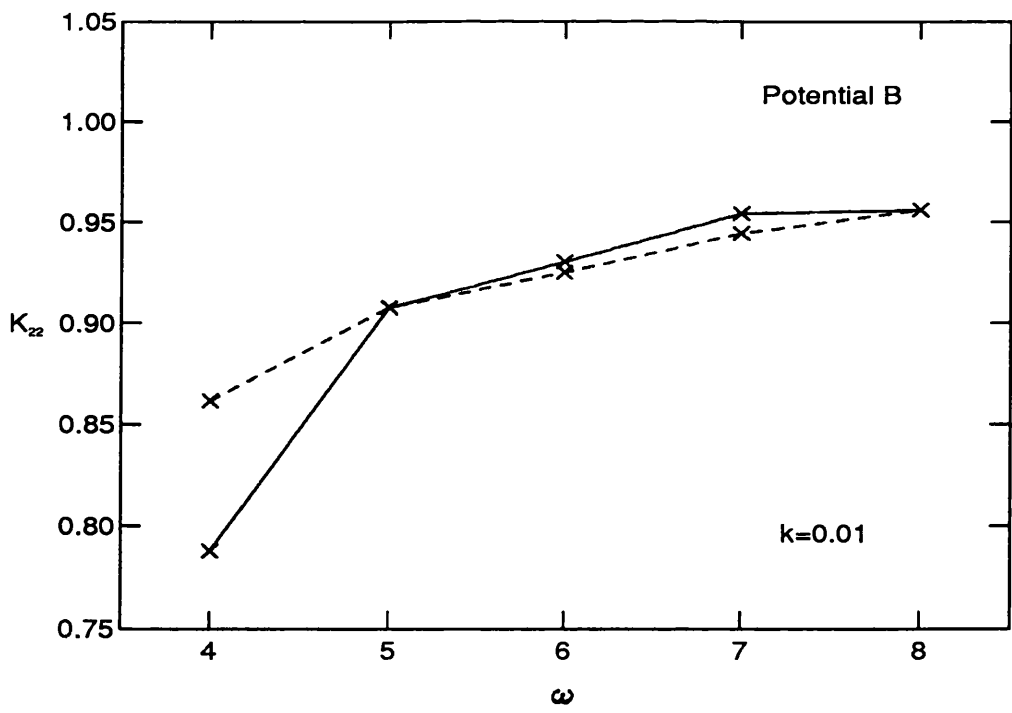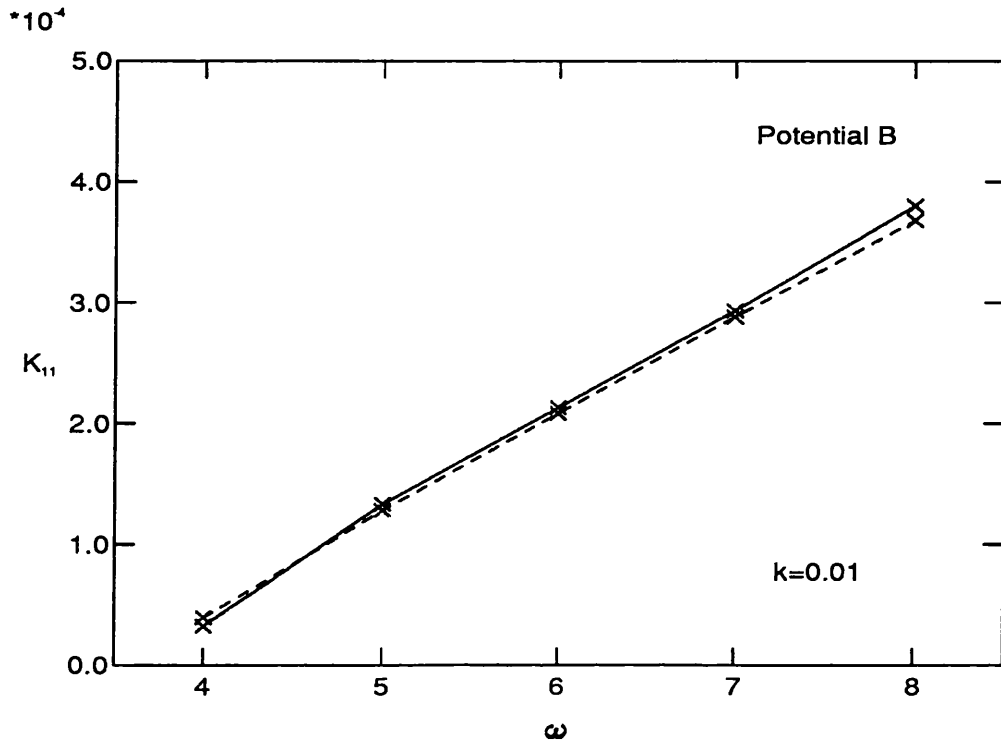
116
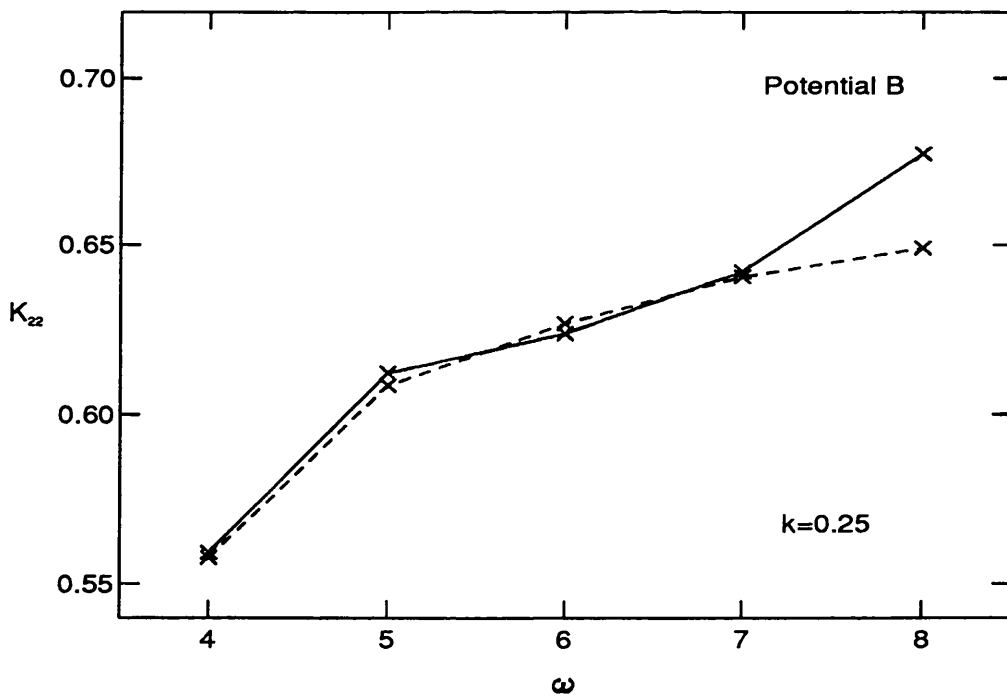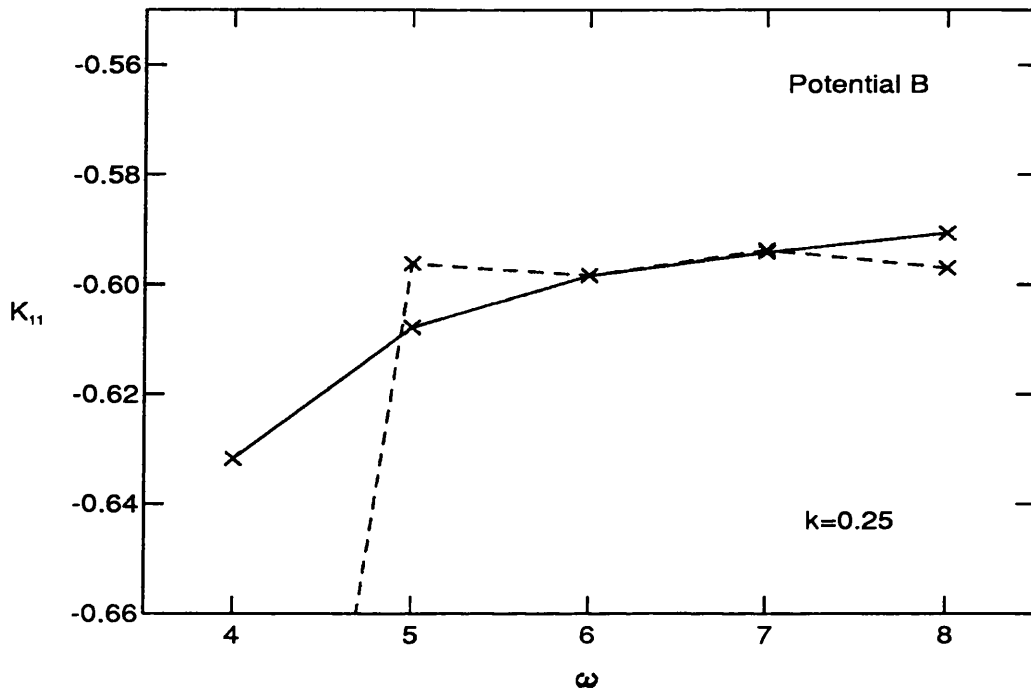
Figure 5.18: Potential B. Convergence of the diagonal K-matrix elements for p-wave positron-lithium scattering. $k = 0.25$

$k(a_0^{-1})$	K_{11}	K_{12}	K_{21}	K_{22}
0.01	0.000483	−0.005892	−0.005901	1.038902
	0.000458	−0.005968	−0.005975	1.038578
0.10	0.024363	−0.129534	−0.129652	0.987039
	0.025127	−0.129083	−0.129209	0.987922
0.20	−0.305067	−0.174105	−0.174106	0.812414
	−0.305150	−0.173758	−0.173756	0.810352
0.30	−0.837268	−0.194916	−0.194981	0.602159
	−0.837350	−0.194980	−0.195044	0.602668

Table 5.5: K-matrix elements for positron-lithium p-wave scattering, potential A. $\omega = 8$.

$k(a_0^{-1})$	σ_{11}	σ_{12}	σ_{21}	σ_{22}
0.01	0.02604	2.00944	0.00089	27.69600
	0.02324	2.06075	0.00091	27.68766
0.10	0.38607	10.04318	0.40969	23.78933
	0.41652	9.96696	0.40653	23.81370
0.20	27.03774	4.80881	0.63129	15.35687
	27.04168	4.79944	0.63008	15.31099
0.30	54.51348	2.08294	0.46292	7.99973
	54.52065	2.08314	0.46297	8.00940

Table 5.6: Cross sections for p-wave positron-lithium scattering, potential A. $\omega = 8$.

$k(a_0^{-1})$	K_{11}	K_{12}	K_{21}	K_{22}
0.01	0.000372	0.006677	0.006686	0.955657
	0.000368	0.006675	0.006684	0.955858
0.10	0.001952	0.149026	0.149172	0.917305
	0.002180	0.148012	0.148128	0.920933
0.20	−0.338811	0.216699	0.216717	0.754776
	−0.339156	0.216596	0.216613	0.753473
0.30	−0.897224	0.267004	0.267063	0.552291
	−0.897230	0.267104	0.267165	0.554133

Table 5.7: K-matrix elements for positron-lithium p-wave scattering, potential B. $\omega = 8$.

$k(a_0^{-1})$	σ_{11}	σ_{12}	σ_{21}	σ_{22}
0.01	0.01477	2.80344	0.00129	26.35524
	0.01439	2.80137	0.00129	26.36102
0.10	0.26819	14.15592	0.59580	22.58500
	0.25457	13.91394	0.58584	22.69071
0.20	33.11405	7.53458	1.01415	14.28206
	33.16421	7.53523	1.01425	14.25157
0.30	58.34417	3.69458	0.83692	7.35275
	58.35238	3.69153	0.83621	7.38770

Table 5.8: Cross sections for p-wave positron-lithium scattering, potential B. $\omega = 8$.
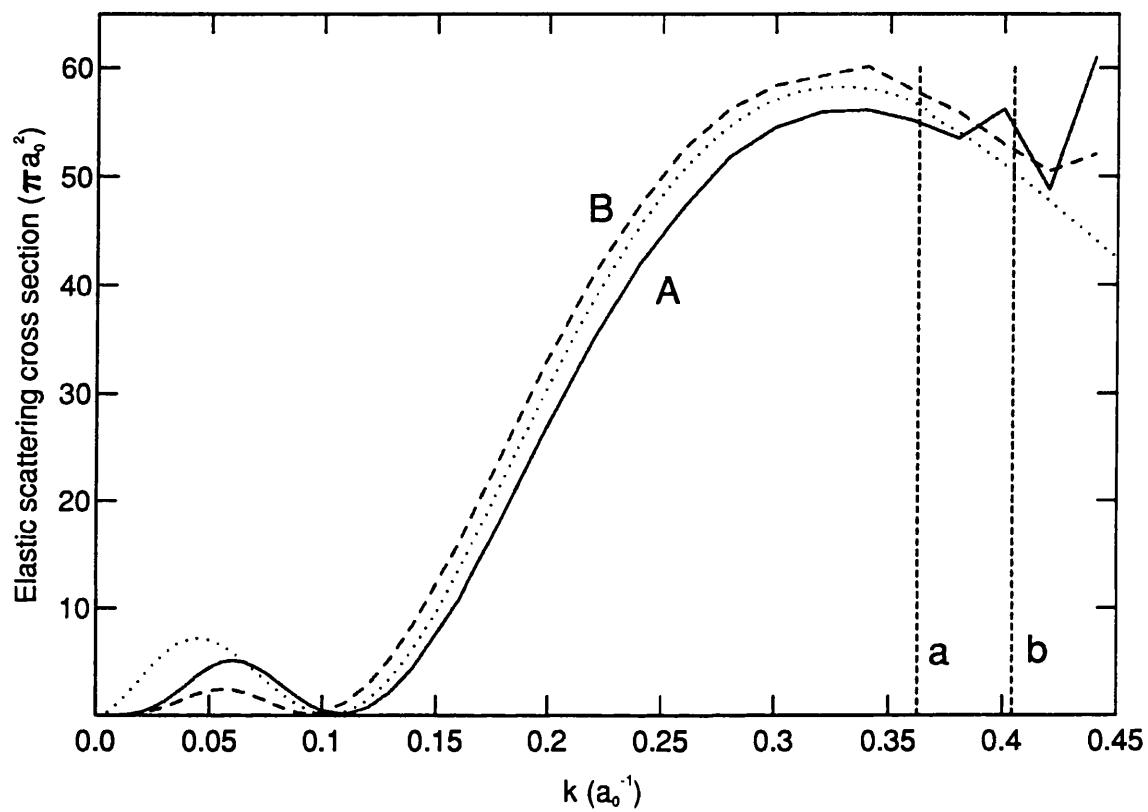
Figure 5.19: Variation of the p-wave positron-lithium elastic scattering cross section with respect to k for $\omega = 8$. The first excitation thresholds of potentials A and B are labelled a and b respectively. The 14 state close-coupling results of McAlinden *et al.* (1994a) are included as the dotted line.
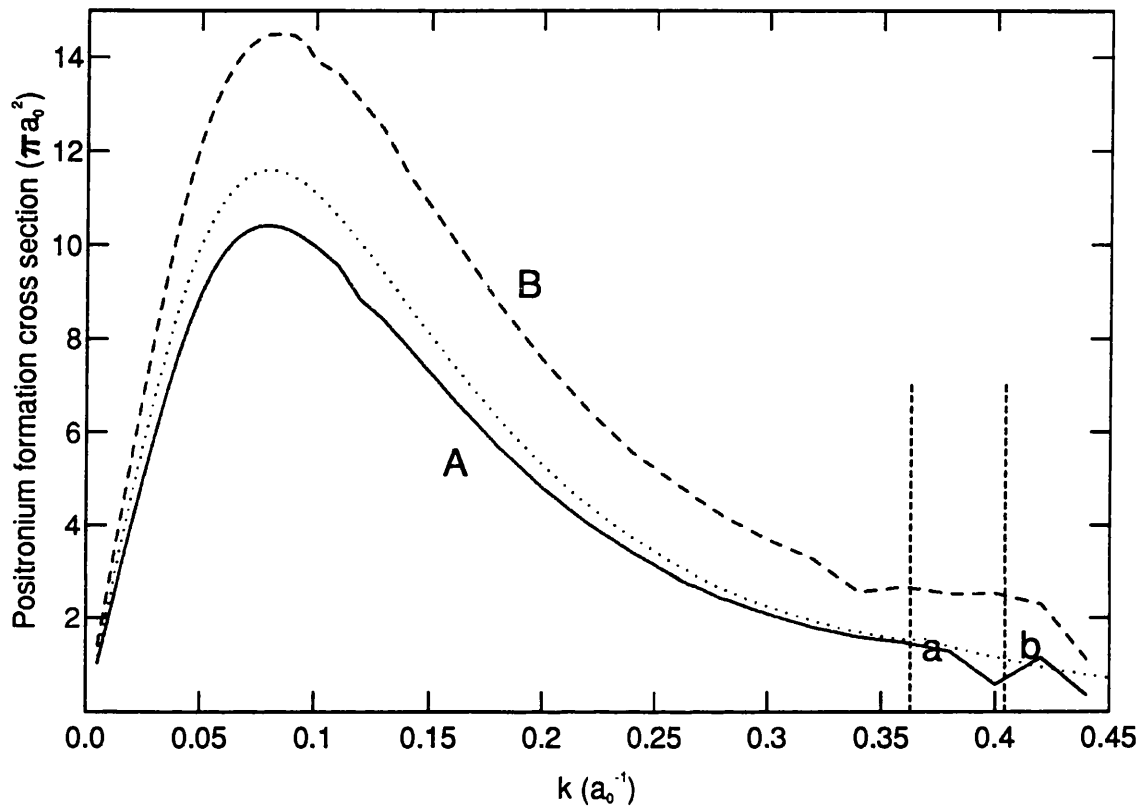
Figure 5.20: Variation of the p-wave positron-lithium positronium formation cross section with respect to k for $\omega = 8$. The first excitation thresholds of potentials A and B are labelled a and b respectively. The 14 state close-coupling results of McAlinden *et al.* (1994a) are included as the dotted line.
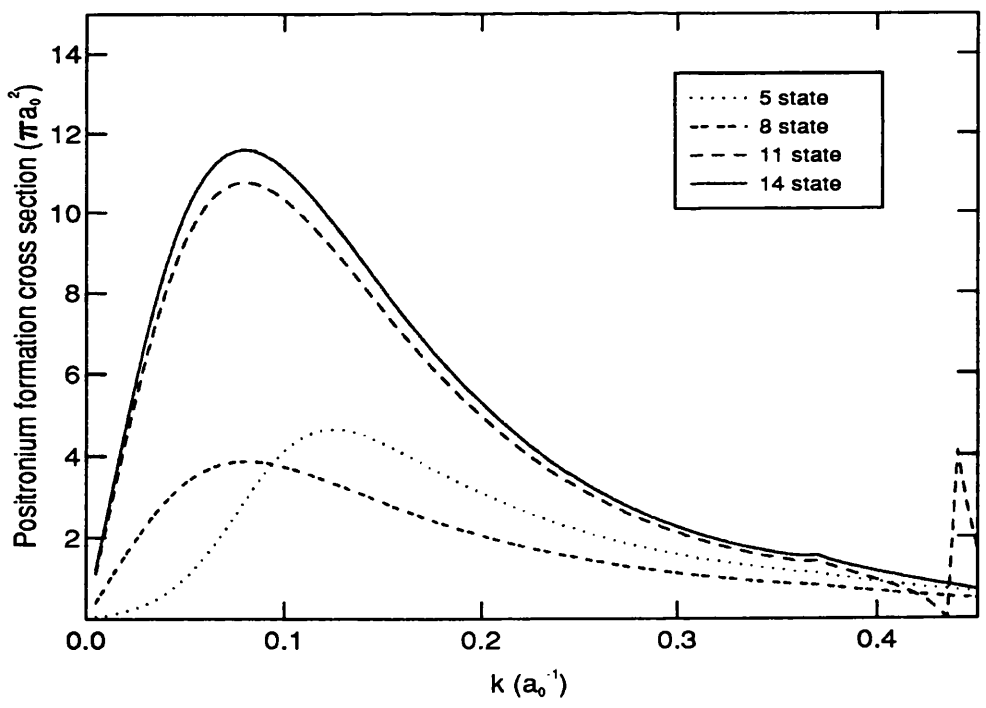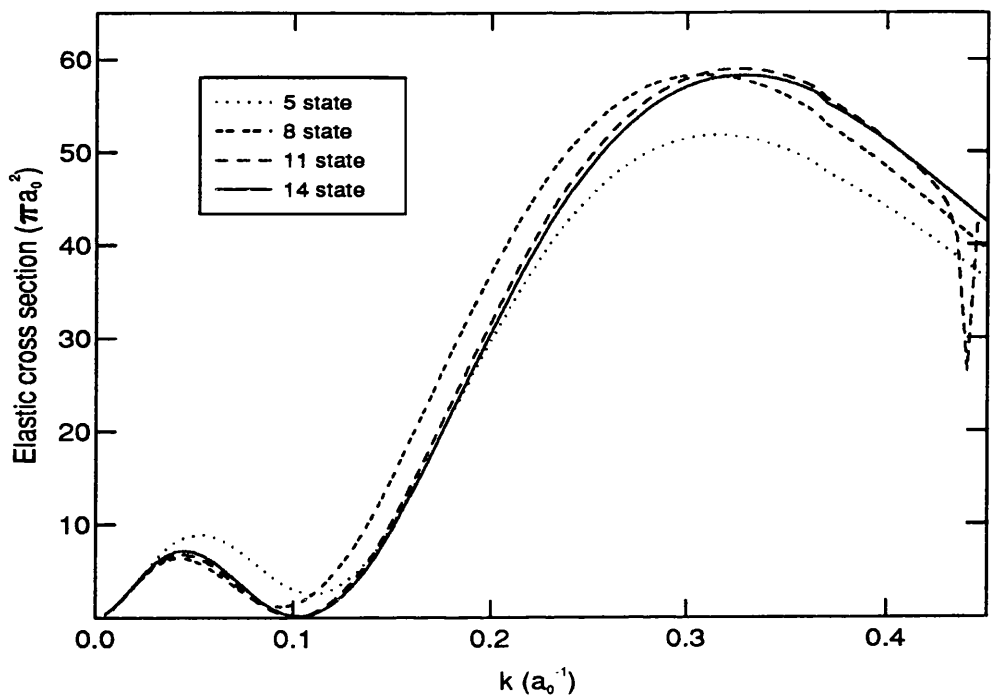
Figure 5.21: Close-coupling results of McAlinden *et al.* (1994a,b) for positron-lithium *p*-wave scattering, showing elastic scattering (top) and positronium formation (bottom) cross sections. Note that the 5 and 8 state positronium formation cross sections are scaled down by a factor of 10.
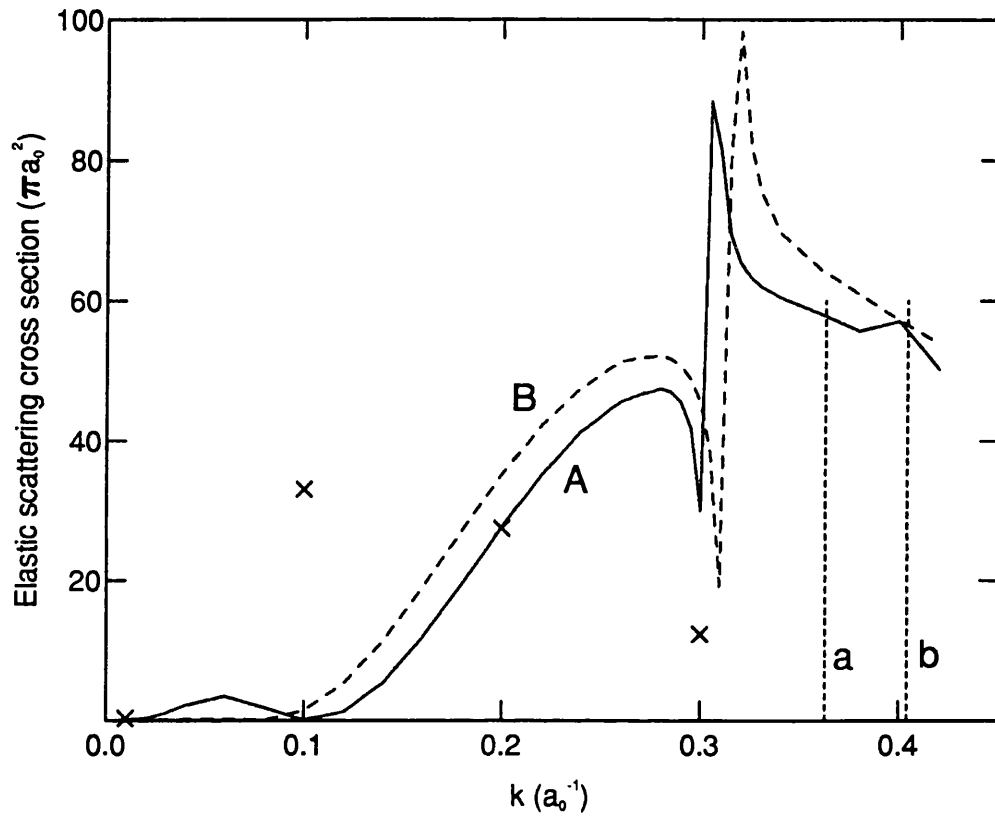
Figure 5.22: Variation of the p-wave positron-lithium elastic cross section with respect to k for $\omega = 8$ with the positronium channel uncoupled. The crosses correspond to results obtained from McEachran (1992) using five states of lithium in a close-coupling expansion. These latter cross sections are scaled down by a factor of ten.

5.3.3 Conclusions for p-wave Scattering

The p-wave elastic scattering results, shown in figure 5.19, illustrate well the importance of selecting a good set of non-linear parameters for the positron-lithium problem, since the minimum feature close to $k = 0.1$ can easily be missed if they are not well optimised. Tables 5.5 and 5.7 show how K_{11} is positive for low k, but passes through zero and becomes negative for higher k-values. The elastic cross section, which is closely related to K_{11}^2, consequently contains a minimum, which is a feature of both potentials. Since the diagonal K-matrix elements converge from below, however, and below $k \simeq 0.1$, K_{11} is only slightly positive, the minimum is only reproducible beyond a certain level of convergence, being initially situated at $k = 0$ and moving steadily to the right with the inclusion of more terms in the trial function. The graphs in figure 5.23, where K_{11} is plotted as an inverse power of ω for $k = 0.1$, show how this matrix element converges upwards, from negative to positive values, with respect to increasing the number of linear parameters in the scattering wavefunction. A comparison with the p-wave results of McAlinden et al. reinforces the authenticity of this feature in the elastic cross section.

As in the case of hydrogen, p-wave scattering contributes much more substantially to the positronium formation cross section than does s-wave, except at very low energies, with σ_{Ps} rising to a maximum at approximately the same k-value as the elastic cross section reaches its minimum. As illustrated in figure 5.22, the uncoupling of the positronium channel produces a very pronounced effect on the elastic cross section, resulting in the introduction of an artificial resonance, for both potentials, close to $k = 0.3$. Below this energy, and in fact where the p-wave Ps formation cross section is much larger, the uncoupled elastic cross section surprisingly agrees well with the fully coupled calculation, although the resonance amply demonstrates the hazards of ignoring an open scattering channel.
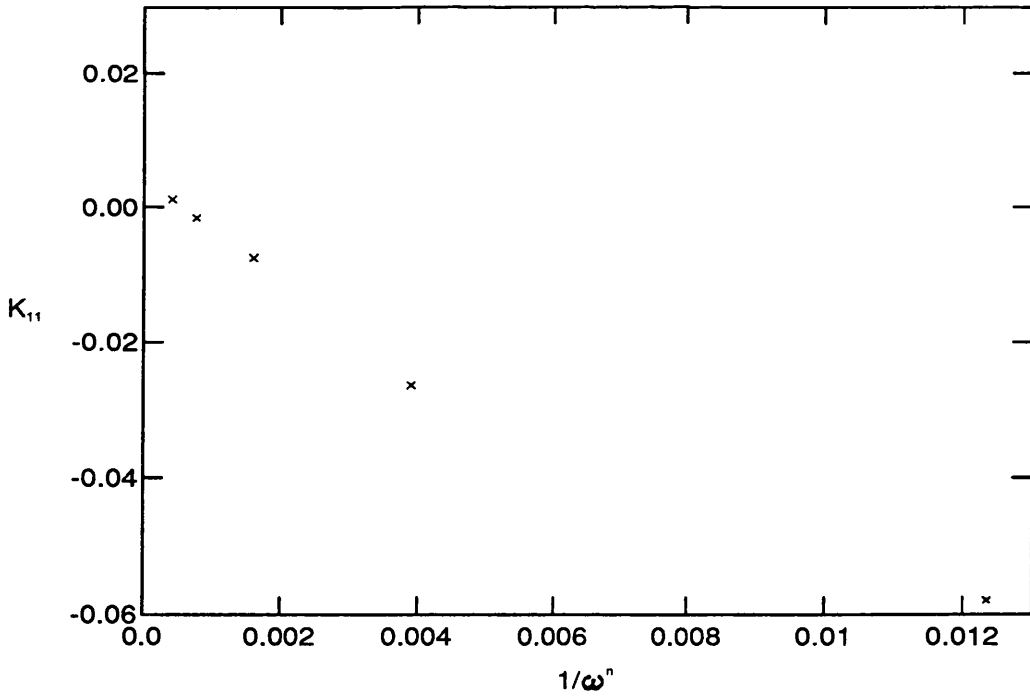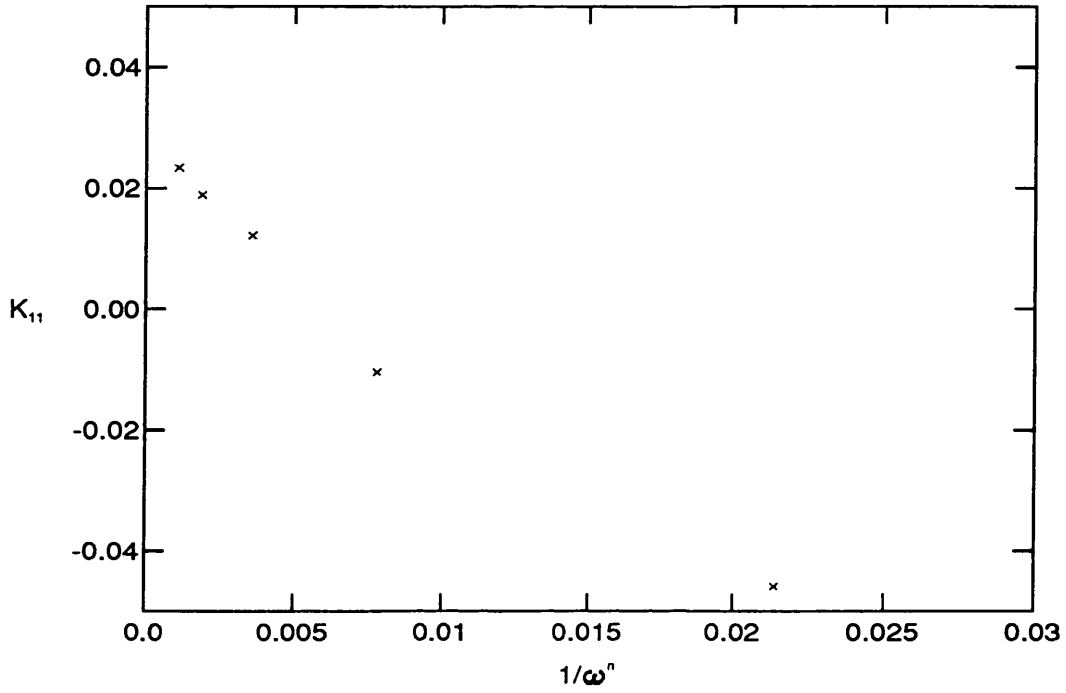
Figure 5.23: K_{11} plotted as a function of ω^{-n} for $k = 0.1$ in p-wave positron-lithium scattering. For potential A (top), $n = 3.5$, and for potential B, $n = 4$.

5.4 Positron-Lithium d-wave Scattering

5.4.1 Trial Function

The modifications to the trial functions required to treat $l = 2$ positron-lithium scattering are analogous to those made by Brown and Humberston (1984) for the positron-hydrogen problem. The long-range components of the wavefunction are the second-order spherical Bessel functions, and Neumann functions appropriately shielded at the origin. At short ranges, three different symmetries of correlation term are required, following the discussion of section 2.3, to allow the two units of angular momentum to be suitably distributed between the positron and electron. Thus:

$$
\begin{aligned}
\Psi_1 &= \Phi_{\mathrm{Li}}(r_2)Y_{20}(\theta_1, \phi_1)\sqrt{k}\left\{j_2(kr_1) - K_{11}^t n_2(kr_1)\left[1 - \exp(-\lambda r_1)\right]^5\right\} \\
&\quad -\Phi_{\mathrm{Ps}}(r_3)Y_{20}(\theta_\rho, \phi_\rho)\sqrt{2\kappa}K_{21}^t n_2(\kappa\rho)\left[1 - \exp(-\mu\rho)\right]^7 \\
&\quad + \exp\left[-(\alpha r_1 + \beta r_2 + \gamma r_3)\right]\left(Y_{20}(\theta_1, \phi_1)r_1^2\sum_{h=1}^{N_1} a_h r_1^{k_h}r_2^{l_h}r_3^{m_h}\right. \\
&\quad \left. +\mathcal{Y}_{20}(\theta_1, \phi_1, \theta_2, \phi_2)r_1 r_2\sum_{i=1}^{N_2} b_i r_1^{k_i}r_2^{l_i}r_3^{m_i} + Y_{20}(\theta_2, \phi_2)r_2^2\sum_{j=1}^{N_3} c_j r_1^{k_j}r_2^{l_j}r_3^{m_j}\right) \quad (5.17) \\
\Psi_2 &= \Phi_{\mathrm{Ps}}(r_3)Y_{20}(\theta_\rho, \phi_\rho)\sqrt{2\kappa}\left\{j_2(\kappa\rho) - K_{22}^t n_2(\kappa\rho)\left[1 - \exp(-\mu\rho)\right]^7\right\} \\
&\quad -\Phi_{\mathrm{Li}}(r_2)Y_{20}(\theta_1, \phi_1)\sqrt{k}K_{12}^t n_1(kr_1)\left[1 - \exp(-\lambda r_1)\right]^5 \\
&\quad + \exp\left[-(\alpha r_1 + \beta r_2 + \gamma r_3)\right]\left(Y_{20}(\theta_1, \phi_1)r_1^2\sum_{h=1}^{N_1} d_h r_1^{k_h}r_2^{l_h}r_3^{m_h}\right. \\
&\quad \left. +\mathcal{Y}_{20}(\theta_1, \phi_1, \theta_2, \phi_2)r_1 r_2\sum_{i=1}^{N_2} e_i r_1^{k_i}r_2^{l_i}r_3^{m_i} + Y_{20}(\theta_2, \phi_2)r_2^2\sum_{j=1}^{N_3} f_j r_1^{k_j}r_2^{l_j}r_3^{m_j}\right) \quad (5.18)
\end{aligned}
$$

The angular functions are given by

$$
Y_{20}(\theta, \phi) = \sqrt{\frac{5}{4\pi}}\left(\frac{3}{2}\cos^2\theta - \frac{1}{2}\right), \qquad (5.19)
$$

and

$$
\mathcal{Y}_{20}(\theta_1, \phi_1, \theta_2, \phi_2) = \frac{3}{4\pi}(3\cos\theta_1\cos\theta_2 - \cos\theta_{12}). \qquad (5.20)
$$

5.4.2 Results for d-wave Scattering

Only rather preliminary investigations were carried out for the d-wave problem, owing to time constraints, and the cross sections presented here are not as well converged as it is hoped they could be. As with the earlier $l = 2$ studies of positron-hydrogen scattering, it was found very difficult to locate suitable values of the non-linear parameters α, β and γ, with the problems of optimisation compounded further in this case by the very high polarizability of the lithium atom. Because of the time-consuming task of generating matrices involving three different symmetries of short-range function, a detailed search of the non-linear parameter space was not practicable. A limited investigation, along the lines of that described for s-wave scattering in section 5.2.2, gave rise to reasonable agreement between Kohn and Inverse Kohn data for $\alpha = 0.5$, $\beta = 0.7$ and $\gamma = 0.4$, and the cross sections obtained for $\omega = 8$ (165 short-range terms of each symmetry) are illustrated in figures 5.24 and 5.25. Again included, for comparison, are the close-coupling results obtained by McAlinden *et al.* (1994a) using their 14-state close-coupling expansion. Although the general trends of both sets of data are similar, further optimisation is clearly warranted in the variational investigations in order to produce smoother and better converged cross sections.

These preliminary studies, however, appear to indicate that the d-wave contribution to the elastic cross section is smaller than for s- or p-wave scattering, but that quite a large contribution is made to the positronium formation cross section for this partial wave.

Figure 5.24: Variation of the d-wave positron-lithium elastic scattering cross section with respect to k for $\omega = 8$, potential A. The first excitation threshold of potential A is indicated. The 14 state close-coupling results of McAlinden *et al.* (1994) are included as the dotted curve.
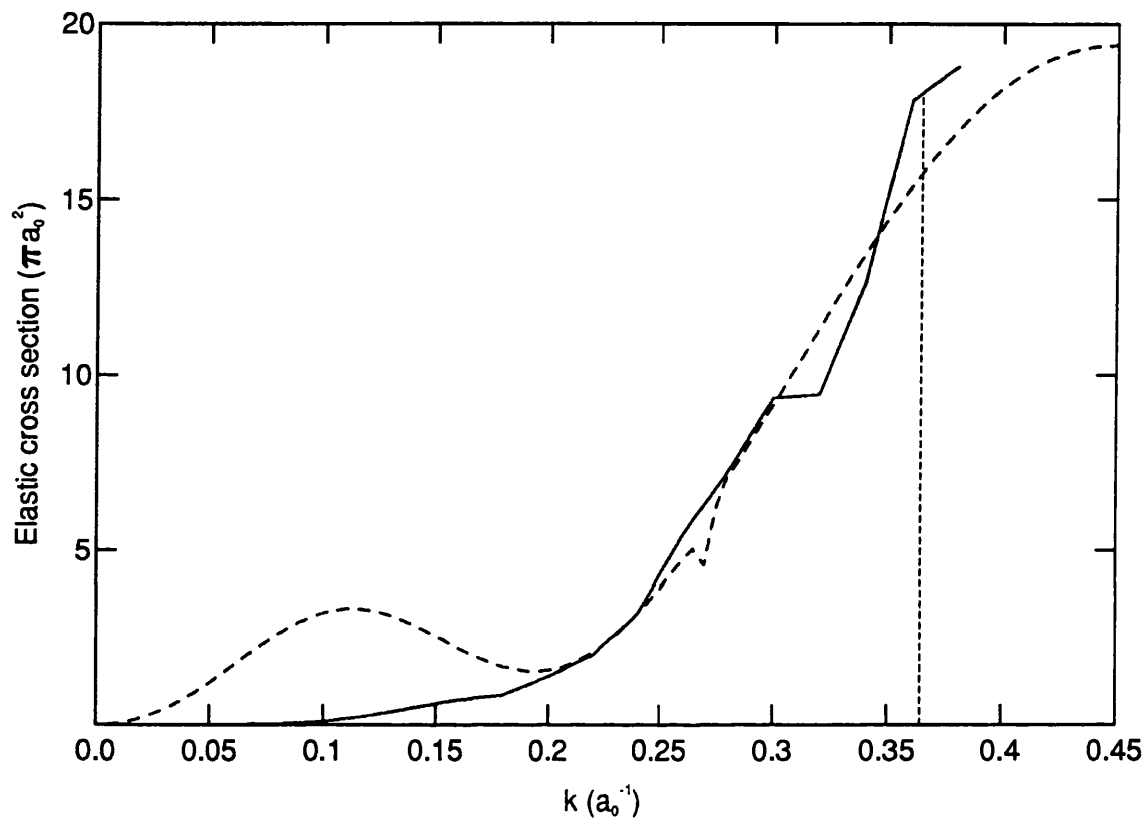
Figure 5.25: Variation of the d-wave positron-lithium positronium formation cross section with respect to k for $\omega = 8$, potential A. The first excitation threshold of potential A is indicated. The 14 state close-coupling results of McAlinden *et al.* (1994) are included as the dotted curve.
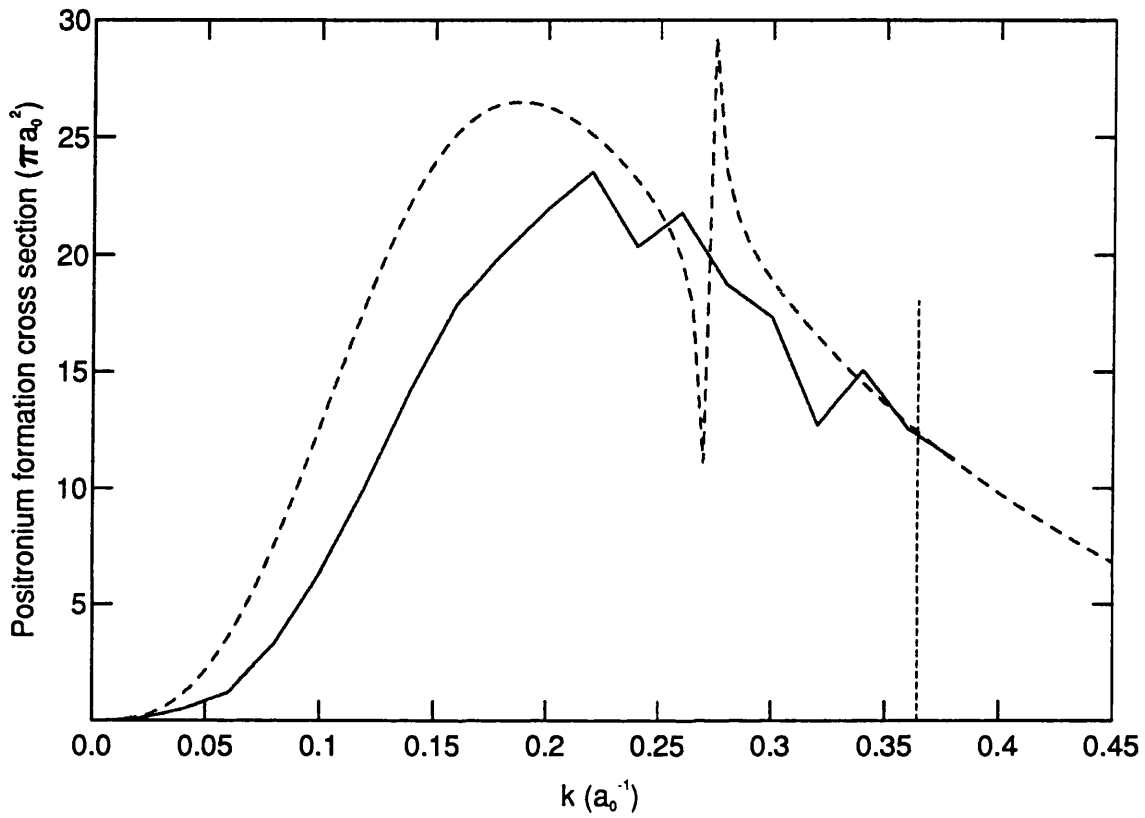
129

Chapter 6

Conclusions

Results have been reported here of variational investigations of positron scattering from atomic lithium and hydrogen at low energies, for the partial waves $l = 0$, 1 and 2. Trial functions using up to 220 terms of a given angular momentum symmetry have been used to obtain cross sections for elastic scattering and positronium formation, to varying levels of convergence, in the energy region where only these two channels are open.

In both the calculations of positron-lithium scattering, and in the generation of ground-state target wavefunctions and eigenvalues for the lithium atom, two phenomenological potentials have been employed to represent the interaction of the weakly bound valence electron with the well localised positive core. The one deemed the more reliable, referred to throughout as potential A, produces a $2s$ eigenfunction with a realistic nodal structure whose energy (−0.193826 Hartree), as calculated using the Rayleigh-Ritz method, agrees with the experimentally determined estimate of the ground-state energy of lithium (−0.198158 Hartree) to within 2.5%. It also has a drawback in possessing a very tightly bound $1s$ pseudostate (at approximately −1.8 Hartree), but it was hoped that in view of the large energy separation between this and the $2s$ state, the scattering calculation would not be adversely affected by its presence.

One of the main reasons for introducing a second potential was to see whether the

absence of the tightly bound pseudostate resulted in the removal or introduction of any particular features of the positron-lithium scattering calculation. Potential B has a short-range repulsive component which prevents the formation of the very tightly bound state, instead producing a $1s$ state whose energy (−0.195718 Hartree) is in good agreement with the experimental estimate of the energy of the $2s$ state, but whose nodal structure is incorrect. In fact, all the s-states of this latter potential have one less node than the states to which they physically correspond. Although the p-state eigenfunctions have the correct forms, their energies are in markedly poorer agreement with experiment than are those of potential A.

In both cases, the effects were assessed of including a term in the potentials which allowed for the polarization of the atomic core. The inclusion of this term in the scattering calculation represented a complication which, it was felt, was best avoided initially if possible. Its introduction altered the position of the ground state energies by only about 2%, with its effects growing smaller still for the higher eigenstates. The forms of the eigenfunctions themselves were affected very little.

The polarizabilities of the model atoms generated using the two potentials were evaluated by means of a further Rayleigh-Ritz calculation which introduced a perturbing electric field into the Hamiltonian for the system. Again the effects of introducing the core polarization term were studied. With the term included, the polarizability calculated for potential A was in excellent agreement with the experimental estimate, being rather less than 1% larger. Excluding it had the effect of increasing the polarizability of the model, leaving it in error by approximately 8%. With or without the term, the calculated polarizability using potential B was in markedly worse agreement with experiment, reflecting the poor representation of the lithium p-states produced by this potential. Including the polarization of the core gave rise to an overall polarizability which was too small by about 16%, although its exclusion improved agreement

with experiment somewhat, giving a value within 12% of the measured estimate. On the strength of the calculations of the energies and polarizabilities, it was felt that potentials A and B, with the core polarization term excluded, still provided a very good representation of the lithium atom.

For the purposes of the positron-lithium scattering calculation, the interaction between the positron and core was taken to have the same form as the electron-core potential (without the core polarization term), but with the sign reversed. This involved the assumption that exchange effects had a very small effect on the form of the electron-core potential, which was reasonable on account of the valence electron being so weakly bound.

For s-wave positron-lithium scattering, two types of trial function were used, which differed only in the forms for their short-range components. The original form was essentially the same as that used in previous positron-hydrogen calculations, but with the simple $1s$ hydrogen target function replaced by the 15 term lithium wavefunction generated in the Rayleigh-Ritz calculation. The presence of this target wavefunction as a multiplicative factor in the short-range Hylleraas expansion proved, however, to be too restrictive for such a polarizable target atom, and convergence was found to be poor. Removing it, though, produced a marked improvement, giving rise to more positive values for K_{11} and K_{22}, and more stable cross sections. For the remainder of the lithium calculations (for the higher partial waves also) this latter type of scattering trial function was used throughout.

After some time spent optimising the non-linear parameters, trial functions containing up to 165 linear parameters were used to calculate s-wave cross sections for elastic scattering and positronium formation for energies between zero and the respective first excitation thresholds of the two potentials. Close to zero energy, Wigner's prediction of a k^{-1} dependence for the Ps formation cross section was seemingly confirmed for

both potentials, although this rearrangement channel contributed negligibly over most of the range considered, elastic scattering being, in general, the dominant cross section by several orders of magnitude. Unsurprisingly, uncoupling Ps formation as an outgoing channel in the calculation produced only a very small effect on the elastic scattering cross section, although discrepancies between the present results and those of McEachran indicated that virtual Ps formation probably still plays a large part in the scattering process.

Convergence of the s-wave results was satisfactory, although the very high polarizability of the lithium atom imposed much greater demands on the trial functions than had been the case for the hydrogen problem, for which they were originally devised. As $k \to 0$, in particular, convergence deteriorated to such an extent that attempts to extrapolate to fully converged values of the diagonal K-matrix elements were impracticable. In order to obtain very reliable results for $k < 0.05a_0^{-1}$, it would be necessary to introduce medium-range polarization terms into the wavefunction. To make this modification worthwhile would also require the inclusion of the core polarization effects in the electron- and positron-core potentials, since it is at these energies that they are likely exert their greatest influence. It should be noted, however, that the infinite Ps cross section at zero energy is always liable to cause convergence problems in this type of calculation. The complicated nature of the positron-atom interaction is well illustrated by the close-coupling results of McAlinden *et al.*, which require the introduction of many states to yield s-wave Ps formation cross sections of even the same order of magnitude as the present Kohn variational data.

For p-wave positron-lithium scattering, the two types of short-range correlation term, arising from the two different angular momentum symmetries, made the calculations more time consuming than for s-wave collisions, and it was not possible to go into as much detail optimising the non-linear parameters. With sufficiently many

linear parameters included in the trial functions, however, it was not difficult to find a set of values which gave rise to smooth cross sections, where agreement between Kohn and Inverse Kohn results was generally good. The results obtained indicated a zero p-wave Ps formation cross section at zero energy, again in accord with Wigner's threshold theory, but a much larger contribution to the scattering process from this channel than for s-wave over most of the energy range. The p-wave Ps formation channel, in fact, dominates the elastic channel at the lower end of the energy spectrum.

Although, for a low value of ω, no structure was observed in the p-wave elastic cross section, a minimum was observed to develop, close to $k = 0.1a_0^{-1}$, as the number of linear parameters in the trial function was increased, as a consequence of K_{11} converging upwards from negative to positive values. This was a feature of both potentials, and also of the close-coupling results of McAlinden et $al.$ Uncoupling the positronium channel in the p-wave scattering calculation had the effect of introducing a spurious resonance in to the elastic cross section, and illustrated the necessity for including all scattering channels in the formalism, if reliable results are to be obtained.

In neither the s- nor the p-wave calculations were any significant qualitative differences observed between results for the two different potentials. This would appear to lend weight to the assumption that the $1s$ pseudo-state of potential A exerts a rather small influence. Since the higher eigenstates and the polarizability of this potential are in better agreement with experiment than are those of potential B, and its eigenfunctions have a more realistic structure, the scattering cross sections obtained using potential A are always taken to be the more accurate.

Only preliminary investigations have so far been undertaken for d-wave scattering, and further optimisation of the non-linear parameters in the trial functions is required. Results obtained exhibit a similar trend to the close-coupling data of McAlinden et $al.$, and suggest contributions to the elastic and positronium formation cross sections similar

in magnitude to those obtained for p-wave scattering. When more fully converged results have been calculated, it will be possible to embark on an evaluation of differential cross sections for positron lithium scattering, which, for scattering from channel ν in to channel ν' are given by

$$\sigma_{\nu\nu'}(\theta) \;\; = \;\; \frac{1}{k^2}\left[\sum_l(2l+1)\left(\frac{K}{1-iK}\right)_{\nu\nu'}P_l(\cos\theta)\right]^2 \qquad (6.1)$$

in units of a_0^2.

Further possible extensions to the present work on positron-lithium scattering might include excitation of the lithium atom in to its $2p$ state, requiring the development of a three-channel Kohn functional. Such a modification would also necessitate more complicated trial functions to allow for more scattering channels and for the possibility of differences in the angular momentum of the incoming and outgoing positron.

New investigations were also performed on the positron-hydrogen system, for the purpose of studying threshold phenomena. Expressions were derived, using R-matrix threshold theory, for the effect on the elastic cross section of the newly opened positronium channel. The infinite slope of the s-wave positronium formation cross section was predicted to give rise to a sharp drop in the elastic cross section, but on a scale which would be unresolvable within the limits of the present calculation. The expression giving the threshold effect in the p-wave elastic cross section was shown to yield quite a good fit to the Kohn results above threshold, by assuming a slowly varying value for the uncoupled phaseshift, δ_l. For both s- and d-wave positron-hydrogen scattering, particularly the latter, the lack of continuity in the elastic cross section in going across the Ps formation threshold indicated that the trial functions were under considerable strain in this energy region. The smoothness of the p-wave cross section, however, indicated that things might be improved by varying the non-linear parameters in the wavefunction, and this would seem the next logical step for these investigations.

Continuing developments in the field of experimental positron physics constantly

provide a renewed stimulus to perform accurate theoretical calculations of positron scattering from atoms, and it is hoped that the results of the investigations reported here will, conversely, help to sustain interest in precise measurements of cross sections for the positron-hydrogen and positron-lithium systems.

Appendix A

The Method of Models

The method of models is a convenient way of simplifying the positron-atom problem, which takes advantage of the fact that there is no exchange of the positron with the atomic electrons. This approach has been used successfully in the Kohn variational studies of positron-helium elastic scattering.

Consider the exact Hamiltonian for an atomic target:

$$H_0 = -\tfrac{1}{2}\nabla^2_{atom} + V_{atom},$$ (A.1)

where ∇^2_{atom} is the sum of the Laplacian operators for all the atomic electrons. It may be possible to derive an exact ground state wavefunction, Φ_0, for this system, such that $H_0\Phi_0 = E_0\Phi_0$; this would be the case if, for example, the potential V_{atom} were purely Coulombic, as in atomic hydrogen. In general, though, such an exact evaluation is not possible and it is usually necessary to make do with some approximation, Φ_m, to the exact wavefunction. The assumption of the method of models is that this approximate eigenfunction can still be considered an exact eigenfunction of *some* model Hamiltonian, which represents a good approximation to H_0, such that

$$H_m = -\tfrac{1}{2}\nabla^2_{atom} + V_m,$$ (A.2)

and thus

$$H_m\Phi_m = E_m\Phi_m,$$ (A.3)

where E_m is the approximate energy eigenvalue which corresponds to E_0.

In considering positron scattering from a target with the Hamiltonian H_m, the total Hamiltonian becomes

$$H_T = -\tfrac{1}{2}\nabla_{e+}^2 - \tfrac{1}{2}\nabla_{atom}^2 + V_{int} + V_m \tag{A.4}$$

where V_{int} is the positron-atom interaction potential. Since the total energy of the model system is given by $E_T = \tfrac{1}{2}k^2 + E_m$, where k is the positron wavenumber, the operator $L = 2(H_T - E_T)$ can be written

$$L = -\nabla_{e+}^2 - \nabla_{atom}^2 + 2V_{int} + 2V_m - k^2 - 2E_m. \tag{A.5}$$

Generating the matrix elements needed for the variational scattering calculation requires L to operate on all components of the scattering wavefunction. Since the positron and electron are distinguishable particles, there is no requirement for the scattering wavefunction to be antisymmetric with respect to exchange of the scattered positron with the electrons of the target. Thus for elastic scattering all terms in the total wavefunction can be expressed in the form

$$F = f\Phi_m, \tag{A.6}$$

where f is in general a function of all the inter-particle separations. We therefore have

$$
\begin{aligned}
LF &= \left(-\nabla_{e+}^2 - \nabla_{atom}^2 + 2V_{int} + 2V_m - k^2 - 2E_m\right) f\Phi_m \\
&= \Phi_m\left(-\nabla_{e+}^2 - \nabla_{atom}^2 + 2V_{int} - k^2\right) f - 2\nabla_{atom}f\cdot\nabla_{atom}\Phi_m \\
&\quad + f\left(-\nabla_{atom}^2 + 2V_m - 2E_m\right)\Phi_m. \tag{A.7}
\end{aligned}
$$

The final term in (A.7) disappears, however, since Φ_m satisfies (A.3), so the expression reduces to

$$LF = \Phi_m\left(-\nabla_{e+}^2 - \nabla_{atom}^2 + 2V_{int} - k^2\right) f - 2\nabla_{atom}f\cdot\nabla_{atom}\Phi_m. \tag{A.8}$$

Hence by making the assumption that Φ_m is an exact eigenfunction of H_m, we arrive at a form for LF in which there is no explicit reference to either the model potential, V_m, or the energy eigenvalue, E_m. Thus, in calculations of purely elastic scattering, the nature of the model Hamiltonian and its eigenvalues can effectively be ignored, once the model target wavefunction has been calculated. The method of models thus provides an elegant, self-consistent means of simplifying the formulation of the elastic scattering problem, when the target wavefunction is not known exactly. When Ps formation is also considered, however, this approach has to be abandoned, since it is then necessary to consider explicitly the interaction of the electron in the outgoing positronium with the residual ion.

In the positron-lithium studies reported here, assumptions are made which are similar to those used in the method of models, to allow the simplification of the integrands for the matrix elements where L operates on terms involving the lithium target wavefunction. The precision of the Rayleigh-Ritz calculation used to generate this wavefunction, however, is sufficient that the Hamiltonian of which ϕ_{Li} is to be considered an exact eigenfunction, differs only very slightly from the full target Hamiltonian. The inconsistency introduced by making explicit reference to the electron-core potential in the other matrix elements is therefore small enough to be negligible.

Appendix B

Symmetry Arguments

The number of matrix elements which require evaluating in order to form the matrices A, B, and (S, LS) of equations (2.15) and (2.17) can be reduced considerably by symmetry arguments and the application of Green's theorem. In practice, it is often not very much trouble to evaluate some of the extra elements and, when this is the case, doing so provides a useful check on the numerical accuracy of the calculation.

Consider two functions, f and g, which could correspond to any of the terms, short- or long-range, in the scattering wavefunctions, and now consider the functional F, which is such that

$$F = (f, Lg) - (g, Lf) \tag{B.1}$$

where $L = (-\nabla_1^2 - \nabla_2^2 + 2V - 2E)$, and the integrals denoted by the brackets extend over all space for both the positron and electron. It is evident that $(f, (V - E)g) = (g, (V - E)f)$, since V and E operate in a purely multiplicative way, so we are left with

$$F = -(f, \nabla_1^2 g) + (g, \nabla_1^2 f) - (f, \nabla_2^2 g) + (g, \nabla_2^2 f). \tag{B.2}$$

Green's theorem states

$$\int_V \phi_1 \nabla^2 \phi_2 d\tau = \int_A \phi_1 \nabla \phi_2 \cdot d\sigma - \int_V \nabla \phi_1 \cdot \nabla \phi_2 d\tau, \tag{B.3}$$

whereupon

$$\int_V \left[\phi_1 \nabla^2 \phi_2 - \phi_2 \nabla^2 \phi_1 \right] d\tau = \int_A \left[\phi_1 \nabla \phi_2 - \phi_2 \nabla \phi_1 \right] \cdot d\sigma, \tag{B.4}$$

where A is the closed surface which forms the boundary of the volume V. Applying this to (B.2), we find that, in the limit as $r_1, r_2 \to \infty$,

$$F = \int_{V_2} \left[\int\!\!\!\int_{A_1} (g\boldsymbol{\nabla}_1 f - f\boldsymbol{\nabla}_1 g)\boldsymbol{\cdot} d\boldsymbol{\sigma}_1 \right] d\tau_2 + \int_{V_1} \left[\int\!\!\!\int_{A_2} (g\boldsymbol{\nabla}_2 f - f\boldsymbol{\nabla}_2 g)\boldsymbol{\cdot} d\boldsymbol{\sigma}_2 \right] d\tau_1. \quad \text{(B.5)}$$

It is therefore the case that, if the surface integrals vanish in the limit as $r_1 \to \infty$ for the first term and $r_2 \to \infty$ for the second term, then $F = 0$ and $(f, Lg) = (g, Lf)$. If the surfaces are taken, without loss of generality, to be spheres of infinite radius, then the surface elements have the form $d\boldsymbol{\sigma} = r^2 \sin\theta\, d\theta\, d\phi\, \hat{\mathbf{r}}$ and, in order that the surface integrals vanish, it is necessary that their integrands tend to zero faster than r^{-2}. The exponential dependence of the short-range correlation terms ϕ_i on all three interparticle coordinates r_1, r_2 and r_3 ensures that $F = 0$ if f or g corresponds to one of these. Thus,

$$(\phi_i, L\phi_j) = (\phi_j, L\phi_i) \qquad \text{(B.6)}$$

$$(\phi_i, LS_1) = (S_1, L\phi_i) \qquad \text{(B.7)}$$

$$(\phi_i, LC_1) = (C_1, L\phi_i) \qquad \text{(B.8)}$$

$$(\phi_i, LS_2) = (S_2, L\phi_i) \qquad \text{(B.9)}$$

$$(\phi_i, LC_2) = (C_2, L\phi_i). \qquad \text{(B.10)}$$

If f is equal to S_1 or C_1, whilst g is equal to S_2 or C_2, then all the surface integrand terms in (B.5) have a decaying exponential dependence on r_2 and r_3, since they depend on both the positronium and lithium wavefunctions. As $r_1 \to \infty$, keeping r_2 fixed, the decay of r_3 kills off the first term, and the second term vanishes as $r_2 \to \infty$ because of the exponential fall-off in the electron coordinate, so we also have

$$(S_1, LS_2) = (S_2, LS_1) \qquad \text{(B.11)}$$

$$(C_1, LC_2) = (C_2, LC_1) \qquad \text{(B.12)}$$

$$(S_1, LC_2) = (C_2, LS_1) \qquad \text{(B.13)}$$

$$(C_1, LS_2) = (S_2, LC_1). \qquad \text{(B.14)}$$

141

If we now consider the case where

$$f = S_1 = Y_{l0}(\theta_1, \phi_1)\phi_T(r_2)\sqrt{k}j_l(kr_1) \tag{B.15}$$

$$g = C_1 = Y_{l0}(\theta_1, \phi_1)\phi_T(r_2)\sqrt{k}n_l(kr_1)(1 - \exp -\mu r_1) \tag{B.16}$$

then the exponential dependence on r_2 in the target function $\phi_T(r_2)$ ensures that the second surface integral in (B.5) vanishes. The first term remains, however, and since we are considering surface elements normal to $\mathbf{r_1}$ we can ignore the angular dependence of ∇_1 to obtain

$$(S_1, LC_1) - (C_1, LS_1) = \int_{V_2} \left[\int_{A_1} \left(C_1 \frac{\partial S_1}{\partial r_1} - S_1 \frac{\partial C_1}{\partial r_1} \right) r_1^2 \sin \theta_1 d\theta_1 d\phi_1 \right] d\tau_2 \tag{B.17}$$

As we are considering the limiting case of an integral over the spherical surface A_1 as $r_1 \to \infty$, we require the asymptotic forms for S_1 and C_1, which are

$$\lim_{r_1 \to \infty} S_1 = Y_{l0}\phi_T \frac{1}{\sqrt{k}} \frac{\sin\left(kr_1 - \frac{l\pi}{2}\right)}{r_1} \tag{B.18}$$

$$\lim_{r_1 \to \infty} C_1 = Y_{l0}\phi_T \frac{1}{\sqrt{k}} \frac{\cos\left(kr_1 - \frac{l\pi}{2}\right)}{r_1}. \tag{B.19}$$

The partial derivatives are thus given by

$$\lim_{r_1 \to \infty} \frac{\partial S_1}{\partial r_1} = Y_{l0}\phi_T \frac{1}{\sqrt{k}} \left[\frac{k \cos\left(kr_1 - \frac{l\pi}{2}\right)}{r_1} - \frac{\sin\left(kr_1 - \frac{l\pi}{2}\right)}{r_1^2} \right] \tag{B.20}$$

$$\lim_{r_1 \to \infty} \frac{\partial C_1}{\partial r_1} = Y_{l0}\phi_T \frac{1}{\sqrt{k}} \left[\frac{-k \sin\left(kr_1 - \frac{l\pi}{2}\right)}{r_1} - \frac{\cos\left(kr_1 - \frac{l\pi}{2}\right)}{r_1^2} \right], \tag{B.21}$$

whereby the integrand reduces to

$$C_1 \frac{\partial S_1}{\partial r_1} - S_1 \frac{\partial C_1}{\partial r_1} = Y_{l0}^2 \phi_T^2 \frac{1}{r_1^2}. \tag{B.22}$$

We therefore find, simply, that

$$(S_1, LC_1) - (C_1, LS_1) = \int [\phi_T(r_2)]^2 \, d\tau_2 \int [Y_{l0}(\theta_1, \phi_1)]^2 \sin \theta_1 d\theta_1 d\phi_1$$

$$= 1. \tag{B.23}$$

Thus

$$(S_1, LC_1) = (C_1, LS_1) + 1. \qquad (B.24)$$

When L operates on S_2 and C_2 it is convenient to use the form

$$L = (-2\nabla_3^2 - \tfrac{1}{2}\nabla_\rho^2 + 2V - 2E), \qquad (B.25)$$

and similar arguments to those above can be used to show that

$$(S_2, LC_2) = (C_2, LS_2) + 1. \qquad (B.26)$$

Appendix C

Angular Integration

As the complexity of the spherical harmonics, Y_{l0}, in the scattering wavefunction increases as we consider higher partial waves, so the angular integrations become more complicated. The problem is simplified considerably, however, by the spherical symmetry of the s-state target system, and also the azimuthal symmetry of the scattering.

As a typical case, consider the evaluation of a p-wave matrix element involving a type 1 and a type 2 long-range term (e.g. (S_1, LS_2), (C_2, LS_1)). The general form of the integration would be

$$I = \int \int Y_{l0}(\theta_1, \phi_1) Y_{l0}(\theta_\rho, \phi_\rho) f(r_1, r_2, r_3) d\tau_2 d\tau_1. \qquad \text{(C.1)}$$

For $l = 1$, the spherical harmonics are given by $Y_{10}(\theta, \phi) = \sqrt{\frac{3}{4\pi}} \cos \theta$ so

$$I = \int \int \frac{3}{4\pi} \cos \theta_1 \cos \theta_\rho f(r_1, r_2, r_3) d\tau_2 d\tau_1. \qquad \text{(C.2)}$$

From the cosine rule we have

$$\cos \theta_\rho = \frac{(r_1 \cos \theta_1 + r_2 \cos \theta_2)}{2\rho} \qquad \text{(C.3)}$$

whereupon a substitution gives

$$I = \int \int \frac{3}{4\pi} \left(r_1 \cos^2 \theta_1 + r_2 \cos \theta_1 \cos \theta_2 \right) \frac{1}{2\rho} f(r_1, r_2, r_3) d\tau_2 d\tau_1. \qquad \text{(C.4)}$$

Here we have an expression which depends on two external angles, θ_1 and θ_2. Although it would be possible to carry out the integration using these coordinates, this would
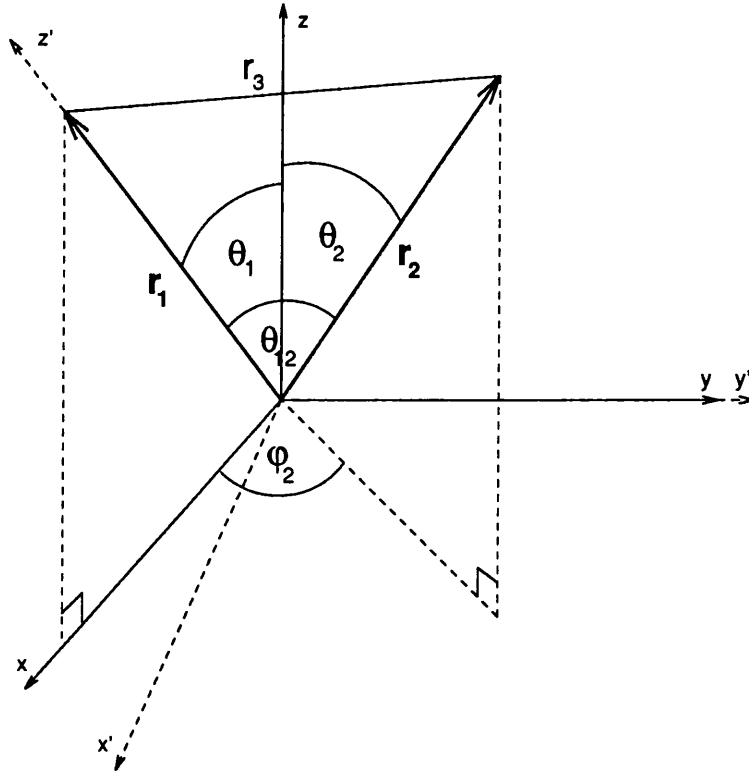
Figure C.1: The coordinates of the positron-atom system

require us to consider the complicated variation of the interparticle distance r_3 as we integrate about the first azimuthal angle. Instead, it is much better to select one of the two position vectors as a z-axis to perform the integration for the other vector, whereupon this complication is avoided. Here, it is most convenient to choose the r_1 vector as the z-axis for the r_2 integration, although the alternative choice would eventually yield the same result.

The coordinates of the positron-atom system for an effective one-electron target are shown in figure C.1. The azimuthal symmetry has allowed us, without any loss of generality, to rotate the x and y axes about the z-axis until r_1 lies in the x-z plane. If we now rotate about the y-axis until the z-axis lies along r_1, then we have a new set of axes (x', y', z') in which the r_2 vector has the coordinates $(r_2, \theta_{12}, \phi_2')$. We now need to express θ_2 in terms of the new coordinates, which is most easily done by finding the components of the unit vectors of the original z-axis $(\hat{k})$ and r_2 in the new system.

Simple trigonometric considerations show that these are given by

$$\hat{\mathbf{k}} = (-\sin\theta_1, 0, \cos\theta_1) \tag{C.5}$$

$$\hat{\mathbf{r}}_2 = (\sin\theta_{12}\cos\phi_2', \sin\theta_{12}\sin\phi_2', \cos\theta_{12}), \tag{C.6}$$

and therefore

$$\cos\theta_2 = \hat{\mathbf{k}}\cdot\hat{\mathbf{r}}_2 = \cos\theta_1\cos\theta_{12} - \sin\theta_1\sin\theta_{12}\cos\phi_2'. \tag{C.7}$$

Substituting this back into (C.4) we obtain

$$I = \frac{3}{4\pi}\int d\tau_1 \int_0^\infty r_2^2 dr_2 \int_0^\pi \sin\theta_{12}d\theta_{12}\int_0^{2\pi} d\phi_2' \left(r_1\cos^2\theta_1\right.$$
$$\left. + r_2\cos^2\theta_1\cos\theta_{12} - r_2\cos\theta_1\sin\theta_1\sin\theta_{12}\cos\phi_2'\right)\frac{1}{2\rho}f(r_1,r_2,r_3). \tag{C.8}$$

Since none of the other variables depends on ϕ_2' this can be integrated over 2π immediately to give

$$I = \frac{3}{2}\int d\tau_1 \int_0^\infty r_2^2 dr_2 \int_0^\pi \sin\theta_{12}d\theta_{12}\cos^2\theta_1\left(r_1 + r_2\cos\theta_{12}\right)\frac{1}{2\rho}f(r_1,r_2,r_3). \tag{C.9}$$

The integration over the remaining external angles θ_1 and ϕ_1 can be done using $d\tau_1 = r_1^2 dr_1 \sin\theta_1 d\theta_1 d\phi_1$, giving

$$I = 2\pi\int_0^\infty r_1^2 dr_1 \int_0^\infty r_2^2 dr_2 \int_0^\pi \sin\theta_{12}d\theta_{12}\left(r_1 + r_2\cos\theta_{12}\right)\frac{1}{2\rho}f(r_1,r_2,r_3), \tag{C.10}$$

which depends only on the internal coordinates of the system. The angle θ_{12} can be expressed in terms of r_1, r_2 and r_3 using the cosine rule:

$$\cos\theta_{12} = \frac{r_1^2 + r_2^2 - r_3^2}{2r_1 r_2}. \tag{C.11}$$

If r_1 and r_2 are kept fixed and the variation of θ_{12} with r_3 is considered, we find

$$\sin\theta_{12}d\theta_{12} = \frac{r_3}{r_1 r_2}dr_3 \tag{C.12}$$

and thus the integral becomes

$$I = 2\pi\int_0^\infty r_1 dr_1 \int_0^\infty r_2 dr_2 \int_{|r_1-r_2|}^{r_1+r_2} r_3 dr_3 (r_1 + r_2\cos\theta_{12})\frac{1}{2\rho}f(r_1,r_2,r_3). \tag{C.13}$$

Numerical integration of this expression is simplified further by the substitution of the perimetric coordinates, described in section 2.2.4.

146

Appendix D

Parameter Values

D.1 Lithium model potential

The lithium model potentials are of the form

$$V(r) = -\frac{1}{r} - \frac{2e^{-\gamma r}}{r}\left(1 + \delta r + \delta' r^2\right) - \frac{\alpha_d}{2r^4}\omega_2(\beta r). \qquad \text{(D.1)}$$

Potential	γ	δ	δ'	$\alpha_d(a_0^3)$	β
A	4.049689462	2.447656964	0.245046253	0.192456	3.910776273
B	3.640580350	−29.204733320	−0.779876393	0.192456	3.910776273

D.2 Non-linear Parameters

D.2.1 Positron-Hydrogen Scattering

Partial wave	α	β	γ
s	0.40	−0.60	0.35
p	0.40	−0.60	0.35
d	0.60	−0.20	0.25

D.2.2 Positron-Lithium Scattering

Partial wave	α	β	γ
s	0.13	0.74	0.17
p	0.20	0.70	0.20
d	0.50	0.70	0.40

References

Anderson C D 1932 *Science* **76** 238

Archer B J, Parker G A and Pack R T 1990 *Phys. Rev. A* **41** 1303

Armour E A G and Humberston J W 1991 *Phys. Rep.* **204**(2) 165

Bhatia A K, Temkin A, Drachman R J, and Eiserike H 1971 *Phys. Rev. A* **3** 1328

Bhatia A K, Temkin A, Eiserike H 1974 *Phys. Rev. A* **9** 219

Blackett P M S and Occhialini G P S 1933 *Proc. Roy. Soc. A* **139** 699

Breit G 1957 *Phys. Rev.* **107** 1612

Brown C J 1986 *Ph. D. Thesis, Univ. London*

Brown C J and Humberston J W 1984 *J. Phys. B* **17** L423

Brown C J and Humberston J W 1985 *J. Phys. B* **18** L401

Brownstein K R and McKinley W A 1968 *Phys. Rev.* **170** 1255

Campeanu R I 1977 *Ph. D. Thesis, Univ. London*

Campeanu R I, Fromme D, Kruse G, McEachran R P, Parcell L A, Raith W, Sinapius G and Stauffer A D 1987 *J. Phys. B* **18** 3557

Carbonell J 1994 *Private Communication* (to be published)

Coleman P G, Johnston K A, Cox A M G, Goodyear A and Charlton M 1992 *J. Phys. B* **25** L585

Dirac P A M 1928 *Proc. Roy. Soc. A* **117** 610

Dirac P A M 1931 *Proc. Roy. Soc. A* **133** 80

Fon W C, Berrington K A, Burke P G and Kingston A E 1981 *J. Phys. B* **14** 1041

Harris F E and Michels H H 1971 *Methods Comput. Phys.* **10** 143

Hewitt R N, Noble C J and Bransden B H 1992 *J. Phys. B* **25** 2683

Higgins K and Burke P G 1993 *J. Phys. B* **26** 4269

Humberston J W and Wallace J B G 1972 *J. Phys. B* **5** 1138

Humberston J W 1973 *J. Phys. B* **6** L305

Humberston J W 1979 *Adv. At. Mol. Phys.* **15** 101

Humberston J W 1982 *Can. J. Phys.* **60** 591

Humberston J W 1986 *Adv. At. Mol. Phys.* **22** 1

Igarashi A and Toshima N 1994 *Phys. Rev. A* (to be published)

Johansson I 1958 *Arkiv för Fysik* **15** 14

Kauppila W E, Stein T S, Smart J H, Dababneh M S, Ho Y K, Downing J P and Pol V 1981 *Phys. Rev. A* **24** 725

Kauppila W E and Stein T S 1990 *Adv. At. Mol. Opt. Phys.* **26** 1

Kohn W 1948 *Phys. Rev.* **74** 1763

McAlinden M T, Kernoghan A A and Walters H R J 1994a (Private Communication)

McAlinden M T, Kernoghan A A and Walters H R J 1994b *Hyperfine Interactions* (to be published)

McEachran R P 1992 *Private Communication*

McEachran R P, Horbatsch M, Stauffer A D and Ward S J 1990 *Annihilation in Gases and Galaxies* NASA Conference Publication **3058** p1

Meyerhof W E 1962 *Phys. Rev.* **128**(5) 2312

Meyerhof W E 1963 *Phys. Rev.* **129**(2) 692

Meyerhof W E 1994 *Private Communication*

Miller T M and Bederson B 1977 *Adv. At. Mol. Phys.* **13** 1

Moxom J 1993 *Ph. D. Thesis, Univ. London*

Moxom J, Laricchia G, Charlton M, Kover A and Meyerhof W E 1994 *Phys. Rev. A* (to be published)

Nesbet R K 1968 *Phys. Rev.* **175** 134

Nesbet R K 1969 *Phys. Rev.* **179** 60

Norcross D W and Moores D L 1972 *Atomic Phys.* **3** 261

Peach G, Saraph H E and Seaton M J 1988 *J. Phys. B* **21** 3669

Register D and Poe R T 1975 *Phys. Lett.* **51A** 431

Schwartz C 1961a *Ann. Phys.* **16** 36

Schwartz C 1961b *Phys. Rev.* **124** 1468

Schwartz C 1961c *Phys. Rev.* **123** 1700

Sperber W, Becker D, Lynn K G, Raith W, Schwab A, Sinapius G, Spicher G and Weber M 1992 *Phys. Rev. Lett.* **68** 3690

Spruch L and Rosenberg L 1960 *Phys. Rev.* **117** 143

Stein T S, Gomez R D, Hsieh Y-F, Kauppila W E, Kwan C K and Wan Y J 1985 *Phys. Rev. Lett.* **55** 488

Stein T S, Dababneh M S, Kauppila W E, Kwan C K and Wan Y J 1988 *Atomic Physics with Positrons* ed J W Humberston and E A G Armour (London: Plenum) p251

Stein T S, Kauppila W E, Kwan C K, Lukaszew R A, Parikh S P, Wan Y J, Zhou S and Dababneh M S 1990 *Annihilation in Gases and Galaxies* (NASA Conference Publication **3058**) p13

Weiss A W 1963 *Astrophysical Journal* **138** 1262

Weyl H 1931 *Gruppentheorie und Quantenmechanik (2nd edn.)* p234

Wigner E P 1948 *Phys. Rev.* **73** 1002

Zhou S, Kauppila W E, Kwan C K and Stein T S 1994 *Phys. Rev. Lett.* **72**(10) 1443

Zhou Y and Lin C D 1994 *Phys. Rev. A* (to be published)

LETTER TO THE EDITOR

Low energy s-wave positron–lithium scattering

M S T Watts and J W Humberston

Department of Physics and Astronomy, University College London, Gower Street, London
WC1E 6BT, UK

Abstract. A detailed investigation has been made of low energy s-wave positron–lithium scattering using the Kohn variational method in the energy range in which only elastic scattering and positronium formation are possible (0–1.84 eV). The positronium formation cross section is infinite at zero energy, but then falls to be several orders of magnitude smaller than the elastic scattering cross section, which has a peak value of approximately $100\ \pi a_0^2$. The elastic scattering cross sections are almost unaffected by the uncoupling of the positronium channel, but the resulting phaseshifts are significantly more positive, and therefore probably more accurate, than those obtained in the most sophisticated previous study using the uncoupled approximation.

Positron scattering by the alkali atoms has been studied theoretically for several years (see Ward *et al* (1989) and McEachran *et al* (1990) for references to earlier work), but the recent experimental measurements of total cross sections by Stein *et al* (1985, 1988, 1990) have stimulated renewed theoretical interest in such systems.

The experimental results show that, unlike for other target atoms, the total scattering cross sections for the alkali atoms are slightly larger at low energies for positrons than for electrons, most probably because of a significant positronium formation component in the case of the former projectile. A further interesting feature is that positronium formation is possible even at zero energy because the ionization energies of all the alkali atoms are less than the binding energy of positronium (6.8 eV). Most previous theoretical studies of low-energy positron–alkali-atom scattering have, however, neglected the positronium formation channel and concentrated instead on elastic scattering and excitation. Even where positronium formation has been included, the methods of approximation have been somewhat crude (for example, the Born and coupled static approximations (Guha and Ghosh 1981) and the distorted-wave approximation (Mazumdar and Ghosh 1986)), yielding possibly rather inaccurate results (see note added in proof). There is clearly a need for a much more detailed study of low-energy positron–alkali-atom scattering, and the initial results of such a study are presented here.

It is a reasonably good approximation to consider the alkali atom as a single valence electron moving in the modified Coulomb field of the core. Positron–alkali-atom scattering therefore reduces to a three-body system, not unlike the positron–hydrogen system which has been studied in great detail using elaborate variational methods (Humberston 1979, 1986). Similar techniques should also give very accurate results for positron scattering by the alkali atoms. We first consider the simplest alkali atom, lithium, even though no experimental results are yet available for this target.

A good representation of the electron–core potential is provided by the form (Peach *et al* 1988)

$$V_-(r) = -\frac{1}{r} - \frac{2}{r}(1 + ar + br^2)\,e^{-\mu r} - \frac{\alpha_c}{2r^4}\,w(\nu r) \tag{1}$$

where the first two terms represent the static interaction with the core, and the third term arises from the polarization of the core, the core polarizability of Li^+ being $\alpha_c = 0.192$. The values of the parameters in V_- are chosen to reproduce the correct binding energy for the electron in the 2s state as well as all excited states, and the fit to the observed spectrum is excellent. This potential also supports a tightly bound 1s state of the electron with an energy of -51.5 eV which has, of course, no existence in the real atom and should therefore be projected out of the scattering wavefunction. Instead, we choose simply to ignore this state, assuming that its large separation in energy from the 2s target state of interest implies a small influence on the scattering process.

The positron–core potential V_+ is derived from V_- by merely changing the sign of the static component in equation (1) to give

$$V_+(r) = \frac{1}{r} + \frac{2}{r}(1 + ar + br^2)\,e^{-\mu r} - \frac{\alpha_c}{2r^4}\,w(\nu r). \tag{2}$$

This procedure is not entirely justified because exchange of the valence electron with the electrons in the core is implicitly included in V_-, whereas there is, of course, no exchange in the positron–core system. A further approximation which is being made initially is to drop the core polarization terms from V_- and V_+ because α_c is so small.

We have thus far confined our attention to the energy region below the first excitation threshold of lithium (1.84 eV), where only elastic scattering and positronium formation can occur. Thus we have the two-channel scattering process:

$$e^+ + Li \to e^+ + Li \qquad \text{elastic scattering}$$
$$\to Ps + Li^+ \qquad \text{positronium formation.}$$
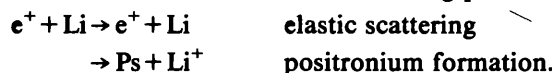
The problem is formulated as a two-channel version of the Kohn variational method, and the Kohn functional for the K matrix takes the form

$$\begin{bmatrix} K_{11}^v & K_{12}^v \\ K_{21}^v & K_{22}^v \end{bmatrix} = \begin{bmatrix} K_{11}^t & K_{12}^t \\ K_{21}^t & K_{22}^t \end{bmatrix} - \begin{bmatrix} (\Psi_1, L\Psi_1) & (\Psi_1, L\Psi_2) \\ (\Psi_2, L\Psi_1) & (\Psi_2, L\Psi_2) \end{bmatrix} \tag{3}$$

where $L = 2(H - E)$. This formulation automatically ensures a symmetric variational K-matrix; that is, $K_{12}^v = K_{21}^v$ even though $K_{12}^t \neq K_{21}^t$. For s-wave scattering the trial functions are taken to be

$$\Psi_1 = \frac{1}{\sqrt{4\pi}}\,\Phi_{Li}(r_2)\sqrt{k}\{j_0(kr_1) - K_{11}^t n_0(kr_1)[1 - \exp(-\lambda r_1)]\}$$

$$\quad - \frac{1}{\sqrt{4\pi}}\,\Phi_{Ps}(r_3)\sqrt{2\kappa}\,K_{21}^t[n_0(\kappa\rho) + \exp(-\lambda\rho)(1 + a\rho + b\rho^2)/\rho]$$

$$\quad + \frac{1}{\sqrt{4\pi}}\,\exp[-(\alpha r_1 + \beta r_2 + \gamma r_3)]\sum_{i=1}^{N} c_i r_1^{k_i} r_2^{l_i} r_3^{m_i}$$

$$\Psi_2 = \frac{1}{\sqrt{4\pi}}\,\Phi_{Ps}(r_3)\sqrt{2\kappa}\{j_0(\kappa\rho) - K_{22}^t[n_0(\kappa\rho) + \exp(-\lambda\rho)(1 + a\rho + b\rho^2)/\rho]\} \tag{4}$$

$$\quad - \frac{1}{\sqrt{4\pi}}\,\Phi_{Li}(r_2)\sqrt{k}\,K_{12}^t n_0(kr_1)[1 - \exp(-\lambda r_1)]$$

$$\quad + \frac{1}{\sqrt{4\pi}}\,\exp[-(\alpha r_1 + \beta r_2 + \gamma r_3)]\sum_{i=1}^{N} d_i r_1^{k_i} r_2^{l_i} r_3^{m_i}$$

where r_1, r_2 and ρ are the coordinates of the positron, electron and the centre of mass of the positronium relative to the core respectively. The lithium function representing the 2s orbital of the valence electron is chosen to be

$$\Phi_{Li}(r) = \exp(-\delta r) \sum_{j=0}^{n} e_j r^j \tag{5}$$

where the variational parameters are chosen to minimize the energy subject to the polarizability being close to the correct value, 165.5.

The wavenumbers of the positron and positronium, k and κ respectively, are related by energy conservation, so that

$$2E = k^2 - 0.396 = \tfrac{1}{2}\kappa^2 - \tfrac{1}{2}. \tag{6}$$

All terms with $k_i + l_i + m_i \leq \omega$ are included in the summations in Ψ_1 and Ψ_2, equation (4), the number of terms, N, being 4, 10, 20, 35, 56, 84 and 165 for $w = 1(1)8$ respectively. This formulation and form of the trial functions is similar to that used by Humberston (1982) and Brown and Humberston (1984, 1985) (see also Armour and Humberston (1991) for further details) in their very detailed investigations of positronium formation in positron scattering by atomic hydrogen.

At each energy, results have been obtained for $\omega = 4(1)8$ and the convergence of K_{11}, K_{22} and the elastic and positronium formation cross sections with respect to ω has been investigated. Apart from the occasional Schwartz singularity, K_{11} and K_{22} both increase monotonically with ω and the convergence pattern is quite well represented by

$$A(\omega) = A(\infty) + \frac{B}{\omega^p}. \tag{7}$$

The elastic scattering and positronium formation cross sections obtained with the most elaborate trial functions, with $\omega = 8$ ($N = 165$), are plotted as the curves labelled A in figures 1 and 2 respectively. Positronium formation is an exothermic process in positron-lithium scattering, and the formation cross section is $\propto 1/k$ at sufficiently low energy, and is therefore infinite at zero positron energy. It then falls rapidly with increasing positron energy to values which are negligibly small compared with the elastic scattering cross section. There is however a significant increase in the positronium formation cross section just below the 2p excitation threshold.

The elastic scattering cross section appears to be converging to a value close to zero at zero incident energy, although the extrapolation of K_{11} to infinite ω suggests that the fully converged value of the elastic scattering cross section may be slightly larger than that shown in figure 1. As the positron energy increases, the elastic scattering cross section rises rapidly to a peak value of approximately $100 \, \pi a_0^2$ at $k \simeq 0.15$ and then falls to approximately $30 \, \pi a_0^2$ at the next inelastic threshold. At energies for which $k > 0.1$ the convergence of the elastic cross section with respect to ω is sufficiently rapid that we are confident that the results plotted in figure 1 are accurate to within a few per cent. For $k < 0.1$, and particularly for values of k just above zero, the convergence shows a marked deterioration although the results still converge smoothly according to equation (7), but with a lower value of p. This deterioration occurs because the trial functions Ψ_1 and Ψ_2 only contain short-range correlation terms whereas long-range dipole terms should also be included if well converged results are to be obtained (Humberston and Wallace 1972). The need for such terms is particularly acute because of the large polarizability of the lithium atom.
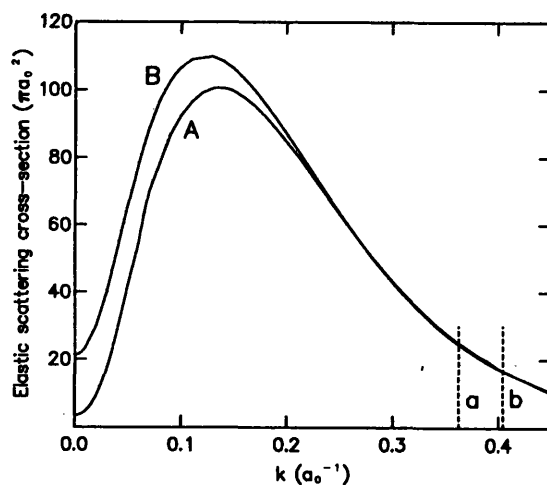
Figure 1. The s-wave positron-lithium elastic scattering cross section obtained with 165 term ($\omega = 8$) trial functions. A, with the electron-core potential which yields a 2s wavefunction for the lithium atom; B, with the electron-core potential which yields a 1s wavefunction for the lithium atom. The two dotted lines, a and b, give the position of the lowest inelastic threshold, 2p, for each of the potentials A and B respectively.
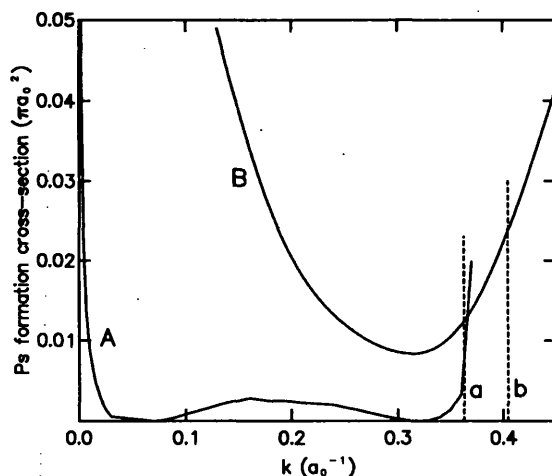

Figure 2. The positronium formation cross section in s-wave positron-lithium scattering. The meanings of curves A and B are given in the caption to figure 1.

The generally small size of the positronium formation cross section in relation to the elastic scattering cross section might be thought to indicate a weak coupling between the elastic scattering and positronium formation channels. However, comparisons with positron-hydrogen scattering (Humberston 1986), where the s-wave positronium formation cross section is also very small, suggest that the p- and d-wave contributions to positronium formation in positron-lithium scattering will be much larger, implying a strong coupling between the two channels.

As previously mentioned, most other studies of positron-lithium scattering have ignored the positronium formation channel, and we have therefore repeated our calculations with the two channels uncoupled so that we can make direct comparisons

with the results of some other previous studies of elastic scattering. The present uncoupled results for the elastic scattering cross section are very similar to those with the coupling present, and, indeed, the two sets of results cannot be resolved on the scale of figure 1.

It is instructive to compare the present uncoupled elastic scattering results with those of Ward *et al* (1989) and McEachran *et al* (1990) who used the close coupling approximation with up to five states of the target lithium atom (results with eight target states have recently been provided for us by McEachran (private communication)). This is the most sophisticated of all the previous studies in which positronium formation has been neglected. The present phaseshifts are more positive, and therefore probably more accurate, than those of McEachran *et al*, as can be seen in table 1, although it should be borne in mind that the model potentials used in the two investigations are not identical.

Table 1. Values of the s-wave phaseshift for positron–lithium scattering in the uncoupled approximation.

	Phaseshift (rad)		
$k(a_0^{-1})$	Present	McEachran *et al*[a] (8 term)	McEachran *et al*[a] (5 term)
0.01	3.123	2.987	2.963
0.1	2.638	1.787	1.703
0.2	1.969	1.046	0.9794
0.3	1.413	0.5815	0.5281

[a] These results have been supplied by McEachran (private communication).

It was mentioned earlier that we have simply ignored the tightly bound 1s state supported by the electron–core potential, equation (1). This problem may be avoided altogether by using as the wavefunction of the lithium atom the ground state of the electron in a modified form of V_- such that this ground state has the correct lithium ground state energy, namely -5.386 eV. Such a potential has been devised by Peach (private communication). Clearly the radial dependence of this nodeless 1s orbital is not the same as that of the 2s orbital, and neither does the polarizability of the modified lithium atom have the correct value of 165.3 (instead it is 138.5), but this new model system is now free of the formal complication of the unphysical tightly bound ground state. The elastic scattering and positronium formation cross sections with this modified form of V_-, and the consequentially modified V_+, are also plotted in figures 1 and 2 as the curves labelled B. The new elastic scattering cross sections are quite similar to those obtained with the original potential, but the new positronium formation cross sections are an order of magnitude larger than the former values, although still very small compared with the elastic cross section except when $k \to 0$. Here also there is a pronounced rise in the cross section just below the next inelastic threshold. It is unlikely that the differences between the positronium formation cross sections for the two potentials will be as large for higher partial waves because the centrifugal barrier will then tend to exclude the wavefunction from the short-range region where the differences between the two potentials are most pronounced.

We are currently improving these calculations by introducing the core polarization terms into the electron- and positron-core potentials, and we are also extending the investigations to higher partial waves.

Note added in proof. The positronium channel has recently been included in a more satisfactory manner within the close coupling approximation by Hewitt *et al* (1992) and by Basu and Ghosh (1991).

References

Armour E A G and Humberston J W 1991 *Phys. Rep.* **204** 165
Basu M and Ghosh A S 1991 *Phys. Rev.* A **43** 4746
Brown C J and Humberston J W 1984 *J. Phys. B: At. Mol. Phys.* **17** L423
—— 1985 *J. Phys. B: At. Mol. Phys.* **18** L401
Guha S and Ghosh A S 1981 *Phys. Rev.* A **23** 743
Hewitt R N, Noble C J and Bransden B H 1992 *J. Phys. B: At. Mol. Opt. Phys.* **25** 2683
Humberston J W 1979 *Adv. At. Mol. Phys.* **15** 101
—— 1986 *Adv. At. Mol. Phys.* **22** 1
—— 1982 *Can. J. Phys.* **60** 591
Humberston J W and Wallace J B G 1972 *J. Phys. B: At. Mol. Phys.* **5** 1138
Mazumdar P S and Ghosh A S 1986 *Phys. Rev.* A **34** 4433
McEachran R P, Horbatsch M, Stauffer A D and Ward S J 1990 *Annihilation in Gases and Galaxies* (NASA Conference Publication **3058**) p 1
Peach G, Saraph H E and Seaton M J 1988 *J. Phys. B: At. Mol. Opt. Phys.* **21** 3669
Stein T S, Dababneh M S, Kauppila W E, Kwan C K and Wan Y J 1988 *Atomic Physics with Positrons* ed J W Humberston and E A G Armour (London: Plenum) p 251
Stein T S, Gomez R D, Hsieh Y-F, Kauppila W E, Kwan C K and Wan Y J 1985 *Phys. Rev. Lett.* **55** 488
Stein T S, Kauppila W E, Kwan C K, Lukaszew R A, Parikh S P, Wan Y J, Zhou S and Dababneh M S 1990 *Annihilation in Gases and Galaxies* (NASA Conference Publication **3058**) p 13
Ward S J, Horbatsch M, McEachran R P and Stauffer A D 1989 *J. Phys. B: At. Mol. Opt. Phys.* **22** 1845

Positron–lithium scattering with the inclusion of positronium formation

J.W. Humberston and M.S.T. Watts

*Department of Physics and Astronomy, University College London,
Gower Street, London WC1E 6BT, UK*

Detailed studies have been made of elastic scattering and positronium formation in low energy collision of positrons with lithium atoms for the two partial waves $l = 0, 1$. For this system, as for all alkali atoms, the positronium formation channel is open even at zero positron energy. A two-channel version of the Kohn variational method is used with trial functions containing many variational parameters, and reasonably well converged results are obtained. The s-wave positronium formation cross section is infinite at zero positron energy but it then falls rapidly to become several orders of magnitude smaller than the elastic scattering cross section which has a maximum value of approximately $100 \, \pi a_0^2$ at a positron energy of 0.5 eV. For p-wave scattering the positronium formation cross section rises to a value of approximately $10 \, \pi a_0^2$ at an energy of 0.1 eV, with the elastic scattering cross section rising to a maximum of approximately $60 \, \pi a_0^2$ just below the first excitation threshold at 1.84 eV.

1. Introduction

Low energy positron scattering by the alkali atoms is of particular interest because the positronium formation channel is open even at zero incident positron energy. Furthermore, recent experimental measurements [1] have shown that, unlike for other targets, the total scattering cross section is larger for positrons than for electrons. This latter feature is very probably a direct consequence of the former, with positronium formation making a significant contribution to the total cross section.

The alkali atom may be accurately represented as the single valence electron interacting with the core via a local central potential, and the positron–alkali atom system therefore reduces to the equivalent three-body system shown in fig. 1.

Numerous theoretical studies have previously been made of positron–alkali atom scattering using a variety of approximation methods. The positronium formation channel was frequently neglected in some earlier studies, for example Ward et al. [2] and McEachran et al. [3] and references therein, but it has been included in more recent calculations by Basu and Ghosh [4], Hewitt et al. [5], and Walters [6] which have all employed some form of the close coupling approximation.

Although no experimental results are yet available for lithium, we have chosen to investigate this system first, and we describe here a very detailed investigation of
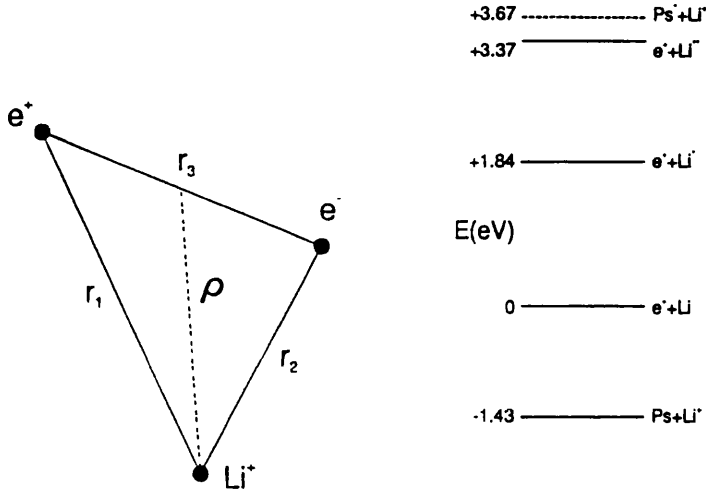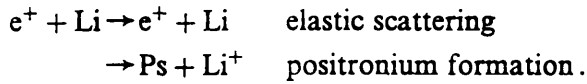
Fig. 1. The positron–lithium system and its energy levels.

lithium scattering by positrons in the low energy region between zero and the first excitation threshold of the lithium atom where only elastic scattering and positronium formation are possible (see energy spectrum in fig. 1); that is

$$e^+ + Li \rightarrow e^+ + Li \quad \text{elastic scattering}$$

$$\rightarrow Ps + Li^+ \quad \text{positronium formation}.$$

2. Method of calculation

A two-channel version of the Kohn variational method is used in a manner similar to that employed by Humberston [7] and Brown and Humberston [8,9] to obtain very accurate results for elastic and positronium formation cross section in low energy positron–hydrogen scattering. The Kohn functional takes the form

$$\begin{bmatrix} K_{11}^\gamma & K_{12}^\gamma \\ K_{21}^\gamma & K_{22}^\gamma \end{bmatrix} = \begin{bmatrix} K_{11}^t & K_{12}^t \\ K_{21}^t & K_{22}^t \end{bmatrix} - \begin{bmatrix} \Psi_1, L\Psi_1) & (\Psi_1, L\Psi_2) \\ \Psi_2, L\Psi_1) & (\Psi_2, L\Psi_2) \end{bmatrix} \tag{1}$$

with $L = 2(H - E)$, and the trial functions for a given orbital angular momentum l, using the nomenclature of fig. 1, are

$$\Psi_1 = \Phi_{Li}(r_2)\sqrt{k}\,Y_{1,0}(\hat{r}_1)\{j_l(kr_1) - K_{11}^t n_l(kr_1)f_1(r_1)\}$$

$$- \Phi_{Ps}(r_3)\sqrt{2\kappa}\,Y_{1,0}(\hat{\rho})K_{21}^t n_l(\kappa\rho)f_2(\rho) + F_1, \tag{2}$$

$$\Psi_2 = \Phi_{Ps}(r_3)\sqrt{2\kappa}\,Y_{l,0}(\hat{\rho})\{j_l(\kappa\rho) - K_{22}^t n_l(\kappa\rho)f_2(\rho)\}$$

$$- \Phi_{Li}(r_2)\sqrt{k}\,Y_{l,0}(\hat{\rho}_1)K_{12}^t n_l(kr_1)f_1(r_1) + F_2, \tag{3}$$

where the functions Φ_{Li} and Φ_{Ps} are the ground state wave functions of lithium and positronium respectively, and the functions f_1 and f_2 are included to shield the singularity in $n_l(x)$ at $x = 0$. These two functions, Ψ_1 and Ψ_2, represent e^+–Li elastic scattering plus positronium formation, and Ps–Li$^+$ elastic scattering plus lithium formation respectively. The wave numbers of the positron and positronium, k and κ respectively, are related by energy conservation such that

$$k^2 + E_{Li} = \tfrac{1}{2}\kappa^2 - \tfrac{1}{2},\tag{4}$$

where the lithium energy $E_{Li} = -0.396$. Short range correlations are represented by the functions F_1 and F_2, the precise forms of which are given later in eqs. (8) and (10).

In terms of the K matrix the partial cross section (in units of πa_0^2) is

$$\sigma_{pq} = \frac{4(2l+1)}{k_q^2}\left|\left(\frac{K}{1-iK}\right)_{pq}\right|^2,\tag{5}$$

where $k_1 = k, k_2 = \kappa$ and σ_{11} is the elastic positron–lithium scattering cross section and σ_{12} is the positronium formation cross section.

A good representation of the e^-–Li$^+$ core potential is given by (Peach et al. [10])

$$V_-(r_2) = -\frac{1}{r_2} - 2\frac{e^{-\gamma r_2}}{r_2}(1 + \delta r_2 + \delta^1 r_2^2) - \frac{\alpha_c}{2r_2^4}w(\nu r_2),\tag{6}$$

where the first two terms constitute the static interaction and the last term arises from the polarization of the core. The e^+–Li$^+$ core potential, $V_+(r_1)$, is derived from V_- by merely changing the static part of the potential. This procedure for generating V_+ is not entirely justified because V_- includes the effect of exchange of the valence electron with the electrons in the core whereas there is, of course, no exchange effect for the positron. Thus far in these investigations we have neglected the core polarization terms in V_- and V_+ because the polarizability of the core is so much smaller than the polarizability of the lithium atom, and also because the core polarization terms, when combined with the three-body term potential which must be added to the total three-body Hamiltonian, tend to cancel when the electron and positron are close together as in positronium.

A very accurate approximation to the wave function of the electron in the potential V_-, our representation of the lithium atom, of the form

$$\Phi_{Li}(r_2) = e^{-Ar_2}\sum_{j=0}^{N_0} e_j r_2^j\tag{7}$$

was generated using the Rayleigh–Ritz method. This wave function has the required character of the 2s orbital of the valence electron with the correct energy, and it therefore represents the electron in the first excited state in the potential

V_-. The ground state, which has no real physical significance but is present in this model we are using for the lithium atom, has an energy of -50 eV. This fictitious state is so far below the energy region of a few electronvolts being considered in the scattering calculation that it can probably be ignored. Nevertheless, we have also used another model of the lithium atom which avoids this problem by having the valence electron in the ground state of a modified form of V_- (Peach, private communication). This state has the correct lithium energy but the wave function is nodeless and does not have the correct radial dependence for small values of r_2. It does, however, give a reasonably good fit to the spectroscopic data for lithium. We shall call the original and modified forms of V_-, and the associated forms of V_+, potentials A and B respectively, and the corresponding two forms of $\Phi_{Li}(r_2)$ are given in fig. 2.

The modification made to V_- to achieve the required 1s ground state energy takes the form of a repulsive short range barrier which is generated by choosing appropriate values for the parameters δ and δ^1 in eq. (6). But, because we have taken the positron–core potential V_+ to be $-V_-$, this repulsive barrier becomes a short range attractive potential well for the positron. However, the intermediate and long range character of the positron–core potential is still repulsive and at the low positron energies being considered here there will be very little penetration of the positron wave function into the short range attractive well. Nevertheless, it must be admitted that in trying to remove an unsatisfactory feature of the original electron–core potential we have introduced an unsatisfactory feature into the positron–core potential. Overall we believe that potential A provides a more reliable model of the electron (and positron)–core potential, but we present results for both A and B in order to convey some impression of the sensitivity of the results to the assumed form of interaction.
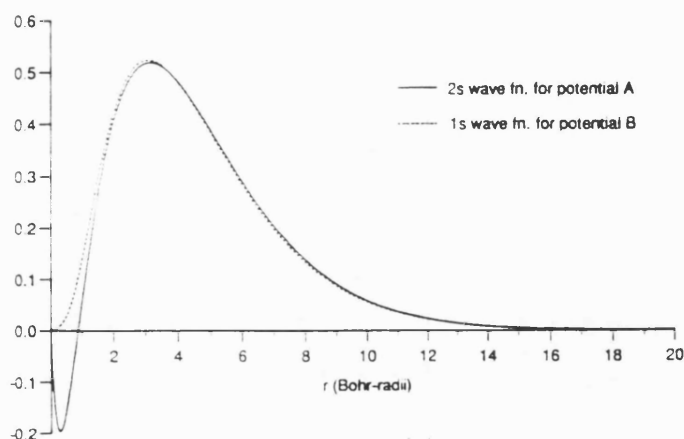

Fig. 2. Lithium wave functions. Plotted here are r_2 versus $\Phi_{Li}(r_2)$ for the two forms of the electron–core potential, A and B.

3. Results and discussion

Results have thus far only been obtained for s- and p-wave scattering.

For s-wave scattering the short range correlation terms in the trial functions Ψ_1 and Ψ_2 are

$$F_1 = Y_{00}(\hat{r}_1) \exp[-(\alpha r_1 + \beta r_2 + \gamma r_3)] \sum_{j=1}^{N} c_j r_1^{k_j} r_2^{l_j} r_3^{m_j} \tag{8}$$

with a similar form for F_2, but with different linear variational parameters. All terms with

$$k_j + l_j + m_j \leqslant w, \tag{9}$$

where k_j, l_j, m_j and w are non-negative integers, are included in the summation, and results have been obtained for $w = 1(1)9$, corresponding to 4, 10, 20, 35, 56, 84, 120, 165, 220, respectively.

Details of the method of calculation and the investigation of the convergence of the K-matrix elements with respect to w have been given by Armour and Humberston [11].

The most accurate values of the elastic scattering and positronium formation cross sections, with $w = 9$, are given in figs. 3 and 4. For $k \approx 0.2$ the results are probably within 10% of the exact, or fully converged, values, but there is some deterioration in the convergence with respect to w for values of k very close to zero and also to 0.36, the first excitation threshold of lithium. Longer range correlation terms
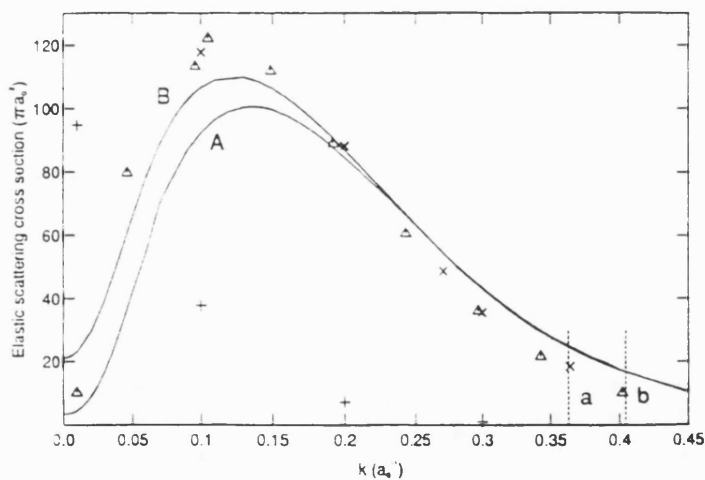

Fig. 3. The $l = 0$ elastic scattering cross section: (———) present results for potentials A and B) the first excitation threshold is marked a and b respectively); (+) McEachran, $\times 10^{-1}$ (private communication, see also refs. [2,3]); ($\times$). Hewitt (private communication and ref. [5]); Walters (private communication, and also ref. [6]).
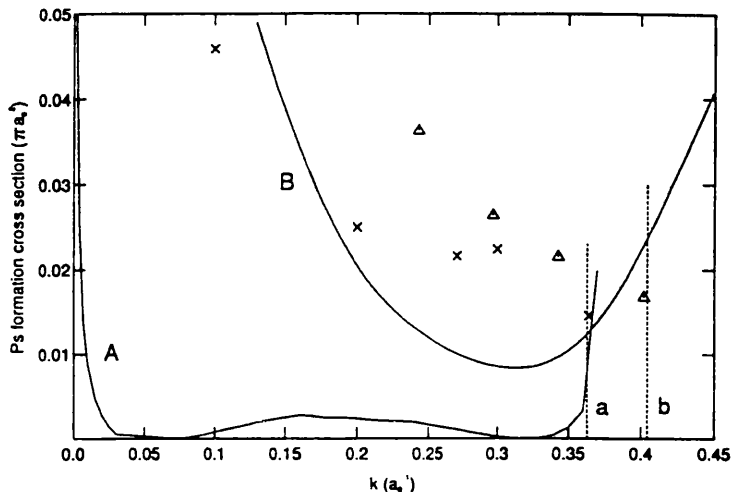
Fig. 4. The $l = 0$ positronium formation cross section: (———) present results for potentials A and B; (×) Hewitt, $\times 10^{-2}$ (private communication and ref. [5]); ($\triangle$) Walters, $\times 10^{-2}$ (private communication and also ref. [6]).

need to be added to the trial functions in order to improve the convergence, particularly because the dipole polarizability of lithium is so large.

At very low positron energies the elastic scattering cross section is quite small, but it then rises rapidly with increasing energy to a maximum value of approximately 100 πa_0^2 before falling away again. Similar elastic scattering cross sections are obtained for the two potential models, and they agree well with the recent results of Hewitt et al. [5] and Walters [6]. Both of these calculations employ the close coupling approximation with pseudostates and they extend over a much wider energy range than that being considered here.

Positronium formation, being an exothermic reaction in positron–alkali atom scattering, has a cross section σ_{Ps} which, according to the Wigner threshold laws, is $\propto 1/k$ for sufficiently small k when $l = 0$, and is therefore infinite at $k = 0$. The rate of positronium formation is, however, proportional to $k\sigma_{Ps}$ and is finite. The positronium formation cross section rapidly falls to a value several orders of magnitude smaller than the elastic scattering cross section and it remains very small throughout the energy range under consideration. Unlike for elastic scattering, the positronium formation cross sections obtained with the two potential models are rather different. This difference is exaggerated by the abnormally small magnitude of the s-wave positronium formation cross section which makes the results depend very sensitively on the model and the method of approximation being used. For both potential models the positronium formation cross section decreases as the flexibility of the trial functions is increased by increasing the parameter w in eq. (9), and the results in fig. 4 are probably upper bounds on the fully converged results. Much larger positronium formation cross sections are obtained for smaller values

of w and it may, therefore, be that the significant discrepancies between the present results and those of Hewitt et al. [5] and Walters [6] arise from the lack of convergence in the close coupling calculations.

We considered the possibility of a positron–lithium bound state by examining the eigenvalues of the total Hamiltonian matrix obtained using the short range correlation functions constituting F_1, eq. (8), as a basis. Unfortunately, because of the very tightly bound state of the electron in potential A there are several energy eigenvalues of the three-body system below the energy of the lithium atom, but none of them provides evidence of a true bound state.

For p-wave scattering there are two types of short range correlation term, and the overall correlation function in eq. (2) for $l = 1$ is

$$F_1 = Y_{1,0}(\hat{r}_1)r_1 \exp[-(\alpha r_1 + \beta r_2 + \gamma r_3)] \sum_{j=1}^{N} c_j r_1^{k_j} r_2^{l_j} r_3^{m_j}$$

$$+ Y_{1,0}(\hat{r}_2)r_2 \exp[-(\alpha r_1 + \beta r_2 + \gamma r_3)] \sum_{j=1}^{N} d_j r_1^{k_j} r_2^{l_j} r_3^{m_j} \tag{10}$$

with a similar form for F_2. Each summation is the same as for the s-wave trial function so that for a given w there are now twice as many short range correlation functions. The most accurate results for the elastic scattering and positronium formation cross sections are given in figs. 5 and 6. Convergence with respect to w is rather less good than for s-wave scattering and the results may differ by as much as 15% from the exact values. As in s-wave scattering, there is again good agreement between the present p-wave elastic scattering cross sections and the corresponding results of Hewitt et al. [5] and Walters [6]. Now the positronium
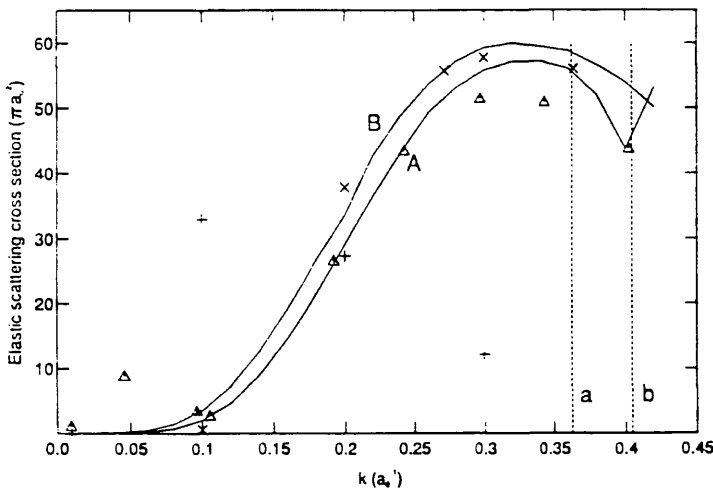

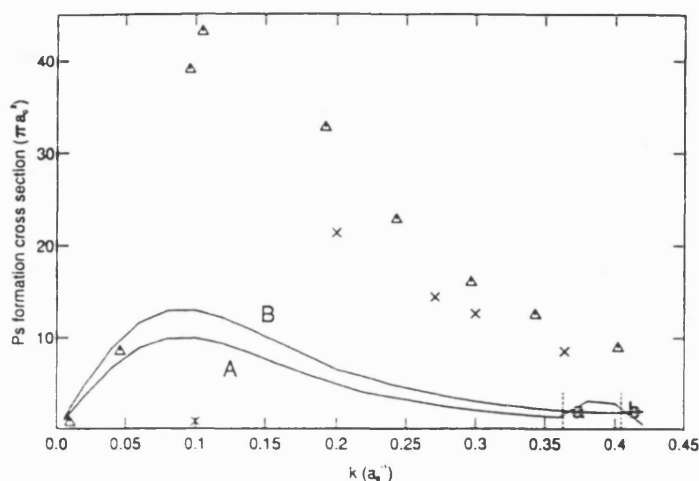Fig. 5. The $l = 1$ elastic scattering cross section. See caption to fig. 3.

Fig. 6. The $l = 1$ positronium formation cross section: (——) present results for potentials A and B; (×) Hewitt (private communication and ref. [5]); ($\triangle$) Walters (private communication and ref. [6]).

formation cross section is a significant fraction of the total cross section, and is very much larger than the s-wave positronium formation cross section except very close to $k = 0$. A similar pattern in the relative magnitudes of the s- and p-wave contributions to the positronium formation cross section has been observed in positron–hydrogen scattering [12].

The present positronium formation cross sections are now in better agreement with the results of Hewitt et al. [5] and Walters [6], being only approximately three times smaller whereas the s-wave results are several orders of magnitude smaller. Again, the discrepancy may be due to the lack of convergence of the close coupling results.

As mentioned in the introduction, the positronium formation channel has been neglected in several previous investigations of positron–lithium scattering [2,3] and we have therefore calculated the elastic scattering cross section with the positronium channel suppressed. In this approximation the Kohn functional becomes

$$K_{11}^{v} = K_{11}^{t} - (\Psi_1 L \Psi_1) \,, \tag{11}$$

where

$$\Psi_1 = Y_{l,0}(\hat{r}_1)\Phi_{\text{Li}}(r_2)[j_l(kr_1) - K_{11}^{t} n_l(kr_1)f_1] + F_1 \tag{12}$$

and F_1 is the same short range correlation function as was used in the two-channel formulation (eqs. (8) and (10)).

The resulting elastic scattering cross sections differ only rather slightly from those obtained in the coupled channel formulation, except for the introduction of a narrow resonance into the p-wave cross section at $k \approx 0.2$, but they differ significantly from the uncoupled results of Ward et al. [2] and McEachran et al. [3] (and McEachran, private communication), particularly at very low energies, as may be

seen in figs. 3 and 5. These authors used the close coupling approximation, but only included the ground and excited states, and pseudostates, of lithium, with no states of positronium. In our present uncoupled calculations we still implicitly include positronium states in the short range correlation function F_1 even though there is no outgoing positronium wave, and it would seem that the inclusion of positronium terms in the closed channel is sufficient to yield moderately good results for elastic scattering.

Our investigations are being continued to higher partial waves and will also be extended to somewhat higher energies where more open channels become accessible.

Acknowledgement

References

[1] C.K. Kwan, W.E. Kauppila, R.A. Lukaszew, S.P. Parikh, T.S. Stein, Y.J. Wan and M.S. Dababneh, Phys. Rev. A 44 (1991) 1620.

[2] S.J. Ward, M. Horbatsch, R.P. McEachran and A.D. Stauffer, J. Phys. B 22 (1989) 1845.

[3] R.P. McEachran, M. Horbatsch, A.D. Stauffer and S.J. Ward, *Proc. Workshop on Annihilation in Gases and Galaxies*, Goddard Space Flight Center, Greenbelt 1989, ed. R.J. Drachman, NASA Conference Publication 3058 (1990) p. 1.

[4] M. Basu and A.S. Ghosh, Phys. Rev. A 43 (1991) 4746.

[5] R.N. Hewitt, C.J. Noble and B.H. Bransden, J. Phys. B 25 (1992) 2683.

[6] J. Walters, Proceedings of this Conference, Hyp. Int. xx (1994) xxx.

[7] J.W. Humberston, Can. J. Phys. 60 (1982) 591.

[8] C.J. Brown and J.W. Humberston, J. Phys. B 17 (1984) L423.

[9] C.J. Brown and J.W. Humberston, J. Phys. B 18 (1985) L401.

[10] G. Peach, H.E. Saraph and M.J. Seaton, J. Phys. B 21 (1988) 3669.

[11] E.A.G. Armour and J.W. Humberston, Phys. Rep. 204 (1991) 165.

[12] J.W. Humberston, Adv. At. Mol. Phys. 22 (1986) 1.